Light forge: a microfluidic high throughput platform for rapid and affordable detection of drug resistant strains of Tuberculosis

Ian Maheti Mbano

Student Number: 210546221

Submitted in full fulfilment of the requirements of the degree Masters in Medical Microbiology

College of Health Science, School of Laboratory Medicine and Medicinal Sciences, Nelson Mandela School of Medicine, 719 Umbilo Road, Durban, 4001

November 2015

Declaration

I hereby declare that the study reported in this thesis was conducted under the supervision of Dr Frederick Balagadde, at the KwaZulu Natal Research Institute of Tuberculosis and HIV (K-RITH), Nelson Mandela School of Medicine, KwaZulu Natal.

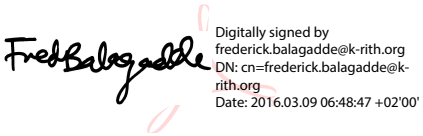

.....	.....
Student	Supervisor
Mr Ian M Mbano	Dr Fredrick Balagadde

Dedication

I would to dedicate this work to my Lord and personal saviour, Jesus Christ who by the power of the Holy Spirit h marvellously guided me throughout this work. I could not have achieved this feat without him; it is as simple as that.

I want to dedicate this work to my family, Fred (father), Rachael (deceased mother), my sisters Beatrice and Natasha, not forgetting my two beautiful and witty nieces Chloe and Lee-ann. I am eternally grateful of the love you people shower me with, the support structure you provided throughout the duration of this work helped through many challenges. I love you.

Acknowledgements

I would like to thank Dr Manormoney Pillay and Dr Adrie Steyn for their assistance in acquiring the test *M. tuberculosis* strains. I greatly appreciate Mr Tawanda Mandizvo, for the relentless effort in the development of the microfluidic platform Light Forge. I also want to appreciate Dr Balagadde for the constant encouragement throughout the duration of this work.

Table of Contents

List of Tables

List of Figures

List of Abbreviations

HIV/AIDS – Human Immune Virus/ Acquired Immune Disease Syndrome

TB- Tuberculosis

TNF- Tumour Necrosis Factor

DC-SIGN- Dendritic Cell Specific C-type lectin receptor

HAART- Highly Active Antiretroviral Therapy

PI- Protease Inhibitors

NNRTI- Nucleoside Reverse Transcriptase Inhibitors

IRIS- Immune Reconstitution Inflammation Syndrome

MDR-TB- Multi Drug Resistant Tuberculosis

XDR-TB- Extensively Drug Resistant Tuberculosis

TDR-TB- Totally Drug Resistant Tuberculosis

PCR- Polymerase Chain Reaction

SSM- Sputum Smear Microscopy

TST- Tuberculin Skin Test

IGRA- Interferon Gamma Release Assays

ESAT-6- Early Secretory Antigen Target 6

NTM- Non-Tuberculosis-Mycobacterium

BCG- Bacillus Calmette–Guérin

LED- Light Emitting Diodes

LJ- Lowstein-Jensen

MGIT- Mycobacteria Growth Indicator Tubes

NAP- β-Nitro Alpha acetyl amine β-hydroxyl propiophenone

MODS- Microscopic-Observation Drug Susceptibility

NAA- Nucleic Acid Amplification

AMTD- Amplified Mycobacterium Tuberculosis Direct

LAMP- Loop Mediated Isothermal Amplification

FRET- Fluorescence Resonance Energy Transfer

ELISA- Enzyme Linked Immunosorbent Assays

HRMA- High Resolution Melting Analysis

NLR- Negative Likelihood Ratio

PLR- Positive Likelihood Ratio

PDMS- Polydimethylsiloxane

IR- Infra-Red

TLC- Thermo-Chromic Liquid Crystals

MLSI- Microfluidic Large Scale Integration

PMT- Photo Multiplier Tube

CCD- Closed Circuit Device

CMOS- Complementary Metal Oxide Semiconductor

CL- Chemiluminescence

PO- Peroxyoxalate

ECL- Electrochemiluminescence

EMR- Electromagnetic Radiation

LED- Light Emitting Diodes

NMR- Nuclear Magnetic Resonance

TAC- Taqman Array Card

POC- Point of Care

GFP – Green Fluorescent Protein

Abstract

Tuberculosis is one of the most deadly infectious diseases currently plaguing the global community. Unfortunately, lack of accessible, reliable and affordable diagnostic tools in the high disease burden, and resource poor regions such as Sub-Saharan Africa has hampered efforts to eradicate the epidemic. This study documents the development of a microfluidic platform called Light Forge, which is capable of detecting genetic drug resistance signatures in *M.tuberculosis* DNA. The first phase of this study involved a molecular drug susceptibility assay on 7 strains of *M.tuberculosis* using the high resolution melt analysis at *the rpoB, katG, mab-inhA* and *gyrA* loci with the Light Cycler96 . These findings compared with phenotypic drug susceptibility testing and Sanger sequencing. The results from the preliminary tests showed that the commercial system could detect positive strains at sensitivity estimates of 86%, 17% , 0% and 100% for *rpoB, katG,* mab-*inhA* and *gyrA* respectively. Detection of non-synonymous mutation in *gyrA* region for all test strains halted further testing. The *rpoB* gene was selected for on chip profiling with the Light Forge system due to the higher sensitivity. The results from the Light Forge showed that the system was capable of detecting test strains with 100% sensitivity, with modest reproducibility and correspondence with the phenotypic drug susceptibility profiles and the sequencing results. A microfluidic TB assay based on the Light Forge system is on the horizon based on the findings of the study. However, more work is required to incorporate other genes and ultimately design the best-equipped device for the clinical setting.

CHAPTER 1: INTRODUCTION

The emergence of drug resistant strains of *M.tuberculosis* demands an increase in the diagnostic capacity of health care delivery programs. Drug resistance leads to treatment failure, increasing the mortality and disease transmission rates [1]. Increasing diagnostic capacity is a major proponent in achieving the goals of the STOP TB strategy. The strategy aims to reduce TB transmission by 80%, TB related deaths by 90% and TB associated costs to the patients by 100% before the year 2030 [2]. These are steep goals, which will require a concerted effort from all TB stakeholders ranging from the pharmaceutical companies, governmental agencies and technological institutions right up to the patients.

This thesis describes the development of a microfluidic assay for the detection of drug resistance linked mutations in *M.tuberculosis*. Microfluidics exploits the miniaturization of reactions in an integrated manner to deliver fast, efficient assays with increased resolution of the product. This introductory chapter is aimed at highlighting the important aspects of tuberculosis disease, more so its synergistic interaction with HIV/AIDS. I further proceed to document the various drugs used to treat the many variations of this disease. A summary of the current diagnostic tools used in tuberculosis research ensures. The chapter concludes by an expose into the arena of microfluidics, with emphasis on devices performing nucleic acid amplification. Chapter 2 shows the methodologies used in the development of the assay from the preliminary to the testing phase. Chapter 3 provides a sequential and chronological presentation of the results from the commercial system leading up to the findings from the Light Forge system. Results from the standard methods are included to verify the observations. The final chapter, chapter 4, discusses the findings of the experiment. It highlights the advances the Light Forge device is making whilst suggesting areas in which assay can be further improved. This study is a collaborative effort with Mr Tawanda Mandizvo from the Kwazulu Natal Research Institute of Tuberculosis and HIV/AIDS, Balagadde lab.

1.1 HIV/TB endemic

Tuberculosis (TB) is a disease caused by infection with *Mycobacterium tuberculosis(M.tuberculosis)s*, which typically infects the lungs (pulmonary TB) but can also infect other organs including the kidneys, spinal cord, and brain (extra pulmonary TB) [3]. TB can be either latent or active, with the former referring to a state in which the *M.tuberculosis* is in a dormant, non-infectious phase. Active TB is when the bacteria are actively dividing in the host thus are easily transmitted [4]. A third of the global population suffers from latent TB. However, due to the body's defence system, clinical symptoms are the result of an immune-compromising event such as the onset of HIV/AIDS. About 9 million TB cases were reported in 2012 alone, with 1.3 million TB related deaths worldwide [5]. Even though this disease is treatable, it remains a challenge to the global community over a century since its discovery. The co-infection of TB and HIV-AIDS ("cursed duet") is a major challenge in resource-limited settings, particularly in Asia and Sub Saharan Africa. This is cemented by the realisation that even though South Africa has less than 1% of the World's population, it is responsible for more than 25% of global HIV-TB co-infection cases [6]. Compared with other countries, such as USA (high income), China (upper middle income), India (lower middle income) and Zimbabwe (low income), South Africa (upper middle income) have the highest incidence of TB in spite of obvious economic and population advantages to the aforementioned countries. In the mid-90s, countries in the Sub-Saharan Africa had a boom in TB incidences (Figure 1) catalysed by an increase in the rate of HIV infection cases. This is in contrast to the USA, China and India, which show a gradual decrease in TB cases even to date. Perhaps issues such as poverty, inequality and social turbulences coupled to a lack of standard health care could have led to more HIV related TB cases in South Africa [7]. A study recently showed that HIV positive individuals of African descent had a 2.5 fold chance of developing tuberculosis disease in comparison to those of Caucasian ancestry [8]. The observation was a result of a mutation in the gene that produces the macrophage migration inhibitory factor (MIF). MIF is implicated inflammation and ultimately infection control. Such a finding implies that the biological make up of an individual might predispose them to disease, but more research is required to support this claim.

Studies have shown that within the human host, the two pathogens—*M. tuberculosis* and HIV—develop a mutual interaction, leading to the fatal disruption of the immune functions when unabated [9]. Infection with HIV increases the risk of activating latent TB infection into active disease by 20-fold [10]. In the following passage, a brief description of the biology of the TB/HIV co-infection, its effect on diagnosis, treatment administration and patient outcome is discussed.

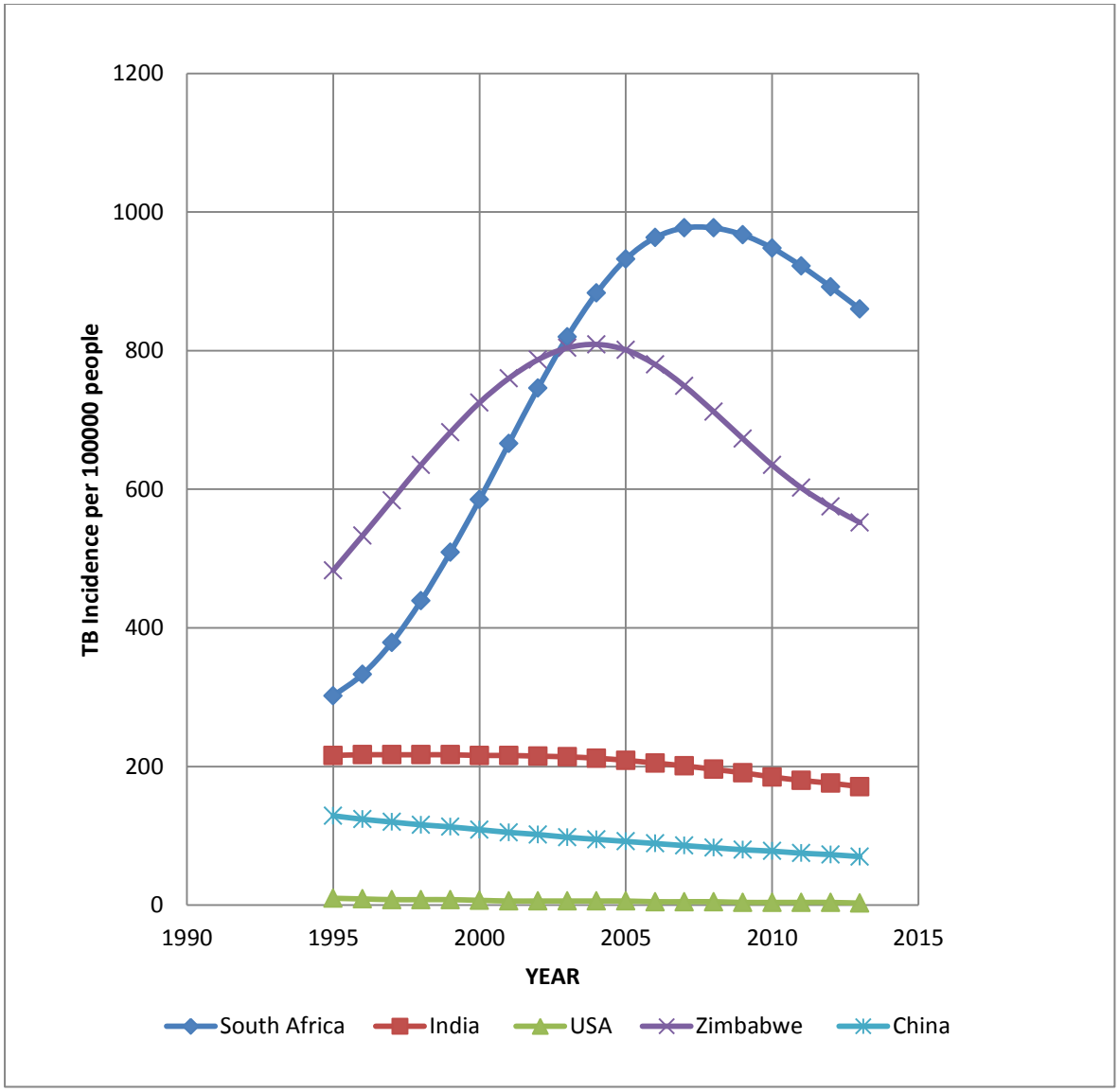

Figure 1: TB incidence rates variation in South Africa, India, USA, China and Zimbabwe adapted from the World Bank [11].

The graph above shows that the TB incidence cases in the USA have been relatively constant for the for the past two decades. Over the same period, China and India gradually reduced the incidences of TB disease but cases are still higher than the rates observed in the USA. South Africa and Zimbabwe, both in the sub-Saharan region, show increase in the incidences of TB from 1995. This increase correlated with the increase in HIV incidences in the region. The rates peaked in 2004 for Zimbabwe and 2007 for South Africa, after which steady declines ensured because of improved intervention by the TB control programs. However, the current rates are still too high in comparison to global standards. More work is required to reduce the incidence rates.

1.1.1 Biology of TB/HIV interaction

One of the most critical outcomes of an untreated HIV infection is the reduction in the number of $CD4^+$ T cells, which increases the risk of latent TB advancing to active TB disease. Coupled to added susceptibility to exogenous superinfecting TB strains [10]. Tumour Necrosis Factor (TNF) is a cytokine that is produced by macrophages or monocytes in response to infection [12]. It has been implicated in the caseous necrosis(aggregation of host immune cells to eliminate *M.tuberculosis*)—observed during infection with TB—that helps to ensure short and long term control of the pathogen [13]. HIV infection inhibits killing of *M. tuberculosis* by macrophages mediated by TNF [14]. Macrophages activate a programmed cell death pathway, creating an acidic cellular environment that eliminates the *M.tuberculosis*. When HIV infects the macrophage, it tends to halt the programmed cell death, allowing the cell to persist [15].This invariably increases the pathogenesis of *M.tuberculosis*. In addition, HIV infection increases the expression of receptors that facilitate the entry of *M.tuberculosis* into the macrophages, allowing the dispersion of *M.tuberculosis* throughout the host [16]. Typically, TB infection is contained within granulomas—highly stratified cellular confines that prevent dissemination of *M.tuberculosis* cells and ultimately help eradicate the infection. Granulomas also serve as a classical indication of *M.tuberculosis* infection. HIV infection compromises the containment of *M.tuberculosis* by altering the granuloma structure. This can be achieved by hampering recruitment of new cells to the granulomas, causing them to be more porous to external tubercular cells whilst releasing previously contained *M. tuberculosis* microbes into the circulatory system [17].

Interestingly, some studies claim that TB disease has a negative effect on HIV infection progression to AIDS although this claim is not completely substantiated [10]. On the contrary, an elevated viral replication rate has been observed in sites with a highly localised *M.tuberculosis* population [18]. This is observed in alveolar macrophages—the primary target cells for TB infection—were elevated rates of HIV replication are observed, spiking transmissions of *M.tuberculosis* from infected macrophages to T cells[10]. It is known that TNF is released by the immune system to arrest bacterial growth but unfortunately it also activates HIV replication in macrophages, thus the body is essentially predisposed to susceptibility to HIV by a positive response to the TB pathogen [19].

Dendritic cells (DC), found on the skin and mucosal surfaces, are responsible for trapping antigens and presenting them to the T cells to activate the adaptive immune response [20]. Both TB and HIV infections repress the host's pro-immunity activities using different mechanisms, specifically the DC-specific C-type lectin receptor (DC-SIGN). *M.tuberculosis* is captured via this receptor and internalised by the cells, where it has been shown to down-regulate the response of the immune system by suppressing cytokines responsible for pathogen eradication such as IL-12 and TNF [21]. HIV on the other hand, hybridizes to the DC-SIGN receptor through its gp120 protein, facilitating the efficient distribution of this virus throughout the host. Targeting of these cells by TB and HIV greatly

limits the controlling ability of the immune system and further complicates efforts to diagnose each of the pathogens as highlighted in the subsequent passage.

1.1.2 Implication of TB/HIV coinfection on diagnosis

HIV co-infection with TB elicits a marked negative effect on their clinical diagnosis, perhaps a consequence of TB/HIV interaction. Firstly, HIV positive patients typically have low tubercle bacilli numbers in their sputum and develop more defined extra-pulmonary TB, leading to sputum negative microscopy results [22]. Clinicians' use symptom screening in resource constrained countries as a method to determine the TB status of patients, prominently relying on a cough sustained for a period exceeding 3 weeks as high confidence marker for active TB disease. However, for patients living with HIV/AIDS, this symptom often has a low sensitivity for TB [23]. Coupling night sweats and fevers to the persistent cough leads to a useful marker in clinical diagnosis of TB disease. Nevertheless care should be taken as reliance on these symptoms invariably increases the chances of false detection of TB since the symptoms are not specific to TB disease [23]. Infection with HIV serves as an avenue for a myriad of opportunistic infections, confounding the interpretation of findings from chest X-rays [24]. In spite of these glaring limitations, the diagnostic algorithms for HIV positive and HIV negative patients are still largely the same for most national disease monitoring programmes. The reality of the situation is that it is difficult to arrive at a high confidence diagnosis without the use of culture based methods which require longer time periods (3 to 8 weeks), dedicated facilities or more expensive molecular techniques that can detect DNA or RNA TB markers in shorter time periods. HIV infection is easy to detect in bodily fluids such as saliva or blood of the patient using a wide array of methods [25]. A thorough scan of the literatures shows that tuberculosis infection does not impede HIV diagnosis.

1.1.3 Treatment of TB/HIV coinfection

Discovery of the highly active antiretroviral therapy (HAART) has improved the clinical outcomes as shown by the decline of the number of deaths in study cohorts in the United States of America from 987 to 78 in 6 years [26]. The same trend was observed in South Africa [27], in which the better survival rates were attributed to HAART and comprehensive TB therapy [28]. Optimal use of both these regimens leads to effective disease management. This raises one of the biggest challenges in TB/HIV treatment: when to initiate HAART for patients already receiving TB treatments. This decision is complicated by the fact that drugs that are in the rifamycin class and routinely used in TB therapy—including rifampin and rifabutin—negatively interact with protease inhibitors (PIs) and non-nucleoside reverse transcriptase Inhibitors (NNRTI) that are used in HIV treatment[29]. Short course TB therapy is a fully supervised 6 month regimen aimed at reducing the cost of treatment as well as increasing patient adherence [30]. Short course therapy involves 2 months of daily rifampin, isoniazid, pyrazinamide and ethambutol, followed by 4 months of isoniazid and rifampin twice a week. There is

minimal description of how the HIV infected patients respond to the short course therapy for TB [31], with some studies suggesting that it leads to lower relapse rates for HIV positive patients [32].

In order to address the challenges encountered in effective treatment of TB/HIV coinfection, treatment plans typically adhere to the notion that TB treatment takes precedence over that of HIV [33]. More often than not, this stance requires adjustments, by taking into account CD4+ counts and drug resistance profiles of the *M. tuberculosis* of the patient. Patients with CD4+ counts greater than 200 cells/ml start HAART after completion of anti-TB therapy, whereas patients with CD4+ counts less than100 cells/ml have to receive HAART shortly after starting anti-TB therapy [33]. In spite of the several nuances, Dean *et al* showed that early initiation of HAART leads to fewer deaths and instances of debilitating TB disease [34]. On the contrary, early initiation of HAART increases the risk of developing Immune Reconstitution Inflammation Syndrome (IRIS), which is a paradoxical immune response to HAART were the clinical condition worsens due to an excessive immune sensitivity to infectious and non-infectious antigens [35]. However, in cases of TB/HIV coinfection, IRIS can lead to an elevated drug toxicity and reduced efficacy of anti-TB therapy [36]. All these dynamics serve to illustrate that coinfection of TB and HIV invariably complicates the treatment planning and outcomes for the patients.

It is clear that TB/HIV confection is a threat to the management of these diseases. Through their pseudo-symbiotic and largely elusive interaction within the host, they have added several layers of complexity to their respective diagnoses and treatment plans. Meaningful efforts should be channelled towards preventing future HIV and TB transmission, improving all of the current treatment plans in high disease burden areas as a cooperative effort from governments, cooperates and the communities at large without delay.

1.2 Tuberculosis drugs

Tuberculosis has afflicted humankind for many centuries. Physicians have treated patients in many different ways over the years. One of the early treatments involved a combination of prolonged exposure to the sun, fresh air and assuming the proper gait [37]. This strategy yielded moderate success probably because patients lungs were not agitated by pollutants found in the cities, and the prescription of rest and prescribed posture allowed the natural healing of TB lesions [37]. This also made it easier to isolate patients who were releasing TB-pathogen packed aerosols. Clinicians in the early 1900s also resorted to collapsing the lungs of the patients to address TB disease as a last alternative for grave cases [38]. This was borne from the observation that healing TB lung cavities close or die off. The major assumption being by seizing function of part or the entire lung, perhaps the patients would recover. Lung collapsing was performed by either a pneumothorax (filling the interplural space with air or nitrogen) [39], phrenic paralysis (inhibiting function of the phrenic nerve, which controls lung expansion) [40] or thoracoplasty (removal of ribs until the lungs seized expanding)

[41]. Even though these approaches may seem bizarre and peculiar to a modern reader, they helped reduce the lung capacity, accelerating the repair of cavities in the lungs and reducing the bacterial load expelled during exhalation[37]. The above methods were rapidly replaced by more scientific remedies when Robert Koch proved that tuberculosis disease was caused by a bacterial pathogenic agent [42]. This paved the path for the development of several antibacterial agents for treating the disease.

The goal of chemotherapy is to reduce the pathogenic load whilst mitigating the effects of pathogen metabolic activity on the host. There exists a wide range of anti-TB drugs, developed in the 1940s. The desired outcome of the chemotherapy is to eradicate all multiplying bacteria, prevent development of TB drug resistance and achieve host sterility to avoid clinical relapse [43]. Combination treatment allows eradication bacteria multiplying at different rates. In the following section, the various drugs administered for different forms of the TB diseases (first- and second-line drugs), while highlighting potential drugs, which are still in the trial phases, are confabulated.

1.2.1 Firs line anti-TB drugs

Four drugs (isoniazid, rifampin, pyrazinamide and ethambutol) constitute first line tuberculosis therapy. These drugs are for TB treatment-naïve patients with the operating assumption that the infection is with drug-susceptible or treatable strain(s) of *Mycobacterium tuberculosis*. The treatment plan involves 2 months of intensive treatment with all four drugs followed by a continuation phase lasting 4 months with only isoniazid and rifampin [44]. These agents represent the first response to the detection of infection, commonly referred to as Group 1 drugs.

1.2.2 Isoniazid

Isoniazid, a nicotinamide prodrug, was discovered in 1952 and has potent bactericidal activity against *Mycobacterium tuberculosis* [45]. It is the most prescribed anti-TB drug. Isoniazid is readily absorbed by host cells and is passively taken up by *M.tuberculosis* [46]. Studies have shown that it interferes with several cellular functions, particularly nucleic acid synthesis [47]. However its potency against *M.tuberculosis* is linked to inhibition of mycolic acid synthesis [48]. This effect is achieved when the oxidised form of isoniazid binds to the Enoyl Acyl Carrier Protein (ACP) reductase InhA [49], a critical enzyme in the fatty acid synthesis complex. NAD is a coenzyme which exists in its oxidized (NAD^+) or reduced form (NADH) functioning as an electron transfer factor in redox processes [50]. It is involved in cellular regulations such as energy generation, DNA transcription and repair. Thus the interaction of isoniazid with bound NAD is thought to dislodge this metabolite from the active form of reductase [51], halting the enzymatic process. Unfortunately, the overuse of this drug has led to the development of resistance. In 50-80% of the cases, drug resistant clinical isolates harboured a point mutation in the *katG* gene, specifically a threonine substitution with serine at residue 315 [43]. Resistance to isoniazid has also been shown to be due to mutations in the *inhA* gene or its promoter *mab-InhA*, maintaining enzyme functionality but reducing affinity to NADH substrate perhaps by

using a different substrate [52] . Mutations in other genes such as *ndh* , *kasA* ,*aphC, oxyR* have been implicated in low to moderate events of isoniazid resistance [53]. In spite of all this knowledge, some clinical isolates with phenotypic resistance lacking mutations in any of the known genes have been detected, suggesting that more rigorous studies are required to elucidate other resistance mechanisms [54].

1.2.3 Rifampin

A member of the rifamycin family, rifampin is a synthetic drug, which is a vital component of anti-TB drug regimens. It exhibits a characteristic delayed bactericidal activity in comparison to isoniazid, making it suitable for killing bacteria which continue to survive (albeit in a diminished metabolic state) for long periods during chemotherapy [55]. Due to its lipid-like properties, rifampin can be easily transported into the extracellular environment of *M.tuberculosis* [52]. Its bactericidal activity is attributed to the ability to bind to the bacterial RNA polymerase inhibiting transcription [43], although the exact mechanism of this action is yet to be fully understood. Similar to isoniazid, prolonged and munificent prescription of the drug has led to development of resistance. In over 90% of rifampin resistant isolates, point mutations were detected in a highly variable 81bp region of the *rpoB* gene, encompassed in codon 507 to 533 [53]. Not all the rifampin resistant strains exhibit mutations in this region and more studies are required to allow full comprehension of resistance conferring gene mutations.

1.2.4 Pyrazinamide

Pyrazinamide is a member of the nicotinamide group of drugs together with isoniazid. Similar to isoniazid, it is a prodrug that is converted to its active form, pyrazinoic acid by the activity of pyrazinamidase [56]. It shows high efficacy against slowly dividing bacteria in a quasi-dormant state under acidic conditions typically found in phagosomes [57]. However, the killing effect is sustained for up to 2 months only during treatment [58]. The accumulation of pyrazinoic acid in the cytoplasm is thought to lead to the disruption of the proton motive force due to the low intracellular pH [59]. Pyrazinamide has been shown to inhibit trans-translation, a pathway designed to ensure production of correct functional proteins and in some instances gene expression in bacteria [60]. Resistance to pyrazinamide is generally attributed to mutations in the gene *pncA*, which codes for the production of the afore mentioned pyrazinamidase [43]. Drug resistance is linked to mutations throughout the 561bp region coding for this enzyme and its 82bp promoter region . This complicates development of a simple assay for detection of genomic signatures of pyrazinamide resistance [61]. As with the aforementioned anti-TB drugs, not all resistance can be attributed to mutations in the *pncA* region, suggesting alternative resistance mechanisms that may reduce accumulation of the drug [46].

1.2.5 Ethambutol

Ethambutol was discovered in 1961 as an anti-TB drug and has since been incorporated into first line TB therapy [43]. A member of the alkanolamines, this drug targets dividing bacteria and is incorporated into the combination treatment to minimise development of resistance to the other first line drugs despite possessing minimal sterilizing ability [62]. It interferes with arabinogalactan synthesis by preventing chain elongation of this biological polymer [63]. It has also been reported to interfere with other cellular activities such as phospholipid synthesis [64]. Point mutations at codon 306 of the *embB* gene are responsible for resistance to this agent for about 50% of the resistant cases [65]. Other cases have been attributed to various factors such as mutations in the *embCA* operon, although cases of resistance which cannot be attributed to any known mutations are still very frequent [43].

Clinical resistance to the aforementioned antibiotics can be a result of several genetic or epigenetic factors. Firstly, some *M.tuberculosis* strains are naturally or intrinsically resistant to these agents as a result of chemical and physical modifications of their cell wall [66]. Secondly, *M.tuberculosis* subpopulations can display an epigenetic phenomenon called persistence, which is caused by non-inheritable changes that alter gene expression with no alterations in the DNA code [67]. This is most likely a result of the re-arrangement of the cellular responses by epigenetic modulators via DNA methylation mechanisms and modification of histones [68]. This leads to a diminished metabolism and growth for protracted periods of time [69]. Finally, most cases of drug resistance are a result of acquired resistance. It occurs when exposure to the discussed antibiotic agents selects for a subpopulation of mycobacteria harbouring advantageous mutations, that eventually thrive in the presence of the drug [70]. This form of resistance is unique in that it occurs at highly predictable rates for the first line anti-TB drugs. For instance David *et al* reported that for isoniazid, rifampin, ethambutol, 190, 3 and 843 cells per 300 million a generation develop mutations upon drug exposure respectively [71]. When resistance arises during patient treatment, some clinicians respond addition of streptomycin to the regimen. However, this drug has been shown to further accelerate the development of clinical resistance [72].

There are several variations of clinical resistance in tuberculosis disease. Multidrug resistant TB (MDR-TB) is when the *M.tuberculosis* strain is resistant to isoniazid and rifampin [70]. Acquisition of an MDR-TB strain by a patient leads to failure of the first line treatment drugs. Another form of TB resistance in Extensively Drug Resistant TB (XDR-TB) which is basically MDR with added resistance to any of the fluoroquinolones and one of the injectable drugs such as amikacin, capreomycin and kanamycin [73]. Cases of MDR- and XDR-TB were reported in 2006 in the province of KwaZulu-Natal, South Africa [74]. Emergence of these strains coincided with alarming rates of mortality in the same study. In such instances, clinicians are forced to switch to second line TB Drugs (Groups 2 to 4), which are shown in table 1.

Group 1 First Line	Group 2 Injectable	Group 3 Fluoroquinolone	Group 4 Bacteriostatic	Group 5 Third Line Drugs
Isoniazid	Streptomycin	Ciprofloxacin	Paraminosalicyclic acid	Clofazimine
Rifampin	Kanamycin	Levofloxacin	Cycloserine	Amoxicillin/Clavulanate[$]
Pyrazinamide	Amikacin	Moxifloxacin	Terizidone	Imipenem/Cilastatin[$]
Ethambutol	Capreomycin[*]	Ofloxacin	Ethionamide	Clarithromycin
	Viomycin[*]	Gatifloxacin	Prothionamide	
			Thioacetazone	
			Linezolid	

Table 1: Second and Third Line Drugs used in TB treatment. The table above shows the various drugs used to treat of infections by *M.tuberculosis*. Group 1 drugs are first line or initial treatment agents. Group 2 to 4 make up the second line drugs. These drugs replace the first line drugs when they fail to treat the infection. Group 3 drugs are third line drugs. Prescription of these agents is normally as the last alternative because of the lack of sufficient clinical information.

[*]Injectable peptide, [$]drugs used in optimised combination ,information from [44].

The term second line drug is allotted to a drug due to either the limited availability of clinical data, unfavourable pharmacokinetic profile or increased incidence of severe side reactions [75]. In most cases, treatment of MDR and XDR TB strains with these drugs has yielded suboptimal outcomes associated with elevated toxicity levels [76]. Kuban *et al* studied the effectiveness of 12 months treatment course that included gatifloxacin, clofazimine, prothionamide, ethambutol, and pyrazinamide throughout supplemented with isoniazid and kanamycin during the first 4 intensive months. Although a cure rate of 89% was observed, almost half of the patients developed hearing impairment[77]. Drugs in Group 5, loosely referred to as third line drugs treat the most lethal form of the disease, Totally Drug Resistant (TDR) TB. This acronym describes strains of MDR which are resistant to all known second line drugs [78]. TDR-TB was first detected in Italy in the year 2007 [79]. In such cases treatment is administered for a minimum of 18 months but very little data exists on treatment efficacy thus this option is only used as a last resort [75]. Cases of TDR-TB were recently reported in South Africa in 2013 and it is clear that

the national TB management infrastructure needs to be revamped to prepare for the inevitable outbreak of these strains [80].

Another variation in resistance observed with *M.tuberculosis* is heteroresistance, defined as the condition in which a single patient is infected simultaneously by a drug resistant and drug susceptible strains of the pathogen [81]. Convention states that for a strain to be categorised as drug resistant, is should be above 1% of the total population as this is higher than resistant strains arising from spontaneous mutation. Mutations tend to be associated with a fitness cost to the pathogen, explaining why these confounding occurrences are missed by the extensively used culture methods [82]. This highlights the need for new methods for *M.tuberculosis* detection which can account for smaller populations, for example it has been reported that the earliest mutant in an isoniazid culture occurs at a rate of 1 in 10^8 cells per generation [83]. Early pathogen detection might lead to improved therapeutic outcomes and an in depth understanding of the pathogenesis of the disease within the host.

Amplification of heteroresistant DNA samples produces a wide range of amplicons ranging from the wild type to the mutant [84]. This was shown when an isoniazid heteroresistant sample run in 10 parallel reactions from the same PCR master mix produced highly variable products [84]. Even though it was difficult to determine which replicate would yield a particular ratio of the amplicons, the pronounced variation was reproducible. Stochastic variations during the early stages of the PCR when the DNA forming complex is being assembled have been suggested to cause the deviant behaviour [85]. This limitation can be addressed by using digital PCR to detect heteroresistance as shown by Phowlat using clinical isolates [86]. It is important to understand the clinical significance of heteroresistance, as this can potentially lead to more personalized therapies, which may be more effective in fighting the TB epidemic. Morand suggested that heteroresistance is a result of evolution, which allows a section of the microorganisms to acquire the mutation that allows survival before the entire population becomes resistant [87]. Thus, it serves as a precursor to full resistance within the host, suggesting interception might halt disease progression. Heteroresistance has also been implicated in increased resistance to other antibiotics, thus it might be an ancient drug evasion strategy [88].

First line therapy still has efficacy against susceptible TB strains, but emergence of MDR, XDR and TDR-TB highlights the need for new drugs. An interesting candidate drug is bedaquiline, currently used to treat MDR-TB as the final option [75]. In spite of encouraging results from earlier trials, it is still relegated to compassionate use as it has been reported to negatively interfere with neural activity of the heart [89]. Other drugs—including nitroimidazoles, fluoroquinolones and rifamycins—are currently being tested and repurposed to the improve efficacy of the combination therapy, seeding hope for better treatment outcomes in the near future.

1.3 TB Diagnosis approaches

Tuberculosis diagnosis is a vital cog in TB control programs as it encompasses the various methods used for case detection. It is very important in the algorithms used by national control programs as it allows early treatment of the TB disease, preventing transmission. Countries such as USA and the more affluent European nations have successfully controlled TB by availing abundant human resources, health care systems and the necessary funding to support diverse efforts to control this disease [90]. Unfortunately, most high incidence areas lack most if not all of these resources, casting a desperate state of affairs. Inadequate tools and appropriate laboratory services mean that a large portion of tuberculosis disease will be uncounted. A large proportion of patients will receive unnecessary treatement for tuberculosis based on their clinical presentation as it takes long for culture results to come back. Such a decision fuels poor resource utilization. There is also a group of patients who receive a delayed diagnosis due to a wide range of socioeconomic factors, increasing the chances of death and disease transmission [91].

Disease detection in TB largely occurs when patients with a continual cough for periods of a few weeks present themselves to health care facilities [92]. The initial approaches involve testing the patient with methods ranging from immunological tests such as tuberculin skin test, imaging techniques such as sputum smear microscopy (SSM), chest radiographic examinations, and bacteriological assays such as culture based testing to molecular diagnostic such as the Xpert/MTB device. These methods have several levels of impact and applicability in TB control. The vast range of existing methods is testament of the major advances t in TB diagnosis, over the last 3 decades.

The next section seeks to discuss these diagnosis methods and their unfortunate drawbacks. It proceeds to highlight the assays that are still in the testing phase and concludes by suggesting the issues the ultimate TB diagnosis will have to address to contribute to the eradication of this disease in the most meaningful way.

1.3.1 Tuberculosis detection

Tuberculosis is thought to have latently infected one third of the human population, with only 10% of these individuals developing active disease [93]. This has led to an increased level of attention towards the detection of latent TB, complicated by the fact that patients lack clinical symptoms of the disease. To circumvent this, assays to detect the immune response elicited by the body upon exposure are currently under evaluation. The main tests to be developed for this purpose include the tuberculin skin test (TST), interferon gamma release assays (IGRA), which use a purified protein derivative (PPD) and early secretory antigen target 6 (ESAT-6); and culture filtrate protein respectively [94]. Unfortunately TST also detects exposure to non-tuberculosis-mycobacterium (NTM) together with Bacillus Calmette–Guérin (BCG) vaccinations, whilst IGRAs offer superior specificity but are unable to differentiate between latent and active TB disease [95]. NTM are *Mycobacterium* species, which are

not part of the *M.tuberculosis* complex, and examples include *M.kansasii*, *M.avium*, *M.marinum* and *M.intracelulare* to name a few. This group is of mycobacteria is responsible for a number of diseases such as pulmonary tuberculosis in HIV positive individuals [96].

Active TB disease is primarily detected using SSM, with a very heavy usage in areas with high TB incidence as it is quite rapid and simple [91]. This has relegated the immune based approaches to a presumptive role. Unfortunately, SSM requires a very high bacillary load (10^3 to 10^5 bacteria/ml), trained personnel and lacks any quality assurance measures to validate findings [97]. Requiring multiple samples on separate days impart a heavy transport cost and potential loss of wages on the patient. This has led to a high number of patients missing the testing and subsequent treatment. The healthcare personnel performing SSM are limited to sixty seconds per slide due to the high demand of the test. The poor sensitivity for extra pulmonary, child and HIV positive TB cases serves to further hamper the test [98]. However, efforts are currently being evaluated to improve the performance of this test by use of light emitting diodes (LED) to perform fluorescence microscopy on sputum samples [99]. This improves the speed of test and the visual clarity of the bacilli to the extent that increases in sensitivity of 10% have been reported [100].

To help clinicians confirm TB disease, they perform chest examinations . Chest examinations are more applicable in cases of pulmonary TB, though a positive reading is not indicative of TB disease. It uses the appearance of lesions in the lungs especially in the lower lobe as indication of disease. It serves primarily as an indicator of disease, but it is not truly a TB diagnostic [91]. In a study detecting mediastinal lymphadenopathy (a TB hallmark in child TB), chest X-rays were found to detect TB cases in 67% of the cases [101]. Imaging methods possess a nontrivial value in TB diagnosis but standardized disease rating and quality assurance measures are critical to amplify its clinical impact [102]. The discussed approaches are indispensable for national TB control programs as they are the first line detection tools in high disease burden countries. Unfortunately, none of these is useful in measuring the drug susceptibility of the tuberculosis detected.

1.3.2 Drug susceptibility testing (DST)

DST can be loosely classified as the monitoring of growth related metabolic activity of the *Mycobacterium tuberculosis* in the presence of drug or detection of mutations within the genome of the pathogen that are associated with drug resistance [103]. The former uses culture-based methods whilst the latter relies on molecular assays. To ensure accurate execution, several parameters are routinely in application to measure their clinical performance. Two parameters that are constantly mentioned in the literature, are the sensitivity and the specificity estimates of the diagnostic tool [104]. Sensitivity is defined as the probability of the tool correctly identifying a person with the tuberculosis disease [105]. This implies that a test with poor sensitivity yields a large percentage of false positive results. Thus the sensitivity of any tool is used to determine if a patient has tuberculosis disease [106].

Specificity is the probability of the diagnostic tool correctly detecting an individual who does not harbour tuberculosis disease [107]. A test with poor specificity produces an increased proportion of false positive results. Specificity is thus used to rule out the possibility of the disease for the patient [106]. It is imperative for any diagnostic tool to have sensitivity and specificity estimates closer to 100%, but this is seldom the case. In spite of their usefulness, cautious interpretations of their meaning is a prerequisite. The levels of disease incidence in the population were pilot trials are done should be similar to that in the population were diagnostic tool is ultimately applied to improve reliability of the result [108].

Culture methods offer the capability of detecting actively metabolising *M.tuberculosis* at an increased sensitivity in comparison to SSM, coupled to the assessment of the bacterial viability in the presence of drugs [91]. It can be performed on various platforms such as solid media, examples including Lowstein-Jensen(LJ) media, utilized to do the proportion and resistance tests within periods of up to 4 to 8 weeks [109]. Such a wait period is too long for the diagnosis of this infectious disease, leading to the development of liquid culture systems. Prominent examples of the liquid cultures include BACTEC 960 TB and the mycobacteria growth indicator tubes (MGIT). The BACTEC system detects radioactive carbon dioxide released from the metabolic activity of the *M.tuberculosis* on the palmitic acid substrate combined with NAP (β-Nitro Alpha acetyl amine β-hydroxyl propiophenone). NAP distinguishes *M.tuberculosis* from NTM. This test takes 5 to 10 days to yield DST results from patient samples [110]. MGIT detects the growth of TB cultured in specific and differential media by using fluorochromes whilst performing DST within 7 to 12 days [111]. These two tests have improved the testing of TB immensely but are prone to contamination, require well-maintained facilities, regular servicing and trained personnel. These requirements limit their applicability to highly centralized laboratories. A variant of liquid cultures is the microscopic-observation drug susceptibility (MODS) for TB [112]. Using an inverted microscope, characteristic TB growth patterns (cords and tangles) can be easily observed facilitating simultaneous detection of TB and drug sensitivity directly from sputum samples [112]. In a study by Moore *et al* MODS was compared to liquid culture and LJ culture systems, sensitivities of 97.8, 89 and 84% were obtained in 7, 22 and 68 days respectively [112]. Other culture-based tests are either in their infancy or under evaluation such that their impact is still to be established.

Significant improvement in TB detection is observed when nucleic acid amplification (NAA) based molecular techniques are used in case finding. These are typically hinged on the polymerase chain reaction (PCR) [113]. Examples of such techniques include the Amplified Mycobacterium tuberculosis direct (AMTD) test from Gene Probe and Amplicor from Roche diagnostics [114]. These tests detect the 16S derived nucleotides amplified from highly specific primers by making use of DNA probes [115] and a colorimetric assay [116] respectively. These tests perform optimally with smear positive samples, but specificity and sensitivity diminishes when applied to smear negative samples. Another example of

the NAA is the Loop Mediated Isothermal Amplification (LAMP) test, a cheap method which does not require the often expensive thermo-cycling and detection devices associated with amplification assays [117]. It has been successfully used to detect TB using specific amplicons such as the 16S rNA and *hspX* [118], successfully distinguishing *M.tuberculosis* from several species of NTM. Unfortunately, in spite of high sensitivity and specificity levels observed when testing sputum positive culture positive samples, the test has a diminished sensitivity of 48.8% for smear negative culture positive cases[119]. All the discussed molecular tools only ascertain the presence strains in the *Mycobacterium tuberculosis* complex, but the rise of MDR and XDR-TB cases worldwide has shifted the emphasis towards rapidly obtaining a drug susceptibility profile for the detected pathogen.

Currently, culture based systems are the gold standard for DST but impressive inroads made by molecular DSTs will likely lead to its widespread use and ultimately replacement of culture methods. An example of a molecular DST is the line probe assays MTBDR*plus*assay [120]. It is a DNA strip based test which combines PCR with reverse hybridization techniques to detect mutations associated with rifampin (*rpoB*) and isoniazid (*katG ,inhA*) resistance [121]. This assay has a modest turnaround of up to 48 hours from sample processing [120]. In a study by Huyen *et al*, the sensitivity of this test was found to be 93.1% rifampin and 92.6% isoniazid with 100% specificity testing cultured isolated[122]. However, this assay still shows a very low sensitivity when used to assess clinical samples[123]. This test needs to expand the range of mutations detected to encompass other drugs and thus still requires confirmation of results as samples showing wild type profiles have been reported to harbour resistance phenotypes. Such instances can be as a result of epigenetic factors modulating drug susceptibility but mechanism are yet to be fully elucidated [124]. It is also confounded by presence of NTM in the sample[125].

To date, the most revolutionary molecular DST tool has been the Gene Xpert system performing the Xpert MTB/RIF assay created by Cepheid [126]. It allows the processing of the patient sample combined with a hemi nested PCR analysis in a largely hands free TB assay and rifampicin resistance detection simultaneously [127]. It relies on a PCR assay that is based on molecular beacon technology, designed to be complementary to the wild type *rpoB* sequence[128]. Molecular beacons are hair pin shaped oligonucleotides (22-44bp) that are designed to bind to a specific amplified sequence by utilizing two fluorescent dyes that use fluorescence resonance energy transfer (FRET) [113] to produce a signal. FRET occurs when the two dyes overlap which is the case when they are spatially close together. When the beacon binds to its target sequence, the reporter and quencher dye are separated as the loop unravels which leads to fluorescence being detected[129]. Mutations in the *rpoB* region have also been reported in most instances to be strongly suggestive of MDR-TB [130]. The integration of sample processing, pathogen detection plus an electronic TB register (patient results automatically updated onto a cloud) within a self-containing module has made this tool a practical alternative with minimal risk to personnel [130]. The time from sample loading to answer can be as short as 1 hour 45 minutes [130]. The

study by Rath *et al* projected that this assay will likely increase case detection by 37% but also increase the cost to the health care systems by about 55% [131]. The assay has been reported to perform optimally with smear positive TB cases with 100% sensitivity, which diminishes when applied to smear negative samples to 68.6% sensitivity in an study which evaluated samples from 429 patients [127]. The same was observed in a study comparing the performance of this device with MODS for smear negative samples from HIV positive patients [132]. The MODS showed a higher sensitivity of 73% compared to the 67% of the Gene Xpert device. Interpretation of these findings is tempered with the realisation that the variability of these readings could very well been a function of the setting and context of this particular study. Irrespective of the impact this tool has made, many limitations are diminishing its impact. It can only be used in areas with a regular electricity supply [133], requires constant availing of single use cartridges with a limited shelf life, needs specific humidity and temperature settings for optimal performance, is operated by trained personnel, requires annual servicing and calibration[134]. It has a limit of detection of 131 cfu/ ml [135] ,cfu being colony forming units. The Xpert device can only detect the presence of a mutant of TB if it has an abundance above 65% in a mixed sample with the susceptible strain[130]. This implies that this device will struggle to detect heteroresistance.

At this moment, it still has intermediate sensitivity, greater than smear test but lower than culture, meaning that it cannot be used to rule out the disease due to false negatives [136]. Unless the science behind this assay is reinvented, ambiguity will always be a confounding factor as rapid amplification of specific loci is an imperfect proxy for slow but effective growing of *M.tuberculosis* [137]. A significant fraction of patients that receive this test still require access to culture facilities, especially for sputum negative samples [138].

1.3.3 Tests currently in the testing phase

Several TB tests are currently in the diagnostic pipeline, example being the breathalyser TB screen, developed by Rapid Biosensor systems [139]. It comprises an easily portable device, which fits a disposable sample collection vessel. Followed by pneumatic transfer of the sample to a reaction centre primed with antibodies for the *M.tuberculosis* specific Ag85B antigen. These antibodies fluoresce upon binding to the target within 10 minutes. McNerney reported that 93% of TB culture confirmed cases accurately detected, but the assay was alarmingly susceptible false positive readings. Another variant of the TB breathalyser tests was reported by Jassal *et a l*[140]. This test detected the degradation of radioactive urea via the urease enzyme within 15 minutes. This technology has decent potential but further evaluation is critical for assimilation into TB control programs.

A more promising point of care tuberculosis immunoassay is the lipoarabinomannan (LAM) detection in urine samples [141]. LAM is a critical component of the mycobacterial cell wall, which can be detected using enzyme linked immunosorbent assays (ELISA). It is favourable sample as acquisition

noninvasively, possessing a reduced risk as opposed to sputum or blood samples. LAM is heat stable and therefore can be detected even after boiling the sample, making it a semi-quantitative TB assay with a 30 minutes turnaround [142]. In spite of a low sensitivity of 56%, this assay was reported to outperform smear microscopy in the case of HIV positive patients, suggesting its use as an additional initial test in the TB diagnosis algorithm [143]. This test has a lot of potential because it is not affected by previous BCG vaccination and the diagnosis is thought to be independent of the anatomical location of the disease [144]. High rates of variability when applied in the field and the inherent low sensitivity are hindering further development of this test, but improvements are on-going [145]. Another promising assay is the TB Patch test, based on the detection of the *M.tuberculosis* complex specific mpb 64 antigen. The assay showed 100% specificity to TB with a sensitivity of 98.1% [146] but it takes 4 days to complete. However, it is very simple, unaffected by prior BCG vaccination such that if incorporated with a plethora of other antigens such ESAT6, HspX etc, it could be the basis of highly useful test in resource constrained areas [147]. In a very different application, a TB patch was used to detect patient sensitivity to second line TB, suggesting that understanding and correctly adapting this technique can potentially lead to a much needed revamp of the TB control efforts [148].

A variant of the phenotypic TB drug susceptibility is the bacteriophage-based assay. When viral particles infect *M.tuberculosis*, they replicate within the host eventually releasing the progeny post the virucide treatment. The release of the progeny is detected as either a plaque on a lawn of fast growing bacteria or by use of specially modified luciferase reporter phages [149]. A positive result suggests drug tolerance whilst a negative result shows drug susceptibility of TB. An example of a commercial version of this assay is the FAST*Plaque-MDRi* [150]. A novel device which detected the presence of the phage using a piezoelectric sensor was reported to have sensitivity and specificity of 91% and 93% respectively [151] in 24 hours. An improvement on the specificity on the phages can make this assay more lucrative.

1.3.4 High Resolution Melting Analysis: a potential TB diagnostic

High Resolution Melting Analysis (HRMA) is a post PCR method used to probe amplicons for sequence deviations such as single nucleotide polymorphisms (SNPs), mutations and DNA methylations [152]. HRMA allows discrimination of PCR amplicons based on their size, GC content and complementarities [153]. The method was introduced in 2002 by Carl Witter and Karl Voelkerding supported by Idaho technologies, whilst conducting research at the University of Utah [154]. It exploits the fundamental ability of DNA to denature when exposed to an ascending temperature gradient (0.008-0.2°C increments), melting at a specific temperature (Tm) reproducibly [155]. The Tm is the state in which half of the total DNA is single stranded whilst the other half remains double stranded. Short amplicons (<300bp) are better suited for analysis as they tend to melt with defined singular peak as opposed to the multiple peaks observed with longer amplicons [156], thus they are normally selected for analysis. This was highlighted when a 544bp product from the human HTR2A gene

coding for production of the neurotransmitter serotonin was subjected to HRMA [154]. The resulting profile showed two melt domains or peaks, making it difficult to identify the peak due to the single nucleotide polymorphisms. The fluorescence is measured by using DNA intercalating dyes such as LC Green, SYBR and Eva Green [157]. The fluorescence readings at each temperature increment are passed through data processing steps such normalization and temperature shifting to produce melt curves and difference plots, from which the variations are easily observed [158]. Several instruments currently perform HRMA including Rotor-Gene 6000, Light Cycler 480, Light Scanner and the Master Cycler.

The application of HRMA in tuberculosis studies has been mainly for detection of mutations linked to drug resistance inadvertently to the first line drugs. It is accurate, cheap and simple to perform thus is very appealing for diagnosis[159]. It is useful in identification and drug susceptibility testing in a number of studies [159-164]. Rifampin resistance has been suggested as a high probability marker for MDR TB, thus HRMA could be a feasible alternative for drug resistance surveillance systems [165]. In the same study, HRMA showed a very high positive likelihood ratio (PLR) and a low negative likelihood ratio (NLR), suggesting that the test can be trusted in ruling in or out cases of rifampin resistance. The test takes about 4 hours to complete, whereas culture based methods can take between 4 to 8 weeks to identify and detect *M.tuberculosis*[166]. By switching the primer sets and reaction conditions, HRMA can easily be expanded to test for isoniazid, fluoroquinolone and streptomycin resistance, which is not possible with the current Xpert MTB device [167].

Year	Ref method	Dye	Genes studied	Sensitivity%	Specificity%	Instrument	Samples(n)	Ref
2008	Proportion method	Syto 9	rpoB	rpoB(98)	rpoB(100)	Rotor-Gene 6000	287	166
2009	BACTEC MGIT 960	Resolight	rpoB	95.9	100	LightCycler480	68	164
2010	Culture	Evagreen	rpoB, katG/ inhA	rpoB (98.6) katG/inhA (84.1)	rpoB (100) katG/inhA (100)	Rotor-Gene 6000	217	159
2011	Concentration method	LC Green Plus	rpoB katG/mab-inhA gyrA	rpoB (94.4) katG/ mab-inhA(95.7) gyrA (100)	rpoB(97.8) katG /mab-inhA(100) gyrA(98.6)	Rotor-Gene 6000	115	160
2012	Proportion method	Resolight	rpoB katG rpsL	rpoB(93.1) katG(80) rpsL(61.8)	rpoB(93.1) katG(93.3) rpsL(100)	LightCycler480	97	168
2013	Proportion method	HRMA dye	rpoB katG/mab-inhA embB rpsL/ rrs	rpoB(100) katG/Mab-inhA(88.8) embB(100) rpsL/ rrs(100)	rpoB(100) katG/Mab-inhA(100) embB(100) rpsL/ rrs(93.7)	LightCycler480	68	162
2014	Proportion Method	Eva Green	rpoB katG	rpoB(95) katG(85.7)	rpoB(100) katG(100)	Rotor-Gene 6000	95	161

Table 2: Description of key studies analysed for the review of HRMA as a TB diagnostic.

Table 2 above shows a brief analysis of studies on HRMA DST in tuberculosis from 2008 to 2014. HRMA has been successful in detecting resistance in a wide range of loci with very high analytical performance, shown by the various sensitivity and specificity estimates. A wide range of dyes, instruments and resistance reference methods have been used in the studies.

Despite the advantages offered by HRMA, there are still a couple of challenges, which require addressing before this technique integrates into the clinical setting. There is need to improve the yield, purity and quantity of DNA obtained from the crude extraction methods used for clinical samples as

this greatly affects the assay[165]. For HRMA to be assimilated as diagnostic assay for *M.tuberculosis*, there is a need for establishing a *modus operandi* (which serves to standardize the instrumentation, reagents, DNA samples etc.) making it applicable at a global scale. During this assay, the intercalating dye binds to any dsDNA including chimera/ nonspecific PCR products leading to an overestimation of the PCR product[169]. This challenge can be addressed by use of hydrolysis probes such as (molecular beacons, taqman probes, scorpion probes etc.) which are designed to hybridize with a specific PCR product[113]. Incorporation of these probes unfortunately complicates the product detection, whilst increasing the cost of the assay. HRMA suffers from the same fate that all molecular diagnostics do, which is the inability to detect mutations outside the classified resistance determining regions.

1.3.5 The Ultimate TB test

The best TB test is one with very high sensitivity and specificity, with the ability to assay for drug resistance during the patient-health care worker contact events [170]. It should be easy to implement at any level of the health care system with equal performance in children and HIV positive sputum negative individuals [92]. This will effectively mean not requiring a steady supply of electricity, refrigeration or water without the need for trained personnel. The cost should be low enough for the test to be affordable by the underprivileged but the device should be able to detect the disease in the earlier stages. From these requirements, it is evident that the likelihood of finding such an assay is very low. The new diagnostic needs to have a minimum of 85% sensitivity and 97% specificity for it to make any meaningful impact as measured by the adjusted lives saved [92].The ultimate TB diagnostic should be able to rapidly identify TB, test for drug susceptibility and determine the particular genotype of the strain for epidemiological studies.

The success of any TB diagnostic is beyond the technology, but more a function of applicability and accessibility but this requires well designed studies with a proper appreciation of the ground conditions affecting patients and the entire health care system. Intensive operations and health delivery research is required to understand how best to implement the new diagnostic [91]. Instead of focussing on low prices for new tests, perhaps emphasis on subsidising the operational costs of existing tools, especially for high disease burden countries is a necessity.

Before development of the ultimate diagnostic, exhaustive efforts are required to maximize the potential of current methods by tailoring each solution for particular TB hotspots. For advantageous patient outcomes to be realised, a synergistic approach in discovery of the diagnosis tools, drugs and the health care delivery systems is of the essence. This should ideally be coupled with the eradication of socioeconomic triggers of TB disease which encourage the vicious disease and poverty continuum [171]. Addressing these issues is as important as the discovery of the ultimate TB test [172], leading to a

comprehensive solution. From this passage, it is clear that TB diagnosis solutions will need to take advantage of latest technological advancements in a manner designed for the resource limited settings.

1.4 Microfluidics and applications in Tuberculosis disease

From the preceding section, it is clear that rapid, accurate technology and cost effective technologies are key in tailoring diagnostic tests for resource constrained high TB burden countries. Microfluidics offers a realistic alternative to solve most if not all of the functional and operational impediments on the current methods. Microfluidics use of minute volumes, in highly integrated systems with improved sensitivity from their bulk equivalents [173]. The aim of the following passage is to provide a succinct exposé to the microfluidic platforms and highlight their potential impact in discovery science and applied research with respect to tuberculosis diagnosis. Preference is given to PCR-based techniques as NAA are currently the most rapid tests in TB diagnosis.

1.4.1The Microfluidics platform

Microfluidics is defined as the science involved in the formulation and production of devices that are capable of manipulating minute quantities of samples or reagents (mostly in the order of nano litres) in a highly integrated manner [174]. Microfluidics allows sample preparation and detection steps to be easily combined in extensively automated devices with high sensitivity, shorter reaction times and smaller device footprints in comparison [175]. Whitesides speculated that the advent microfluidic technology was a result of critical developments and requirements in four seemingly unrelated areas [176] . Development of molecular analytical tools such high-pressure liquid chromatography; combined sample separation and high-resolution detection were critical catalysts. Advancement in micro analytical methods especially during the rapid development of the genomics field about two decades ago hastened the need for devices capable of performing a high number of parallel reactions with high precision and accuracy. The third proponent of microfluidic technology was the need for devices that could detect small quantities of substances implicated in biological and chemical attacks post the cold war. The final driver of microfluidics came from methodologies successful in microelectronics, as they proved to be easily transferable to microfluidics in creating biological circuitry. The combinatorial effect of the rapid developments in these fields formed the bedrock of microfluidic technology.

The miniaturized experimental platform afforded by microfluidics allows for conservation of the biological sample and often costly reagents [177]. Small volumes then translate into diminished thermal masses, increasing the heating and cooling rates of the reaction mixtures, a critical requirement for PCR [178]. The mixing dynamics improved at this scale. Hansen *et al* showed that microfluidic systems could be used to significantly improve protein crystallization using free interfacial energy by deciphering more conditions necessary for optimal reaction kinetics [179]. The ability to perform identical reactions many fold helps to improve the statistical significance of the measurements. The

closed system minimises sample contamination and leakage, making it appropriate for application in clinical settings.

Microfluidic technology has immensely benefited from advances in fabrication methods and materials used to create these devices, but it is yet to be fully integrated into mainstream biology [180]. The major reason for developing this technology is to replace the existing methods by outperforming them, but in most cases, this has come at the cost of application specific devices, which are not readily usable by the average scientist. It is encouraging to note that recently, there has been an increase in collaborative efforts between engineers developing these tools and biologist with a finer appreciation of the end user necessities. This has led to the production of applicable and reliable devices based on solid scientific considerations [181]. Such efforts are poised to yield devices that are efficient at performing the desired task whilst being easy to produce at a large enough scale for integration into research and commercial settings [176]. These factors will likely propel the application of this technology into extensive use in TB diagnosis and research.

1.4.2 Materials used for device fabrication

Substrates used for the production of microfluidic devices have rapidly changed from the inception of this technology. Initial devices were produced from silicon , a direct consequence of using clean room fabrication techniques from the semiconductor chip industry [180]. Silicon has very high thermal and electrical conductivity, making it easy to integrate micro-sensors and heaters. However, silicon is opaque, preventing optical detection, is brittle and inhibitory to biological processes especially (PCR) [182]. The use of glass circumvented the opacity of silicon as it had been properly characterized [183]. The same with silicon, glass chip fabrication is too expensive to allow production of disposable units [182], a critical part for low cost diagnostics. This prompted development of alternative materials.

In light of the shortcomings of these entry-level substrates, elastomeric microfluidics are under development. Polydimethylsiloxane (PDMS), has emerged as promising material as its adoption has led to the unprecedented development of soft lithographic techniques [180]. PDMS is a highly transparent, permeable and flexible polymer, with reduced costs of production and superior biocompatibility with in comparison to silicon and glass [182]. The elasticity of the PDMS can be exploited to incorporate micro pumps, valves and mixers [184]. However, PDMS is incompatible with nonpolar solvents due to its hydrophobic nature ,which increases its permeability leading to loss of biological material [182]. This is a bio-hazardous challenge in clinical settings. Regehr *et al* have shown that uncured PDMS can leach into the reaction mixture, affecting the observations during cell culture experimentation [185]. It has been suggested that the hydrophobicity of PDMS leads to the adsorption of small non-polar molecules, limiting use of this material in non-aqueous chemistry based processes [186]. West *et al* used a hybrid of this polymeric material with silicon in order to exploit advantages offered by both materials, with moderate success in demonstrating the PCR reaction [187]. Due to several

application specific modifications made to PDMS based devices cited in the literature, large scale production for commercialization is going to be challenging [188].

The limitations of PDMS have compelled researchers to explore additional materials, including thermoplastics such as polystyrene, a cyclic olefin copolymer [180], polymethyl methacrylate [189] , and polycarbonate [190]. Use of these materials circumvents some of the drawbacks of PDMS including adsorption and evaporative loss, but production methods are still limited. Other materials that have been explored include paper, wax and cloth, preferred because they are low cost and easily destroyed typically by incineration, a necessity in low resource settings [180].

The consensus is that more research is required in developing materials that address the scalability and compatibility issues. The solution will likely be a combination of various materials directed towards specific applications as opposed to trying to adapt a single substrate to various biological and diagnostic assays. However, it should be noted that new substrates will likely lead to an overhaul in the current device designs and fabrication methods [180].

1.4.3 Temperature control and measurement systems

Microfluidic technology allows integration of several functionalities, which ideally allow the "sample in answer out" work flow [191]. Key to facilitating this integration is the ability to exert a high degree of control on the various reaction parameters. Of the several parameters, temperature and fluidic controls are critical for devices performing the PCR reaction. This section highlights these two parameters, condensing the major variations on the theme found in the literature.

Heating methods are critical in microfluidics as they are of importance in attaining desired temperature thresholds rapidly. The choice of method employed will depend mainly upon the temperature ramp rates required, which are critical in reducing the reaction time. Heating methods can be classified as either contact or non-contact methods[182]. Contact heating entails direct physical fastening of the microfluidic device to the element supplying the heat. This contact can be established by using a thin film element embedded in the microfluidic device [192] or a heating block [193], with the latter limited by increased power consumption, slower ramp rates due to the larger thermal mass. Heating blocks tend to exhibit a higher degree of temperature spatial variation, but this can be addressed by using an oxygen free copper wafer as reported by Erill *et al* [194]. There is a need to develop much improved contact heating methods which allow differential heating of specific locations on chip, but these can have a negative effect on the ubiquitous nature of chip design [195]. The microfluidic platform that will be discussed in the methodology sections utilizes the contact heating method.

In an advanced variation of contact heating, thin metal film heat supply elements can be used for temperature control [196]. These are characterized with higher thermal efficiency and consume less

power than heating blocks, whilst being easy to fabricate, pivotal for portable modules [197]. Daniel *et al* [198] showed that a microfluidic device with a platinum based thin film heater rapidly amplified a 260bp product [199]. However, these films are dogged by high costs and spatial variations that compromise accurate control of the thermal state of the system [200]. Inherent limitations of the contact methods have prompted experimenters to devise non-contact alternatives of heat supply.

Non-contact heating involves temperature cycling of the microfluidic device without physical contact with the heat-supplying unit, greatly diminishing the thermal mass of the process setup. Such a configuration is advantageous in terms of integration with down- and upstream processes in the reaction [201]. Some of the earlier work on these types of heaters involved differentially heated streams of air, with very high ramp rates [202]. Other non-contact methods rely mainly on the absorption of electromagnetic radiation (EMR) by the device, mainly optical radiation (infra-red) and microwave radiation [203]. Infra-Red heating uses a tungsten lamp that has been shown to produce detectable quantities of a 800bp product in 240s [204]. In spite of this, lamp based heating yields non-focussed light, which reduces the efficiency of the overall process. To circumvent this issue, researchers have developed laser based heating methods, with ultra-fast ramp rates [205], but require precise positioning of the reactor and the light source. Microwave heating has proved to be very useful in PCR reactions, with an almost instantaneous temperature response ,whilst being easy to focus on reaction mixture [201]. Another variant of the non-contact heaters is induction heating, which involves placing the microfluidic device in close proximity to a heated element monitored and regulated by a programmed temperature control loop [201]. This method has been shown to require less complicated fabrication techniques and achieve fast temperature transition rates [206].

Temperature measurement is as important as temperature control in PCR, serving as feedback for the control system. Following on the previous theme, temperature measurement systems divide into contact and non-contact methods. Contact based measuring devices include thin film sensors, thermocouples and electrical resistance heaters [201]. The larger the temperature-measuring device, the more there is an undesirable increase of the thermal mass of the system. This is true for the thermocouples and the resistance heaters. These methods measure the temperature at a discrete location on the chip, compromising the accuracy of the measurement, as they cannot infer on chip spatial variation of the temperature. In spite of these drawbacks, these methods are popular as they are easy to install and use. The thin film sensors are an attempt to circumvent some of these limitations. They have been increasingly applied as developments in thin film deposition techniques are occurring [207]. Non-contact sensors of temperature offer the ability of measuring the temperature with no physical interference with the sample, obtaining a more realistic depiction of the thermal state of the system rapidly. An example of such a sensor is infra-red (IR) thermometry, which uses the emission thermograph to determine the temperature after appropriate calibration [182]. In spite of these advantages, environmental factors such as the background noise, chip emission characteristics

diminish performance of the IR sensor. IR only measures surface temperature readings. Some researchers have proposed the use of thermo-chromic liquid Crystals (TLC) to measure temperature [208]. These molecules have liquid-like mechanical properties whilst retaining the optical behaviour typifying solid substances and they readily respond to variation in temperature. They are still to be properly converted to the actual functioning forms as studies on them are still on-going [209].

1.4.4 Fluid transport

This section provides a brief overview of the fluidic handling capabilities of the microfluidic platform. It is in no way exhaustive but rather a small window into the colossal arena of fluid flow within the microfluidic devices.

One of the pioneering fluid transport mechanisms is the lateral flow. Based on capillary action, this form of fluid migration is dependent on the absorptive properties of the substrate[210]. In such tests, the operation is typically simplistic, with a sample loading area and result detection window. To date, this method has been demonstrated to perform best with immuno-based assays which can detect the presence of specific antigens from several samples by combining several loading, reaction, and detection steps in a simple flow-through process which typically takes a couple of minutes [211]. In spite of being easy to implement, the simplicity of the platform means it is very difficult to have high precision liquid control, limiting the amount of different operations that can be performed on such platforms [212]. Another form of fluidic movement is linear actuation, in which the liquid is moved via mechanical displacement [213]. Devices using this type of system have loosely connected cavities or channels, for single use reactions. They are easy to calibrate using internal controls. As with the lateral flow systems, complex assays are difficult because of imprecise control. Another variation of fluidic transport involves the use of pressure driven laminar flow of the fluid streams[214].This is achieved by establishing differential hydrodynamic gradients with the flow routes [210], which facilitates the implementation syringes, pumps, micro pumps etc. This methodology allows predictable velocities to be established in the channels with biphasic flow streams[215], with very accurate focussing of micro particles. The requirement for pressure sources complicates the portability of devices using this form of fluid actuation, together with the taylor dispersion of fluid streams potentially altering the concentration of the reagents in longer sample routes[216]. Other fluid transport methods include segmented flow[217], centrifugal flow[218] and electro kinetics [219], each with their own strengths and limitations. This review will not discuss these in detail, as application in microfluidics research is still limited.

Perhaps the most revolutionary fluid flow technique has been the microfluidic large scale integration (MLSI) system, which was first reported in 1993[220]. A layer of fluid flow with another layer pneumatically controlling the fluid called the control layer guides the fluid flow. The combination of several control layers leads to the ability to have several hundred micro pumps and micro mixers on a

single chip [210]. This method requires simple soft lithographic fabrication to produce the masks and moulds used to produce the micro sized features on chip, with PDMS as the main substrate[221]. The impact this technology was displayed when the Quake group developed multilayer soft lithographic techniques that enabled the binding of several flow and control layers[222]. The company Fluidigm in the USA, has championed the fabrication of these densely packed chips with complicated plumbing. Devices boasting such architecture are useful in various operations including DNA isolation, protein crystallization and immunoassays [222-225]. In demonstration of the scale at which these devices operate, a 250pL sized microfluidic chip with 1000 individually addressed reactors with 3574 valves was reported [226]. Microfluidic chips have been shown to be cheap and sturdy, together with being easily programmable either by the design of the actual circuitry or externally by preferential addressing the individual valves [210]. The only drawback with this technology is that PDMS is not compatible with organic solvents and there is a need for a pressure source for the control and flow layers which complicates the design of POC systems[227]. However, with adequate funding and intellectual resources, these challenges are amenable.

1.4.5 Detection methods

Microfluidic technology strives to miniaturize all aspects of their macroscopic counterparts, but this is only true for some aspects as devices do not simply scale down that easily. Miniaturization provides improved analytical performance at lower reagent cost but this also means a reduction in the detectable analyte[228]. It is imperative for any sensing systems to balance sensitivity with the scalability. Several methods for detection have been developed which include electrochemical (EC), mechanical and optical detection methods[229]. Electrochemical sensing occurs when the progress of a reaction results in the release of an electric signal sensed using either an electrode or probe as shown in the work by Lee *et al*[230]. Unfortunately the reading is affected by variations such as temperature, pH and the ionic activity, limiting their applicability[229]. Micro-scale mechanical sensing systems, based on cantilever beam technology can be useful in diagnostic tests. The detection in such systems is done by either a static micro-sized module which alters its surface forces leading to a deviation of the cantilever beam[231] or a resonant module in which analyte attachment leads to a deviation in frequency at which the beam resonates[232]. Unfortunately, the detection limits of these devices are constrained by the mechanical losses associated with the beams. As consequence of the current limitations of both EC and mechanical sensing, optical sensing methods are still more prevalent in microfluidic technologies.

Optical detection is widely applicable in microfluidics as it allows the detection in a wide range of assays using absorbance, chemiluminescence and more so fluorescence. Light focusses on the chip using pinholes, and by combining this to photo multiplier tube (PMT) and closed circuit device (CCD) camera, low detection limits are realised. Absorbance by definition is the ratio between the incident and transmitted light through a material or solution[233].It has been widely applied in detecting

analytes in large quantities but rarely used at a microfluidic scale. This a direct consequence of miniaturization, which significantly reduces the optical path from the light source to the detector, compromising the measurement[234]. A microfluidic chip which could measure the amount of ammonia was reported by Du *et al*[235]. The chip facilitated the indophenol reaction, detecting the product using a liquid core wave-guide spectrometer, obeying Beer-Lamberts Law in the range 1-100µM of the Fe^{2+} calibrating solution. An integrated complementary metal oxide semiconductor (CMOS) imager bonded to a polystyrene microfluidic network was then used to measure the uric acid content in urine[234]. Currently there is no reported study, which used absorbance to detect PCR amplicons.

Chemiluminescence (CL) occurs when a chemical reaction produces a highly unstable product that decomposes and releases energy in the form of light as it assumes a more stable resting state [236]. The internal excitation of the analyte makes such reactions very attractive for use on the microfluidic platform as there is no need for a light source but is obviously limited to reagents which are able to emit light [234]. A PDMS microfluidic device was used to detect the antioxidant capacity of different solutions using the peroxyoxalate (PO) assay where CL was used to detect the product in which the reagents were loaded by injection [237]. Analytically, the assay performed very well and it showed potential for applications in the field. Unfortunately, a bulky inverted microscope was used for detection the product. A device which resembled the monolithic strata was reported to perform the PO assay using thin film photodiodes to facilitate the micro-scale CL[238]. The device had very good analytical performance and a low reaction time of 11 minutes. Delaney *et al* reported a variation of CL in which the reaction was triggered by the application of an electric pulse to the reaction in what is known as Electrochemiluminescence (ECL) [239]. This device was shown to be low cost (paper based), easy to manufacture (produced from an inkjet printer) and more importantly only required the camera from a standard cell phone for detection of NADH. ECL is yet to be shown to be capable of monitoring a PCR amplification process [201].

Fluorescence occurs when a substance releases light after absorbing electromagnetic radiation (EMR) [240].The emitted light is always of a lower energy (higher wavelength) in comparison to the absorbed radiation. It the most widely used sensing system in microfluidic devices. Several excitation sources can be used which include lasers, xenon and argon lamps [241,242]. Lasers tend to be easily miniaturized, producing EMR which is very coherent with low divergence, enabling them to easily focus on the chip and deliver high energy radiation [234]. Lamp based systems are significantly cheaper than lasers and also offer a wide range of excitation wavelengths. Lamp based light sources have been largely used in microscope based detection modules with excellent results. Developments in the laser technology have been extended to the lamps leading to high energy stable lamps with increased wavelength range from ultraviolet to infrared with very long shelf lives [242]. A microfluidic device simultaneously detecting multiple fluorochromes was reported which used a halogen lamp [243]. An alternative light source in fluorescence based systems is the light emitting diodes (LEDs), which

consume less power and are easy to integrate into micro-sensing systems [244]. Fluorescence detection takes a central role in systems that perform PCR assays as virtually all detection dyes such as saturating dyes, probes; molecular beacons etc. are detected using fluorescence imaging. LEDs have been combined to smaller PMTs in a portable PCR device [245]. In spite of its applicability, fluorescence detection is still limited by background signal especially when using components that auto fluoresce, coupled to their often prohibitive pricing [229].

The brief exposé on the fundamental elements of microfluidics from substrates to detection highlight some of the basic considerations when fabricating these devices. A lot more work is required to miniaturize all the components. For all the functional elements of the chip from fluid movement to product detection, a compromise is necessary to produce robust and applicable devices. An efficient and consistent fabrication method for easy implementation of this technology in the life sciences is the missing link. If it could take a similar route as electronic chips, that is to have separate unit modules which can be combined for a very specific outcome, that would surely be a game changer [210]. The following section discusses some of the publications that have reported the use of microfluidics in TB related research.

1.4.6 Application of microfluidics in TB research

The discussed advantages of microfluidics make it a very strong candidate in revolutionizing the way in which future diagnostics will operate. This is relevant because it allows diagnostics to be created that are more applicable to developing countries as opposed to the developed countries [246]. Devices that have been applied so far in TB related research have been to detect either whole *Mycobacterium*, nucleic acids from *M.tuberculosis* or to measure the immune response from patients with TB [247]. With no immunological reaction unique to TB disease reported, an immuno-diagnostic is still elusive. This section sheds light on some of the research applied in TB related work. Most of the devices to date have concentrated on the detection of *M.tuberculosis* whilst the exceptions extended the devices capabilities to detecting drug resistance.

Ke *et al* reported in 2004 a microfluidic chip amplifying and detecting amplicons from the *rpoB* region of *M.tuberculosis* [248]. The device was fabricated using silicon, using a high power halogen lamp as the heat source. However, the amplicons were detected using gel electrophoresis, which is not applicable at the POC level. This is because electrophoresis only reveals information only about the size and not the sequence of the amplicon. Rosenfield used the activity of the *M.tuberculosis* specific β-lactamase enzyme on a fluorogenic substrate to detect the presence of *M.tuberculosis* using droplet based microfluidics [249]. The study was a proof of concept using *E.coli* for optimisation with a moderate rapidity of 150 minutes. It was reported by Xie *et al* that fluorogenic substrates could be used to detect and distinguish *Mycobacterium tuberculosis* complex from other environmental bacteria within 10 minutes [250] , using a LED excitation source with a very portable imaging unit. Gold

nanoparticles were shown to be very efficient in detecting *M.tuberculosis* amplicons from the *1S 6110* loci on a paper based microfluidic chip [251].Optical detection was via a mobile phone camera with a reaction time of 1 hour. Unfortunately, amplification on a separate device with the product detection modules suggests the assay is not ready for deployment. The gold particles were further developed to detect mutations in the MTB genome linked to drug resistance in different study [252]. A microfluidic device was coupled to a nuclear magnetic resonance (NMR) biosensor for the detection of *M.tuberculosis* [253], on the principle that binding of the biomarker alters the spin of the water molecules. The reaction time was 30 minutes using various samples from blood, saliva, sputum etc. with a detection limit of 20 cfu/ml. The detection module costs about 200 USD, whilst a single microfluidic cartridge costs one USD, which is very attractive for the emerging markets.

A microfluidics platform for *M.tuberculosis* strain genotyping was reported [254].Such a device will prove to be indispensable in monitoring outbreaks to discover and understand transmission events, adding precious value to the clinician- patient contact sessions. The chip used variable number tandems repeat (VNTR), which identifies TB strains by the number of mycobacterial interspersed repetitive units. Unfortunately, the entire process requires a long turn around and complex machinery limiting use to central laboratories [255]. A microfludic device was used to confirm that exposure to bedaquilline causes *M.tuberculosis* to reorganise metabolism in the first 4 days [256]. Using time-lapse microscopy with GFP construct of the pathogen, the bacteria depressed consumption but increase production of ATP. Perhaps the most comprehensive application of microlfuidics in TB diagnosis was reported in the study by Phowlat using a taqman Array Card (TAC) [163]. The study documented an assay capable of detecting mutations known to confer TB drug resistance using hydrolysis probes, simultaneously detecting unknown mutations using (HRMA). TAC accurately interrogated 10 different genes linked with drug resistance. When applied to 230 clinical isolates, the assay had accuracies of 96.1% and 87% when compared with the Sanger and Culture based methods respectively. However, there was still need for a benchtop centrifuge to disperse samples amongst the 384 wells. In addition, performing bulk PCR means that the assay TAC struggle to detect heteroresistance. HRMA could not detect transversion mutations.

Several authors have demonstrated the successful incorporation of microfluidics into the POC, offering superior functionality in comparison to conventional methods. This section showed the different facets that make up microfluidics, together with their application in the fight against TB. The current challenges technology are solvable through a concerted multi-disciplinary towards this epidemic.

1.4.7 Reality of TB diagnosis situation

TB infects about 9 million people annually, whilst 2 million people die each year[257]. On average, an individual carrying the active and dispensable *M.tuberculosis* can infect around 15 individuals each

year if disease progression is not disrupted[258]. For the transmission of this highly infectious agent to be timely disrupted, the disease needs to be detected at a very early stage and appropriate treatment commenced as soon as the diagnosis is made[259]. The most accessible tool in high disease burden resource limited countries is sputum smear microscopy (SSM). SSM only detects *M.tuberculosis* in 50% of cases with diminished sensitivity for children and HIV-positive individuals [260].An increase in the case of drug resistant strains such as MDR, XDR and TDR-TB [78] at a global scale demands a higher level of information from the diagnosis, which is the drug susceptibility profile of *M.tuberculosis* strain. Thus, the replacement of SSM with a test applicable and accessible in any primary health care facility is of paramount importance.

1.4.8 Problem statement

The current health care systems in developing countries cannot cope with the burden of *M.tuberculosis* diagnosis resulting in over 3 million cases being missed annually throughout the world[261]. The emergence of drug resistance forms of *M.tuberculosis* has only served to worsen the situation as now secondary information on drug susceptibility is a must for each positive diagnosis[262].

1.4.9 Research rationale

There is a need to develop alternative diagnostic systems that to detect *M.tuberculosis* and its accompanying drug susceptibility profile at a primary health care level in a cost effective manner. This is achievable through the development of a reliable, reproducible and rapid assay by exploiting the strengths of microfluidics and HRMA.

Aim

To develop a microfluidic based diagnostic tool to detect mutations that are linked to drug resistant *Mycobacterium tuberculosis*.

Objectives

1. Develop and optimise a PCR based assay for detecting drug resistance using a conventional system

2. Perform assays with isolates of *M.tuberculosis* using the microfluidic platform

3. Evaluate performance of microfluidic platform using the laboratory strains of *M.tuberculosis* isolates in comparison with standard methods.

CHAPTER 2: METHODOLOGY

This chapter documents the various methods used during the course of the study. Some *M.tuberculosis* strains are supplied as heat-killed cells. These will undergo the DNA extraction protocol summarised in a subsequent section. The purpose of this step is obtaining a pure sample with a high yield. The DNA samples are directly applicable in the assay post evaluation of their purity and DNA concentration. The phenotypic drug susceptibility of the test strains for use as a benchmark for the findings, accompanies the strains. The next section is detailing the primers selected for the assay. Primers carefully designed ensure efficient amplification of the product. The subsequent sections show the PCR master mix constituents for use on the Light Cycler96. A brief description of the Sanger sequencing reactions follows. Sanger sequencing allows accurate detection of single nucleotide polymorphisms within the various genes. A segment on the succinct method used to design and produce the microfluidic device coupled to the reaction master mix and reaction profile conclude the chapter.

2.1 *M.tuberculosis* test strains

Two groups of *Mycobacterium tuberculosis* samples are available. The first group consists of H37Rv, R35, KZN 605 and R271, cultured at the Nelson R. Mandela School of Medicine (Durban, South Africa). These strains have known drug susceptibility phenotypes and genotypes as reported in a previous study [7]. The second group consists of DNA from clinical isolates Tkk-062, Tkk-050, Tkk-043 and Tkk-039 obtained from the KwaZulu-Natal Research Institute of Tuberculosis and HIV (K-RITH), (Durban, South Africa), after proper characterization of the phenotypic drug susceptibility patterns.

DNA extraction

The first group of MTB strains were supplied as heat killed samples and the DNA is extracted using the CTAB method as reported [263]. In summary, the sample is mixed with 450µl of GTE buffer and 50µl of 10mg/ml lysozyme (Sigma, Germany) with an overnight incubation at 37°C. 150µl of a 2:1 mixture of SDS (Sigma, Germany) and 10mg/ml proteinase K (Sigma, Germany) is added with 40-minute incubation at 55°C. This is followed by the addition of 200µl of 5M NaCl (Sigma, Germany) and 160µl of heated CTAB (Sigma, Germany) followed by a 65°C incubation for 10 minutes. 1ml of 24:1 chloroform/isoamyl alcohol was added to the samples, followed by centrifugation and removal of the top aqueous layer. This step was repeated and the extracts were recombined. 560µl of isopropanol (Capital Labs, South Africa) the extract with gentle mixing. A micro centrifugation step for 10 minutes followed. After discarding the supernatant, 70% ethanol was added to the pellet with mixing and another microcentrifugation step for 10 minutes. The supernatant was discarded and the

air-dried pellet was then suspended in TE Buffer. The final DNA concentration of the extracts was determined using the Nano Drop Lite (Isogen, Netherlands) and the results are shown in the appendix.

2.3 HRMA primer

To detect mutations for rifampin, isoniazid and olfoxacin resistance primers corresponding to the resistance determining regions *rpoB*, (*katG* and *mab-inhA*) and *gyrA* were used. For rifampin resistance, *rpoB* primers amplify the 81bp region between codons 507 to 533, for *katG* the primers amplify the 315 site whilst the *mab-inhA* amplify the -8 and -15 sites, forming the basis for isoniazid resistance. The *gyrA* encompasses several sites associated with ofloxacin resistance. The primer information is summarised in table 3, as adapted from [160].

2.4 Realtime PCR and HRMA

The PCR Master Mix was prepared by adding 25µl of 2X Xtreme™ Buffer (Novagen, Toyobo), 10µl of dNTPs (Novagen, Toyobo), 5µl of LC Green (Idaho Technology Inc, Salt Lake City, UT), 0.3µM of each primer, 1µl of KOD Xtreme™ Hot Start DNA polymerase (Novagen, Toyobo) and 5µl of template DNA containing 200ng of the DNA make a final volume of 50µl. PCR was performed using the Light Cycler96 (Roche Diagnostics, Switzerland). The initial denaturation temperature was 95°C for 300s, followed by 35 cycles of 95°C for 10s, 60°C for 10s, 72°C for 10s (fluorescence readout step). A non-template control (NTC) was included in all experiments, in which distilled water was used instead off the DNA template.

For the HRMA step, the following profile was used: 95°C for 60s, 40°C for 60s, 65°C for 1s then at a 0.07°C/s ramp rate, acquiring 15 readings every degree until 97°C. Difference plots were generated using H37Rv as the baseline signal and then normalizing the test readings (all the other samples) with respect to this standard.

2.5 DNA sequencing of *rpoB, katG,gyrA* and *mab-inhA*

The PCR amplicons generated from *rpoB, katG, mab-inhA* and *gyrA* genes were sequenced by Inqaba Biotech Industries (Pretoria, South Africa) using the same primer sets used to produce them. In summary, the Sanger sequencing method was used post a clean-up step using the ZR-96 DNA Sequencing Clean-up Kit™ (D4052). The products were sequenced in both the forward and reverse directions using the Big Dye® Terminator v3.1 Cycle sequencing kit from Applied Biosystems (California, USA). The cleaned products were injected on the ABI3500XL analysers and the data was analysed using software at Inqaba Biotech Industries (Pretoria, South Africa).

2.6 Microfluidic realtime PCR

2.61 Microfluidic device fabrication

A co-partner on this project, Mr Tawanda Mandizvo, carried out the process of device fabrication. The device was produced in line with the principles of Microfluidics Large Scale Integration (MLSI), previously discussed [226]. A succinct summary of the process is provided in the following paragraph. The initial step involved designing the control and flow layer of the 2 layer push up chip. This was followed by the production of the photomask and consequently the mould. The mould was used to replicate with high fealty the features on the design. The flow layer was a 5:1 mixture of PDMS and Part B (curing agent) and the control layer a 20:1 mixture of the same constituents. They were partially baked at 80°C separately for 30 minutes, carefully stacked with the control layer at the bottom (aligning with a stereomicroscope), and then bonded to a silicon wafer during an 8-10 hour final bake at 80°C.

The Master Mix used for the on chip experiments was modified from the one used in phase 1 in order to compensate for the losses that occur when the chip is being loaded, an approach adopted in a previous study by [264]. The PCR mixture was prepared using 30µl of 2X Xtreme™ Buffer (Novagen, Toyobo), 15µl of dNTPs (Novagen, Toyobo), 9µl of LC Green (Idaho Technology Inc, Salt Lake City, UT), 0.46µM of each primer (Life Technologies), 3µl of KOD Xtreme™ Hot Start DNA polymerase (Novagen, Toyobo), 0.08%(v/v) 1% Tween 20 and 3µl of template DNA with a total quantity ranging from containing 100ng to make a total volume of 75µl. For the 20 reactor chip, 8 reactors were used for H37Rv, 8 for the test strains (R35, Kzn 605) and the other two reactors contained the non-template controls. For the the final experiment, 6 reactors contained H37Rv, 6 contained Tkk-062, 2 contained non-template control reactions and the other 2 had an H37Rv reaction with *gyrA* primers as a positive control.

The thermal cycling was performed using a modified G-STORM GS1 (Somerten, UK) thermocyler, measuring the fluorescence in real-time using an Olympus MVX10 (New York, USA) macroscope. The thermal profile was 99°C for 8 minutes, followed by 35 cycles of 99°C for 65s, 60°C for 115s, 74.5°C for 130s, and 40°C for 90s, and 97°C for 120s.

For the HRMA step, the temperature increased from 75°C to 94°C at a ramp rate of 0.5°C/s with 0.25°C increments for each step. The real-time and HRMA steps on the chip were captured using the Light Forge software, which was developed in house by Dr Frederick Balagadde. The software is essentially temperature feedback system is capable of acquiring fluorescence readouts at easily programmable steps whilst displaying the reaction progress.

Gene	Sequence	Annealing temp (°C)	Nucleotide position$$	Product Size(bp)	Product %GC	Accession Number
rpoB F	CGCGATCAAGGAGTTCTTC	65	2339 to 2357	118	36	L27989.1
rpoB R	TGACAGACCGCCGGGCCC		2456 to 2439			
mab-inhA F	GTCACACCGACAAACGTCAC	64	100 to 119	190	57.9	U66801.1
mab-inhA R	CTCCGGTAACCAGGACTGAA		296 to 271			
katG F	GCGGTCACACTTTCGGTAA	64	2781 to 2799	233	68.7	X68081.1
katg R	GGTGTTCGTCCATACGACCT		2950 to 2931			
gyrA F	GGTGCTCTATGCAATGTTCG	63	2467 to 2486	169	65.2	L27512.1
gyrA R	GCTTCGGTGTACCTCATCG		2700 to 2682			

Table **3:** Information about the primer sets adapted from [160]**.** The table above shows the primer sets that were used for the PCR and Sanger sequencing. The primers annealing temperatures ranged between 63 to 65°C, amplicon size between 118 to 233bp and GC content between 36 to 68.7%. The nucleotide positions are numbered relative to the transcriptional start position of each of the genes. The accession numbers for the sequences on the National Centre for Biotechnology Information (NCBI) site are provided. It is interesting to note that the annealing temperature in table 3 is higher than the 60°C used in the actual reactions.

CHAPTER 3: RESULTS

3.1 HRMA with Light Cycler96

The following section documents the findings when the test strains were evaluated using the Light Cycler96 machine. A short description of the significance of each of the results is given.

For each gene, a histogram documenting the average cycle threshold numbers (Cq) observed for each strain is given. A Cq number is essentially the number of cycles required for the fluorescent signal from each well to cross a particular reaction threshold. The threshold is typically located in the early exponential phase of the amplification process. For accurate HRMA, the amplification has to occur efficiently and reproducibly. Thus, for reactions accumulating product at the same rate, the Cq value will more or less be the same [265]. A threshold number less than 29 shows efficient amplification. The Cq value is only valid if the non-template control does not cross the threshold during the course of the reaction. It should be noted that Cq values are only comparable within the same run [266].

A table showing the numerical measurements of the melting point temperature (Tm) for each gene follows. The findings in the table are normalized estimates melt curve data (not shown) transformed by generating a negative derivative to the give melt peaks. The melt peak data is fitted to the Savitzky-Golay [267] function automatically by the software to produce smoothened data. Emphasis is placed on the estimates of the standard deviation (stdev) and the standard error (sem) for each test strain. The standard deviation shows how variant are the observed Tm from the average Tm also shown in the table. It describes how spread the data is from the mean and an estimate many fold less than the mean whilst being closer to zero shows minimal variation in the Tm value. Another important parameter in the table is the standard error, which documents the reliability of the calculated average. For successful HRMA, these estimates will be more than 100 fold less than the calculated mean, whilst 68% of the observed Tm estimates should be within plus or minus one standard deviation [268]. The technical specifications of the Light Cycler96 state that the replicates of the Tm measurement vary with 0.4°C. Thus the melting temperature alone, cannot be relied upon if the difference between the standard and test strains Tm is less than or equal to 0.4°C.

A visual depiction of the replicated readings of the melting point temperatures follows the table. These are useful in clearly showing the deviation of the melting point temperatures of the test strains using H37Rv as the standard or susceptible strain. This graph is useful in distinguishing the variants from the reference strain. A test strain is called variant if its Tm values are not in the same horizontal region with H37Rv, whilst those located in different regions are classified as wild type or non-mutated strains.

The final graph used in the decision-making i.e determining whether a test strain is called variant or non-mutated is the difference plot, generated by subtracting the normalized fluorescence of the

reference strain from that of the test strain. The resultant figure depicts the different profiles showing the mutation controlled deviation of normalized melt curves. Some mutations tend to lead profiles above the standard or baseline, whilst other mutations are located below that of the reference. Mutations, which do not significantly alter the thermal denaturation profile such as class 3 and 4 single nucleotide polymorphisms, will likely be very similar if not identical to the reference.

Thus by individually and collectively analysing results from these plots and tables, a conclusion is reached on the drug susceptibility of each strain at the various loci. The accuracy of the assay is reported as percentage sensitivity, the probability of the assay detecting a strain with the mutation. The findings from this section are used as the basis for evaluating the light forge assay in the subsequent section.

3.1.1Rifampin resistance assay

rpoB

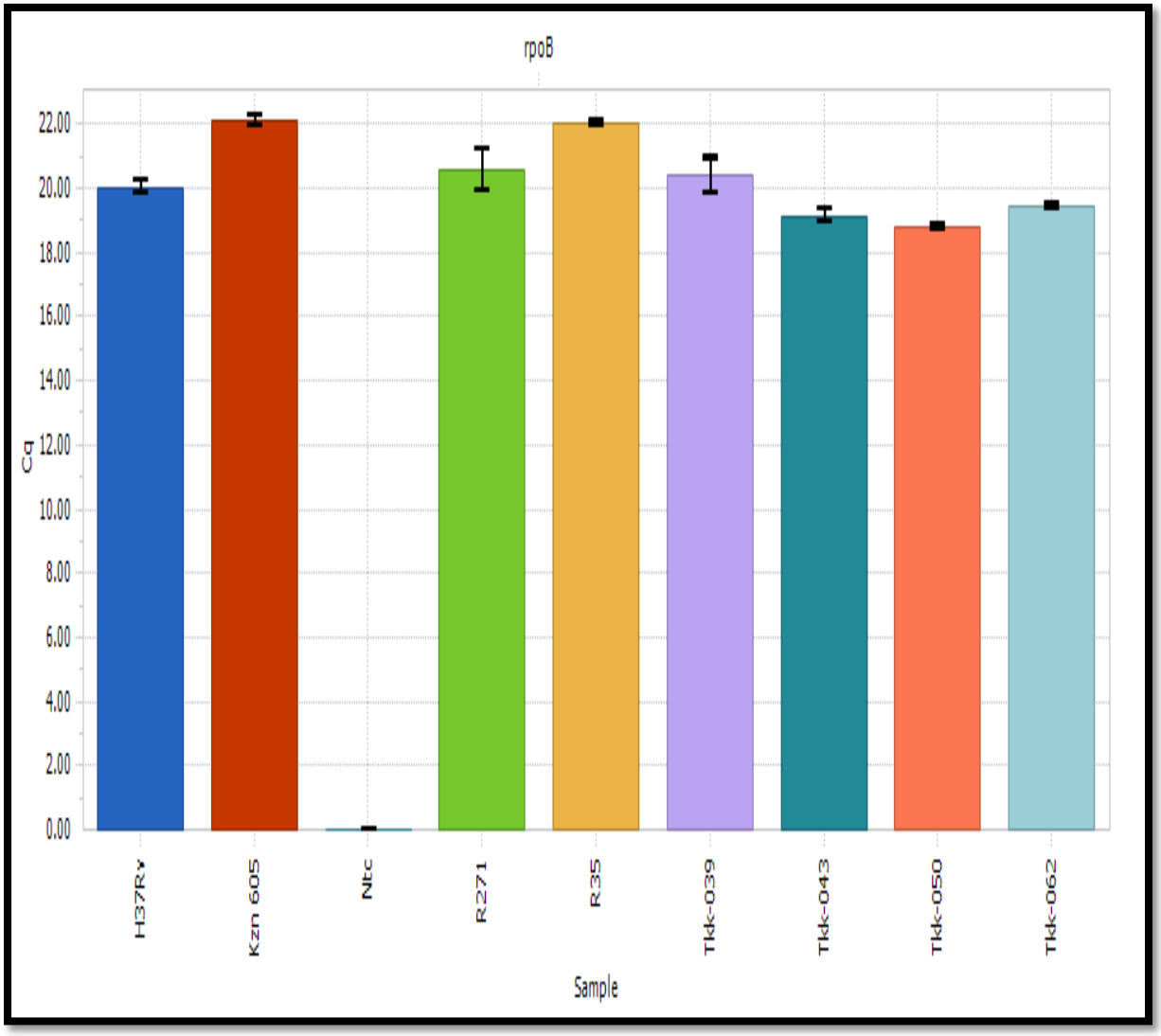

Figure 2: Cycle threshold (Cq) values for the laboratory *M.tuberculosis* at the *rpoB* loci. The diagram above shows the average Cycle threshold values for the *rpoB* amplification of replicates of the clinical samples. All the observed values were below 29 and the non-template control was negative, suggesting that the reaction was successful. Within this run, it is plausible to conclude that all the strains amplified efficiently enough to proceed to the next analysis step.

	H37Rv	R35	Kzn 605	R271	Tkk-050	Tkk-062	Tkk-043	Tkk-039
	88.69	88.99	89.4	88.51	88.44	88.8	88.52	88.5
	88.7	88.9	89.33	88.42	88.45	88.71	88.5	88.5
	88.75	88.9	89.3	88.36	88.43	88.78	88.51	88.44
	88.66	88.92	89.32	88.56	88.42	88.65	88.4	88.44
	88.77	88.86	89.34	88.48	88.42	88.73	88.42	88.46
	88.65	88.88	89.32	88.55	88.41	88.7	88.45	88.4
	88.76	89.01	89.29	88.48	88.4	88.69	88.45	88.4
	88.69	88.93	89.3	88.47		88.71	88.47	
Count	8	8	8	8	7	8	8	7
Mean	88.71	88.92	89.33	88.48	88.42	88.72	88.47	88.45
Stdev	0.046	0.052	0.035	0.066	0.017	0.049	0.043	0.041
Sem	0.016	0.018	0.012	0.023	0.0065	0.017	0.015	0.016

Table 4: Melting point temperatures of individual replicates for the laboratory strains at the *rpoB*. The table above shows the melting point temperatures obtained for each of the replicates for the different samples. Both estimates of the standard deviation and the standard error are smaller than the mean value whilst being closer to zero. On inspection, it is clear that at least 68% of the observed values are within one standard deviation of the mean, showing that the data is normally distributed. The data suggests that there is minimal variation with the observed readings and the differences in the average temperatures are a result of the differences in the melting point temperatures.

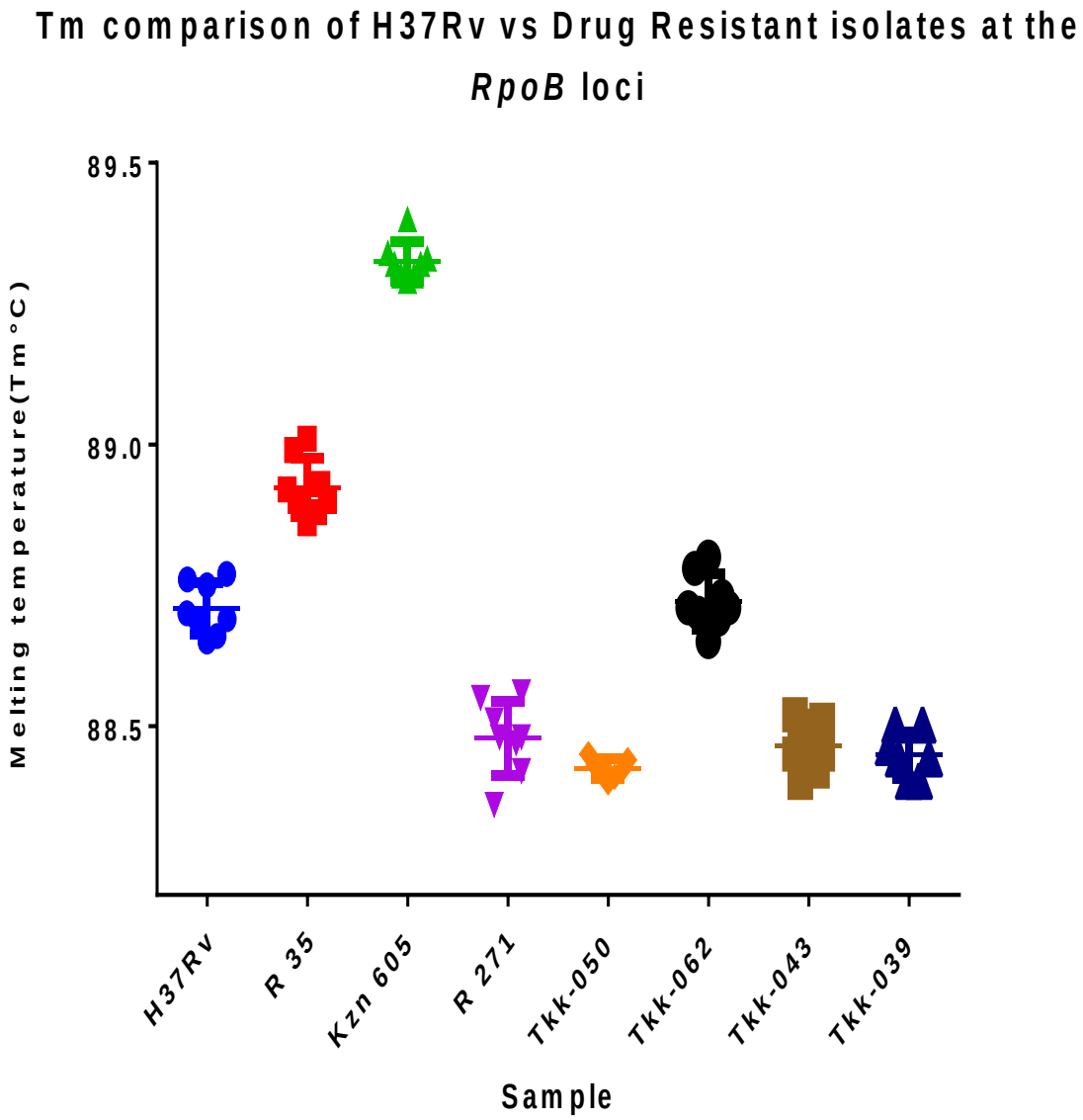

Figure 3: Visual depiction of the variation of the melting temperatures of the various strains at the *rpoB* region. Figure 3 depicts the variation in the melting point temperatures of the amplicons from the reactions involving different test strains and H37Rv. H37Rv and Tkk-062 were located in the same melting point temperature region. R271 and the remainder of the Tkk strains showed a melting point, which was lower than that of the standard H37Rv. R35 and Kzn 605 showed melting point temperatures that were elevated in comparison to the standard. The high degree of cluttering amongst the replicates follows on from the suggestion from Table 4 that the results are reproducible and reliable.

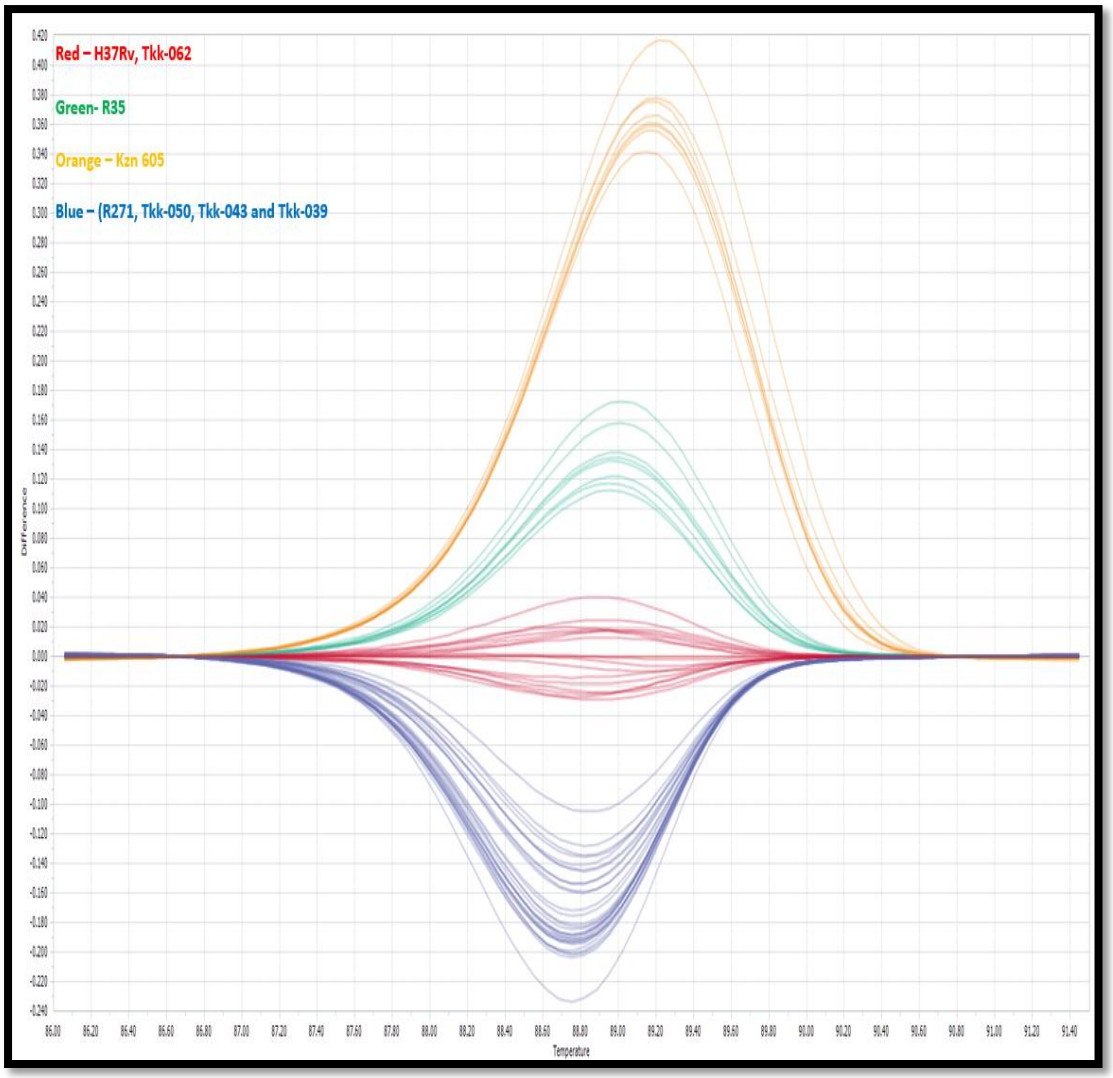

Figure 4: Difference plot showing the variation of the thermal dissociation profiles of the *rpoB* amplicons of the test *M.tuberculosis* strains. The figure above shows the different plots of the various amplicons, highlighting the profiling pattern in which each strain clustered into four different profiles. H37Rv and Tkk-062 cluttered into the same class, the red baseline. R271 and the remaining Tkk strains clustered in a profile that occurred below that of the baseline H37Rv. R35 and Kzn 605 had profiles located above that of the standard, with increased magnitude in their difference. This is consistent with the melting point temperatures in figure 3.

In summary, the rifampin results shows that the assay could detect six out of seven of the strains with mutations, a percentage **sensitivity of 86%**. The Tkk-062 strain result is classified as a false negative, as it contains a mutation but was not detected with the rifampin assay. Specificity estimates cannot be calculated because the assay had no drug susceptible strains in the test panel. Thus, thesestrains are suitable for evaluation of the rifampin assay on the Light Forge system.

3.1.2 Isoniazid resistance assay

katG

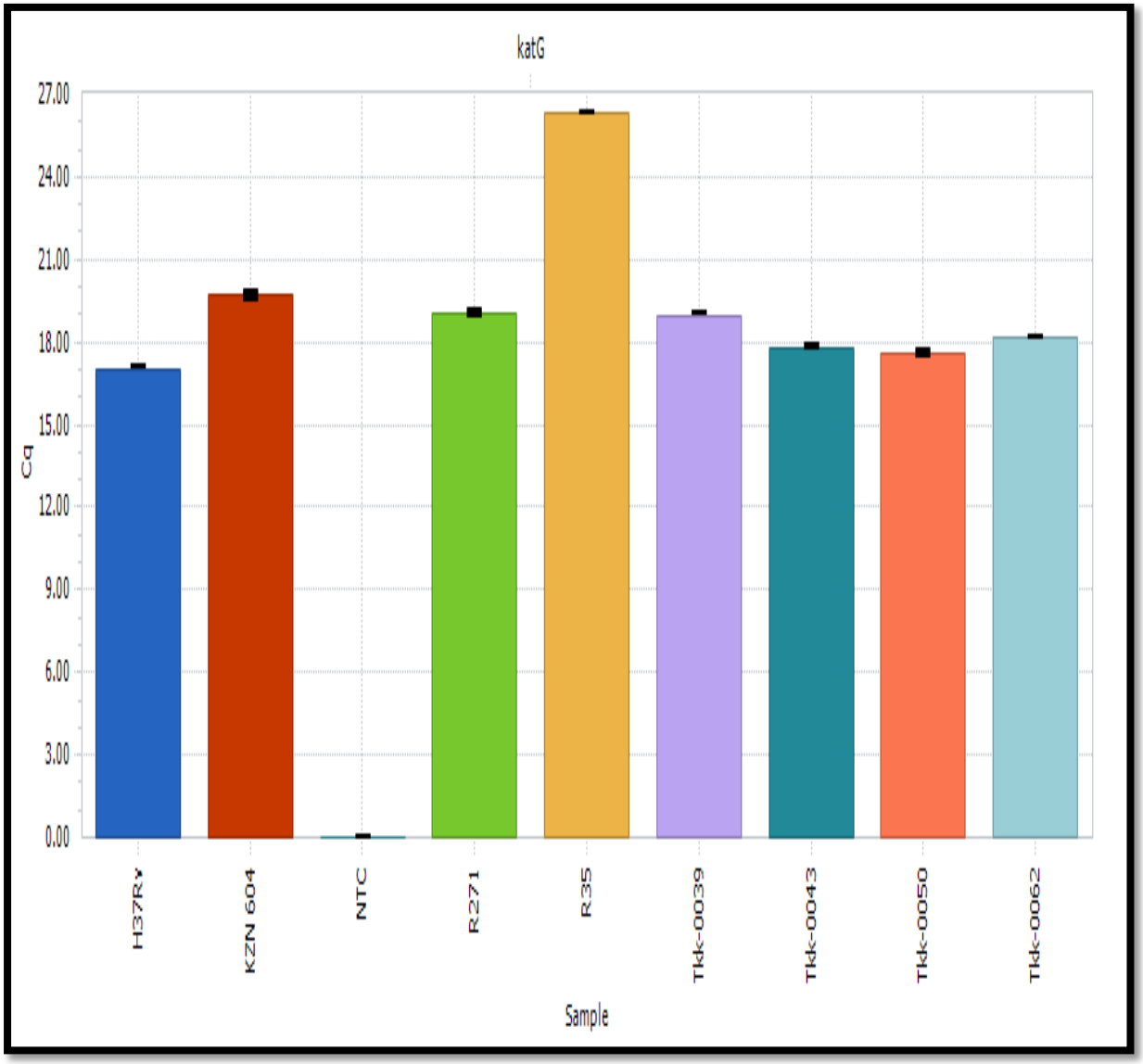

Figure 5: Cycle threshold values achieved during amplification of the *katG* gene for the various laboratory strains. The graph above shows the amplification of a segment of the *katG* gene in the *M.tuberculosis* panel. The average Cq values were less than 29, suggesting that amplification was efficient enough for HRMA. The reaction data shows that with the exception of R35, the different *M.tuberculosis* strains amplified the *katG* product to detectable levels between cycles 17 to 20. This suggest that all the other strains with the exception of the late amplifier R35 (Cq of 26) accumulated the PCR product at almost similar rates . The non-template control showed no appreciable amplification, thus the findings are reliable and is appropriately useful in the subsequent analysis.

	H37Rv	R 35	Kzn 605	R 271	Tkk-050	Tkk-062	Tkk-043	Tkk-039
	89.94	89.95	89.92	89.96	89.89	89.92	89.94	89.75
	89.9	89.83	89.93	89.95	89.91	89.85	89.76	89.75
	90.01	89.83	89.98	89.95	89.9	89.86	89.83	89.82
	89.99	89.78	89.87	90.07	89.82	89.98	89.78	89.81
	90.02	89.86	89.85	90.01	89.87	89.85	89.75	89.84
	89.98	89.81	89.89	89.94	89.89	89.84	89.78	89.72
	89.89	89.81		89.94	89.87	89.83	89.78	89.79
	89.94	89.73		89.92	89.79	89.91	89.8	89.67
Count	8	8	6	8	8	8	8	8
Mean	89.96	89.83	89.91	89.97	89.87	89.88	89.80	89.77
Stdev	0.049	0.064	0.047	0.049	0.042	0.052	0.061	0.057
Sem	0.0061	0.008	0.0078	0.0061	0.0052	0.0065	0.0076	0.0071

Table 5: Melting point temperatures for the katG amplicon of the test *M.tuberculosis* strains. Melting point temperatures of the *katG* amplicons for the various *M.tuberculosis* test strains. The mean melting point temperatures ranged from 89.77 to 89.97°C and the standard deviation from 0.042 to 0.064°C. In all of the test strains, 68% of the observed Tm values were with the range of ± standard deviation, suggesting that the data is normally distributed. Kzn 605 had two of replicates where no amplification was detected for unclear reasons. In conclusion, the observed variation in the Tm amongst the test strains is result of the sequence of the amplicons as opposed to random experimental variation.

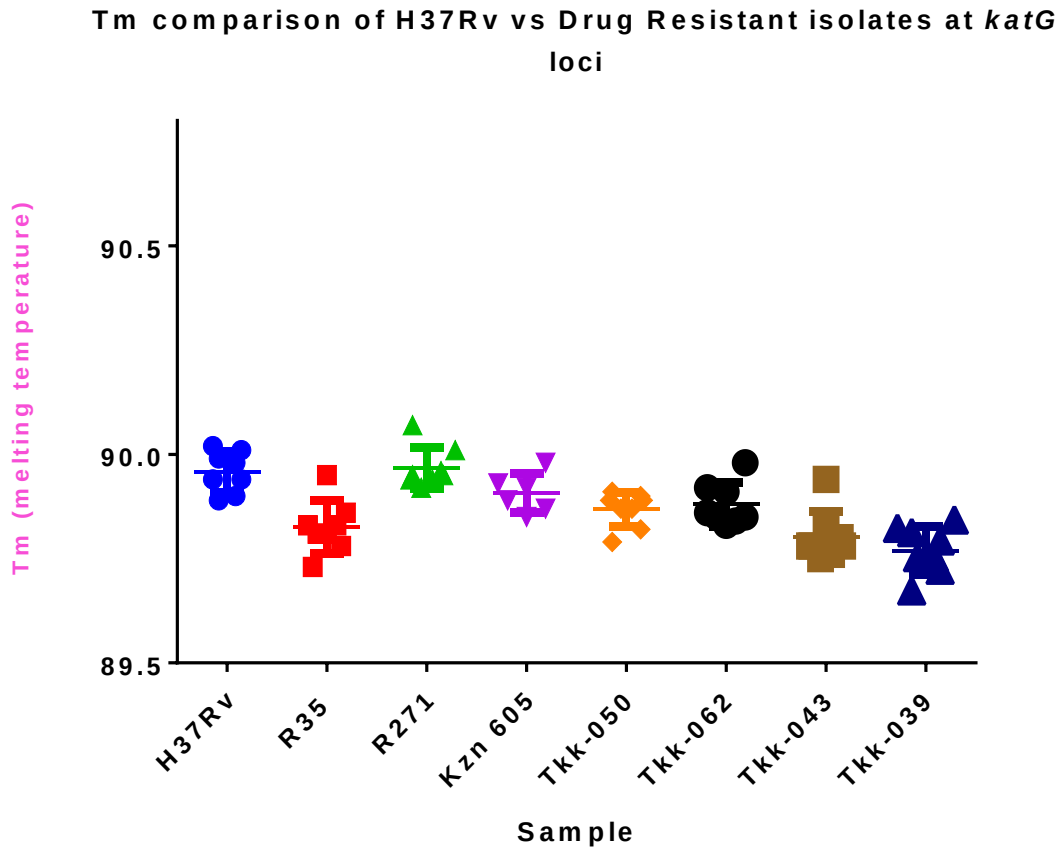

Figure 6: Pictorial variation of the melting point temperatures of the katG amplicons generated from the *M.tuberculosis* strains. The variation of the melting point of the amplicons figure 6 above. R35 and Tkk-043 are in the same temperature region that is slightly lower than that of H37Rv. All the other strains with the exception of R271 (which had no mutation detected by Sanger sequencing as shown in table 8), showed a similar melting point temperature. Tkk-039 displayed a curiously lower melting point temperature. In summary, this graph shows minimal variation in the Tm when the amplicons amongst the strains are studied.

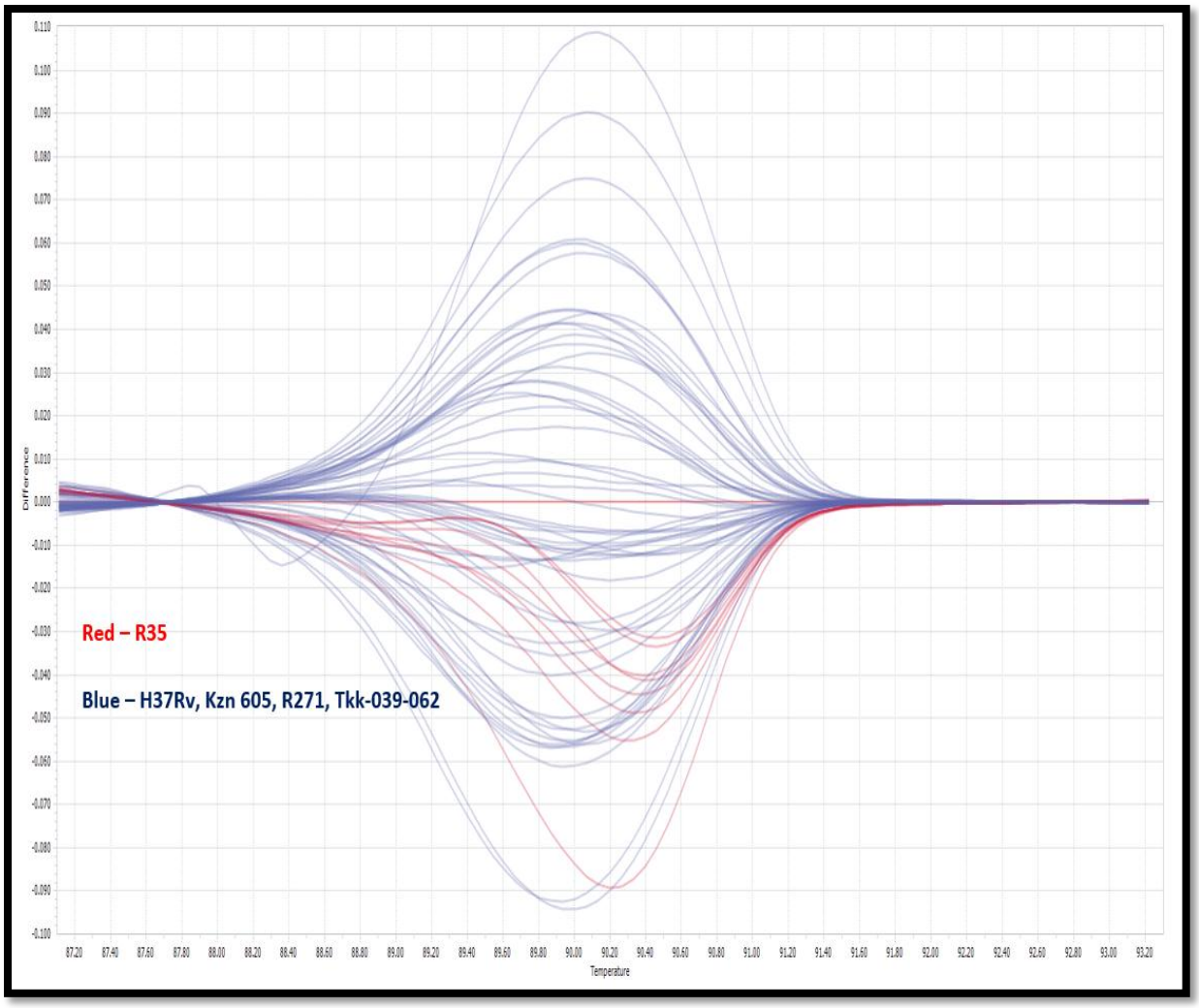

Figure 7: Difference plot generated from the dissociation curves of the katG amplicons of the test *M.tuberculosis* strains. Only two dissociation profiles were observed for the *M.tuberculosis* amplicons of the *katG* gene. R35 showed a distinct profile but the same was not observed for Tkk-039. Thus a disparity is observed between the melting temperature graph (figure 6) and figure 7. All the other strains had a profile that was similar to H37Rv, consistent with the sequencing results in Table 8. The baseline signal for H37Rv was clustered with all the other strains, making it difficult to isolate the profiles.

In summary, one out of six strains was detected, a **sensitivity of 17%.** All the test strains are classified as false negative results as table 8 shows that they contain the mutations. Due to the low sensitivity, this gene is not evaluated on the Light Forge system.

Mab-inhA

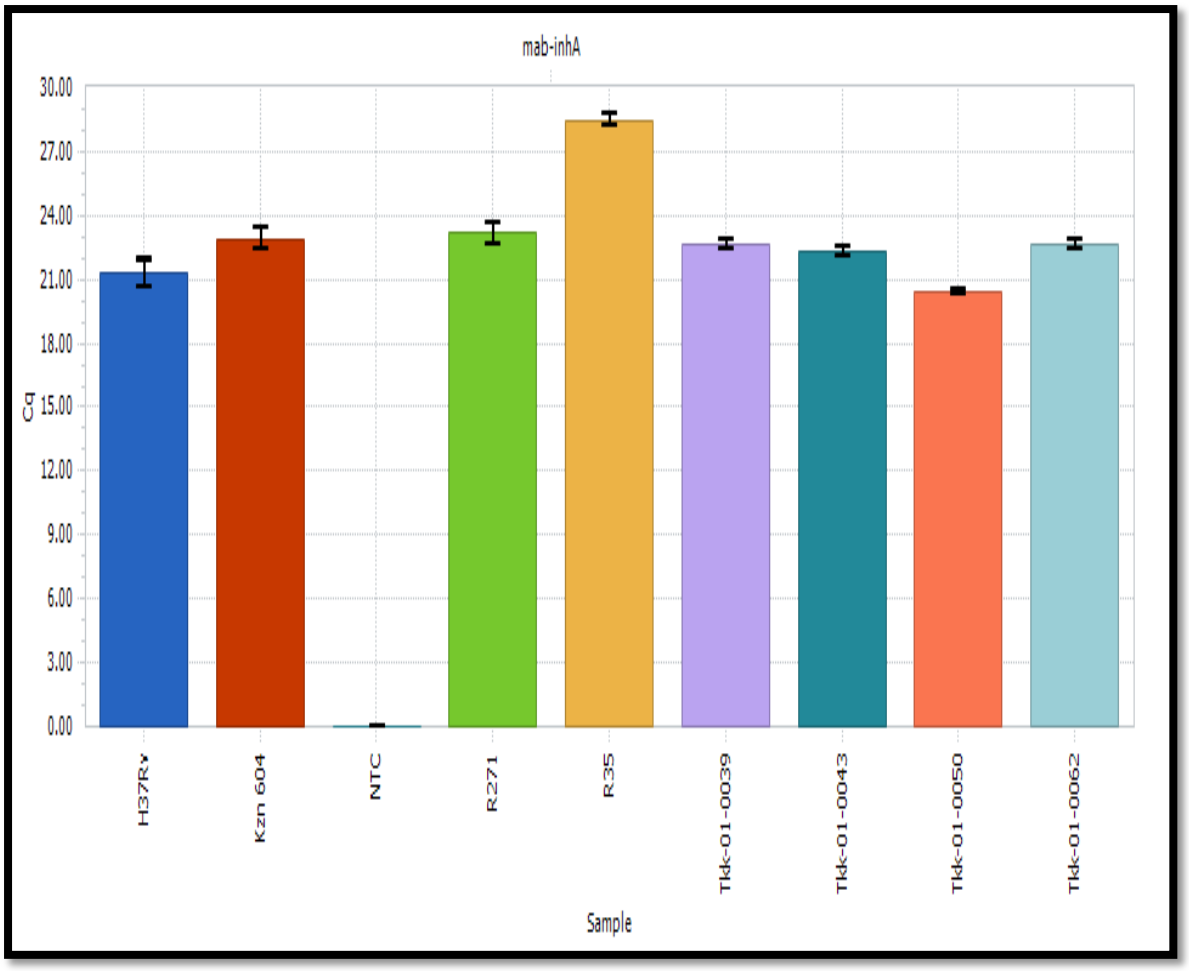

Figure 8: Cycle thresholds of the various M.tuberculosis strains during mab-inhA amplification. The pictogram above detailed how each of the *M.tuberculosis* DNA samples behaved during during the amplification process. From the statistical analysis, the reactions at average Cq values less than 29. R35 was a late amplifier, as shown by the

	H37Rv	R 35	Kzn 605	R 271	Tkk-050	Tkk-062	Tkk-043	Tkk-039
	90.67	90.51	90.65	90.68	90.55	90.52	90.69	90.74
	90.56	90.49	90.59	90.68	90.51	90.45	90.61	90.73
	90.6	90.5	90.62	90.68	90.5	90.46	90.69	90.67
	90.66	90.5	90.64	90.8	90.54	90.51	90.71	90.68
	90.69	90.52	90.67	90.67	90.53	90.51	90.67	90.7
	90.58	90.48	90.59	90.6	90.49	90.5	90.64	90.71
	90.56	90.48	90.55	90.6	90.47	90.49	90.64	90.65
	90.6	90.52	90.62	90.58	90.51	90.51	90.65	90.72
Count	8	8	8	8	8	8	8	8
Mean	90.62	90.5	90.62	90.66	90.51	90.50	90.66	90.7
Stdev	0.051	0.016	0.039	0.070	0.027	0.026	0.033	0.031
Sem	0.018	0.0057	0.014	0.025	0.0094	0.0091	0.012	0.011

Table 6: Melting point temperatures of the mab-inhA amplicons from various test *M.tuberculosis strains*. The table above shows the variation in the melting point temperature for amplicons of *mab-inhA* gene amplified from different test samples. The melting point temperature varied from 90.5 to 90.7°C, with small estimates of standard deviation and error observed amongst the replicates i.e. over a 1000-fold less than the mean. Again, for the test strains, 68% of the observed Tm values are within the first standard deviation, thus the data is normally distributed. It was concluded that the variations in the Tm were a result of the differences between the amplicons themselves as opposed to unknown variability.

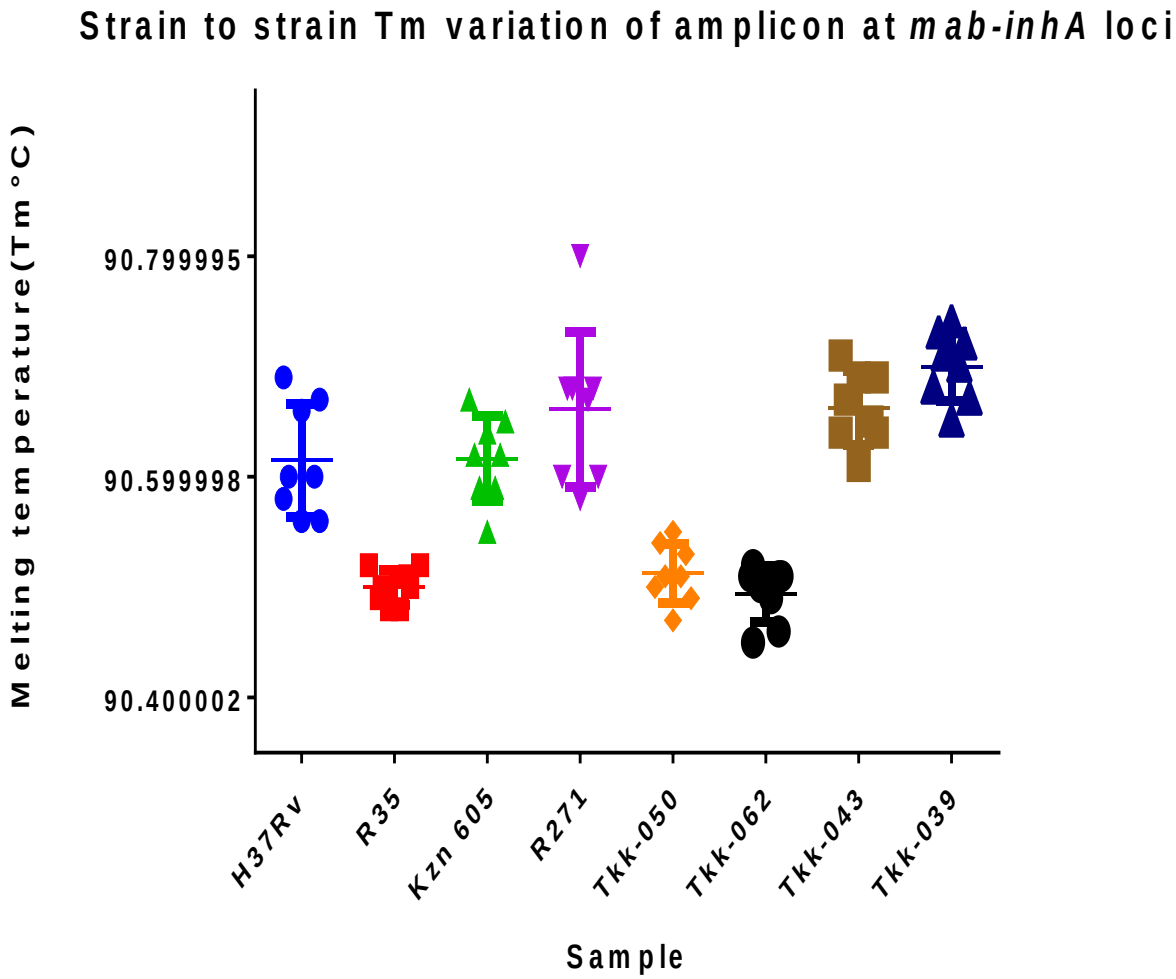

Figure 9: Visual variation of the melting point temperatures of the *M.tuberculosis* strains at the *mab-inhA* locus.The visual representation of the melting point temperature. Two strains, Tkk-043 and Tkk-039 were within a temperature region above that of H37Rv. Tkk050,Tkk062 and R35 were located in melting temperature regions below H37Rv. R35 did not have any detectable mutation as shown in table 8.The class one mutation in Kzn 605 showed no detectable difference from H37Rv. The remainder of the strains, which had no detectable mutations, showed profiles similar to H37Rv. In summary, only five of the test strains showed distinguishable Tm profiles.

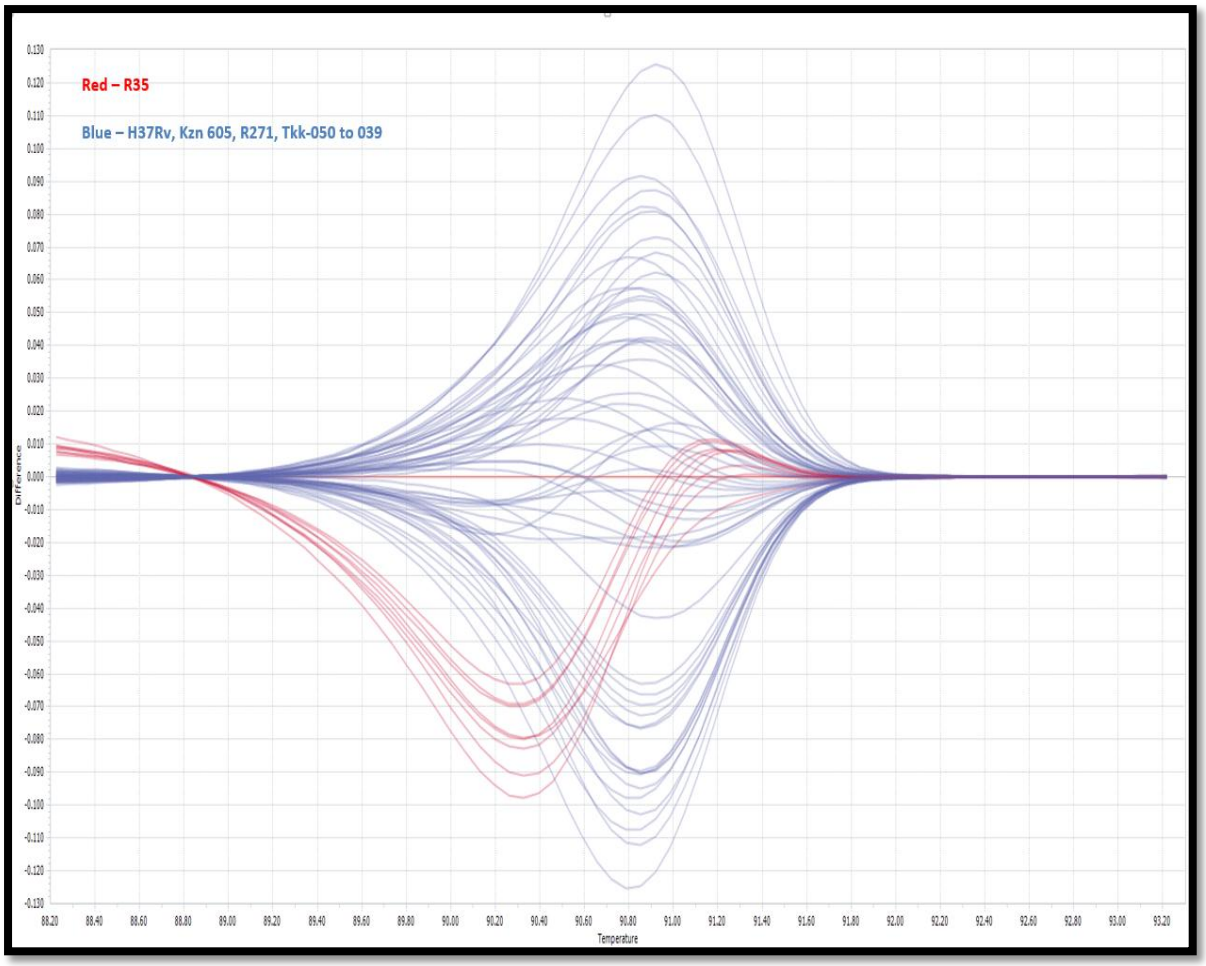

Figure 10: Difference plot generated from the thermal dissociation curves of the various *M.tuberculosis* strains at the *mab-inhA* loci. As shown in Figure 9, only two profiles were observed on the difference plots. R35, which had no mutation in this region as ascertained by sanger sequencing, had an unusual profile. The rest of the samples have the same identical profile with H37Rv, in spite of having mutations that were skewing the melting point temperature as shown in figure 9.

In summary, it is quite clear that the findings from the melting temperature graph and the difference plot do not easily align. Based on the difference plot, the isoniazid assay at the *mab-inhA* gene had **0% sensitivity**. Due to the failure of the assay to detect the resistance-linked mutations, the assay was not evaluated using the Light Forge system.

3.1.3 Ofloxacin resistance results

gyrA

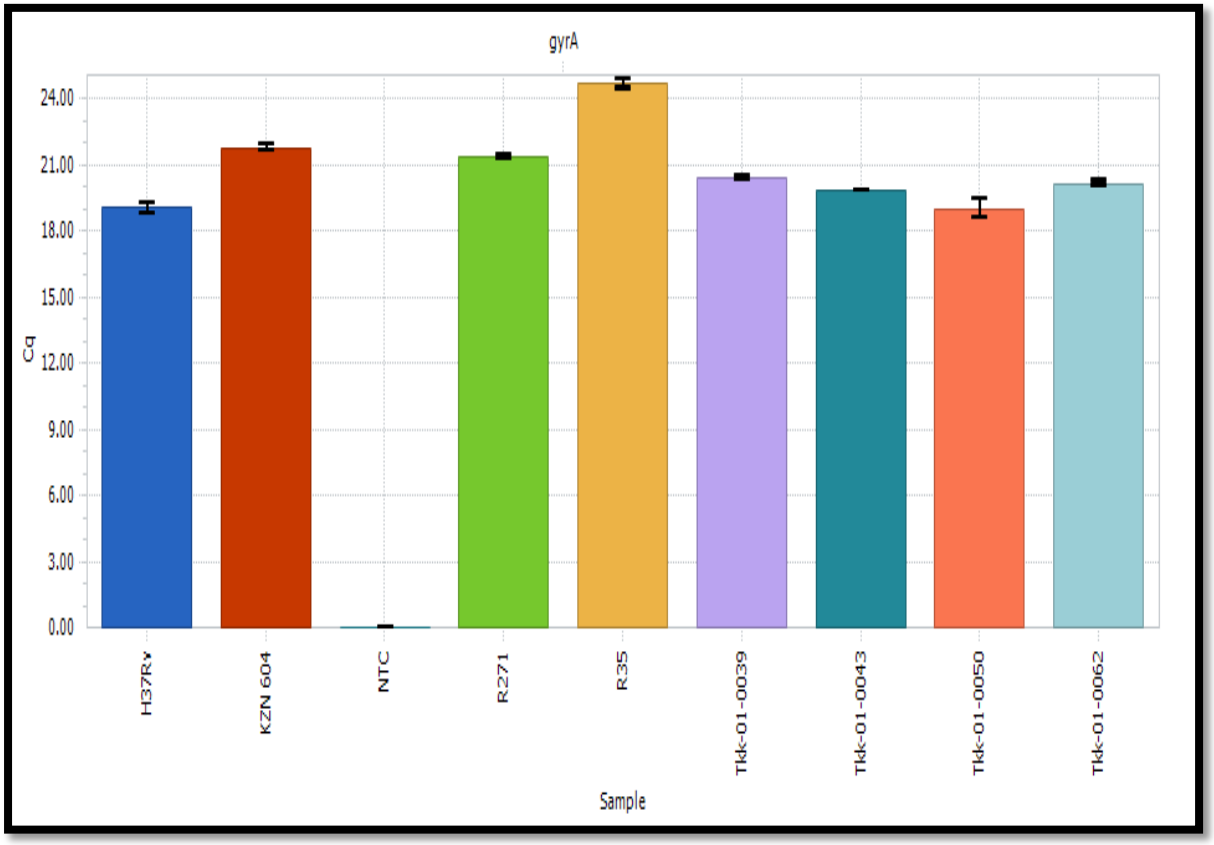

Figure 11: Cycle threshold numbers for each of the *M.tuberculosis* strains observed during amplification of the *gyrA* amplicon. The figure above shows the average cycle threshold for pooled replicates of each of the test DNA samples. The reactions produced detectable quantities of product between cycles 18.5 to 24.5. As all the Cq values were below 29, thus it was concluded that the amplification was efficient. As shown in the preceding figures, R35 appears to be a late amplifier, with a Cq value of 24.5. The non-template control showed no appreciable quantity of product.

	H37Rv	R 35	Kzn 605	R 271	Tkk-0050	Tkk-0062	Tkk-0043	Tkk-0039
	91.92	91.96	91.78	91.94	91.94	92.04	92.02	92.07
	92.01	91.96	91.73	91.95	91.98	91.92	91.93	91.98
	91.81	92.03	91.7	91.9	92.02	91.93	92.08	92
	91.99	92.05	91.79	91.93	92.01	91.9	91.97	92
	91.84	92	91.74	91.94	92.01	91.98	91.93	92.03
	91.95	92.01	91.67	91.89	91.96	91.91	91.97	91.97
	91.99	91.94	91.69	91.94	91.88	91.97	91.92	91.98
		91.91	91.7		92.19	92.04	91.99	91.98
Count	7	8	8	7	8	8	8	8
Mean	91.93	91.99	91.73	91.93	91.97	91.95	91.97	92.00
Stdev	0.078	0.041	0.045	0.023	0.050	0.050	0.058	0.035
Sem	0.030	0.014	0.016	0.0087	0.018	0.018	0.021	0.012

Table 7: Melting point temperatures from the dissociation curves of the *gyrA* amplicons of the *M.tuberculosis* strains. The table above shows how the melting point temperature for each replicate of the *M.tuberculosis* strains varied during the melt analysis. The average melting point temperature ranged from 91.95 to 92°C. Consistent with the theoretical assumptions of the normal distribution, 68% of the observed temperatures are with a single standard deviation. This shows that the variation observed was normal and not reflective of inaccurate measurements of the Tm. Low estimates of the standard error show that the average Tm is highly reliable.

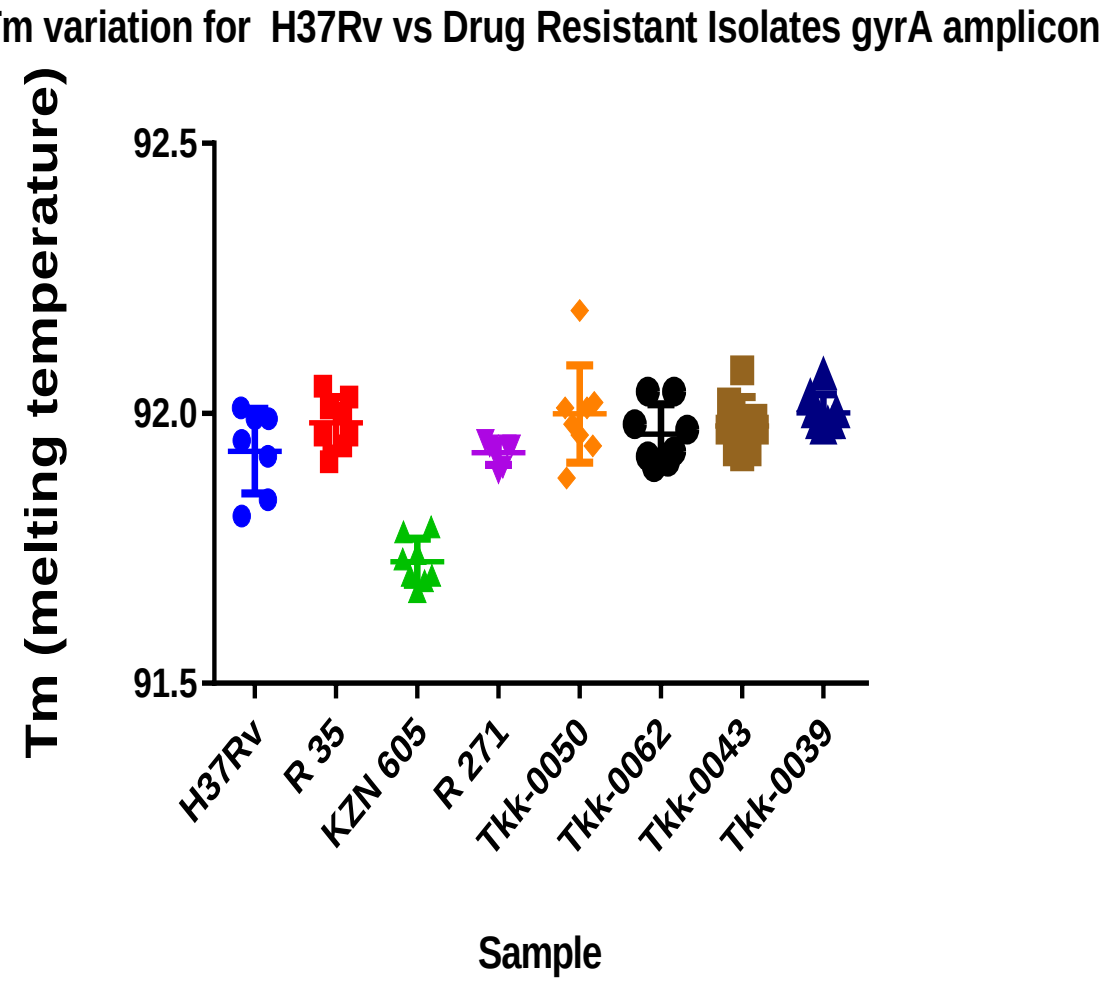

Figure 12: Visual distribution of the melting point temperatures of the *gyrA* amplicons of the test *M.tuberculosis* strains. The figure above is a visual depiction of the melting point temperature of the various *M.tuberculosis* test strains. The majority of the test strains were within the same Tm region as the standard H37Rv. The only exception was Kzn 605, which had a reduced melting point temperature region located below that of H37Rv. The other strains were located within the same temperature region with H37Rv, suggesting the similarity of their products.

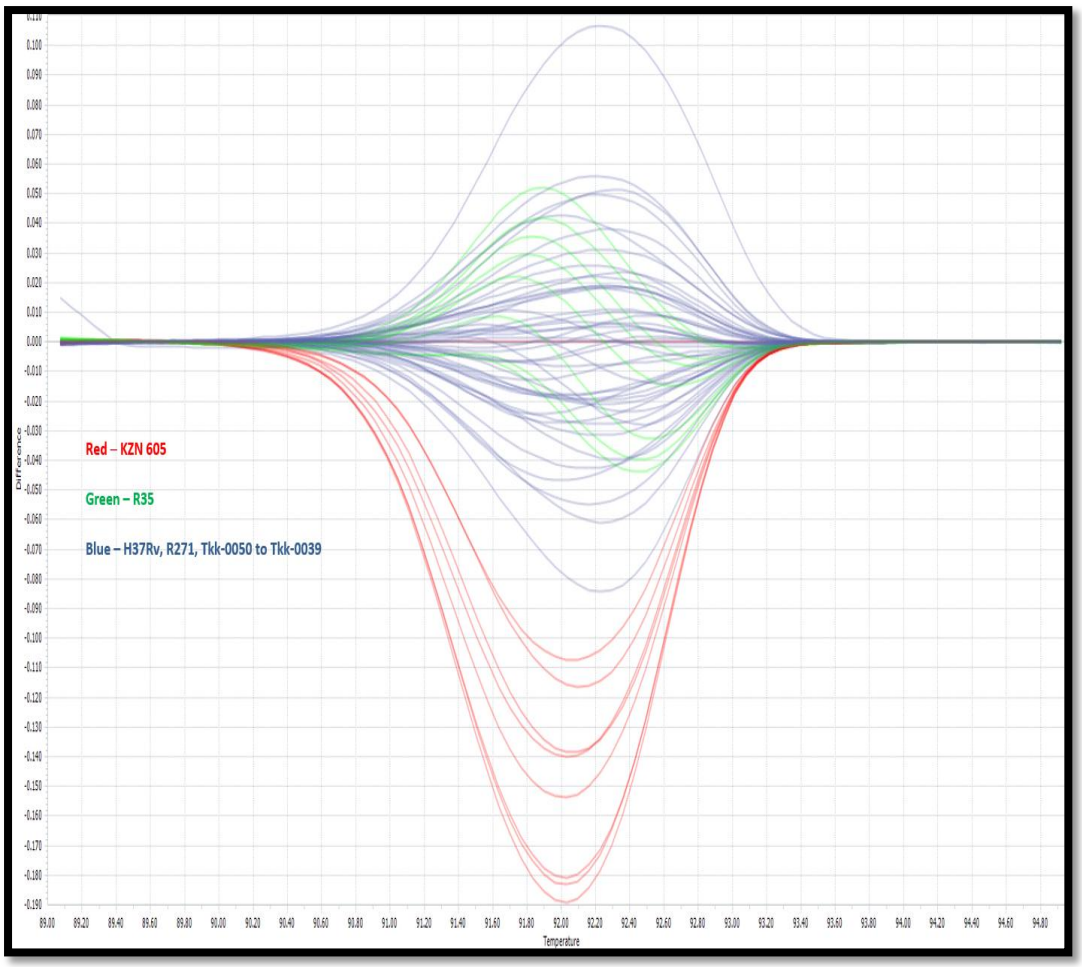

Figure 13: Difference plot generated from the dissociation curves of the various amplicons from the gyrA loci. The figure above shows the difference plot for the various *M.tuberculosis* strains at the *gyrA* region. R35 had profile that spanned up and down that of the H37Rv, in spite of not having any mutation within this region as shown by Table 8. Kzn 605 showed a profile that was very distict from that of H37Rv. The profile was located below that of the H37Rv baseline, consistent with the observation made in figure 12. Kzn 605 had two mutations, which skewed the melting point temperature. Unfortunately, all the other strains on the test panel had a mutation, which is not linked to ofloxacin drug resistance (S95T).

In summary, the ofloxacin managed to detect resistance with a **100% sensitivity**. The presence of the non-synonymous mutations meant that the other strains could were not suited for use in the resistance detection assay. In spite of the perfect sensitivity, the ofloxacin assay proved feasible for one strain, thus it was not evaluated using the Light Forge System.

3.2 HRMA with Light Forge

Following on from the findings from the initial phase, the rifampin assay was used to study drug-linked mutations in the test panel of *M.tuberculosis* strains with the Light Forge device. The initial image shows the 2D appearance of the microfluidic chip under bright field microscopy view. Followed by a snapshot view of the chip before and after product amplification using the green fluorescent protein (GFP) filter. These images are acquired using a LabView based system. They are processed using a Matlab script to produce the amplification, melt and the derivative plots. The current chip can only be used to test one strain per reaction, with the other reactors being occupied by the standard and non-template control.

Following on from phase 1, the amplification plots serve to show efficient amplification of the product. The microfluidic chip used had 20 reactors thus an identical assay of the Cq values is not possible. An empirical rule is used, such that if the fluorescence picks up before the 20^{th} cycle i.e it has reached the logarithmic amplification stage (exponential phase), the reaction is considered as an efficient amplifier. No signal from the non-template control is ideal.

Melt curves then follow, which show the progression of the gradual denaturation of the amplicons. These plots are used to detect variants from the H37Rv. Ideally the melt curves should show that the non-template control has a lower melting point temperature than the reaction with DNA [124].

Derivative peaks generated from the melt curve data are presented. These show the negative derivative of the normalized melt curve data. The presence of a mutation is shown by the of shifting of the peak by the test strain in comparison to H37Rv. The peak for the test and standard strains are expected to be located at a higher temperature in comparison to that of the non-template control. Non-template control peaks located in the same region as the desired product strong suggest the possibility of contamination.

The results are then conclude by a visual depiction of the Tm values for each of the tested strain. This graph is useful in deciding if a test strain is assigned as mutant or wild type together with, the information supplied from the other plots.

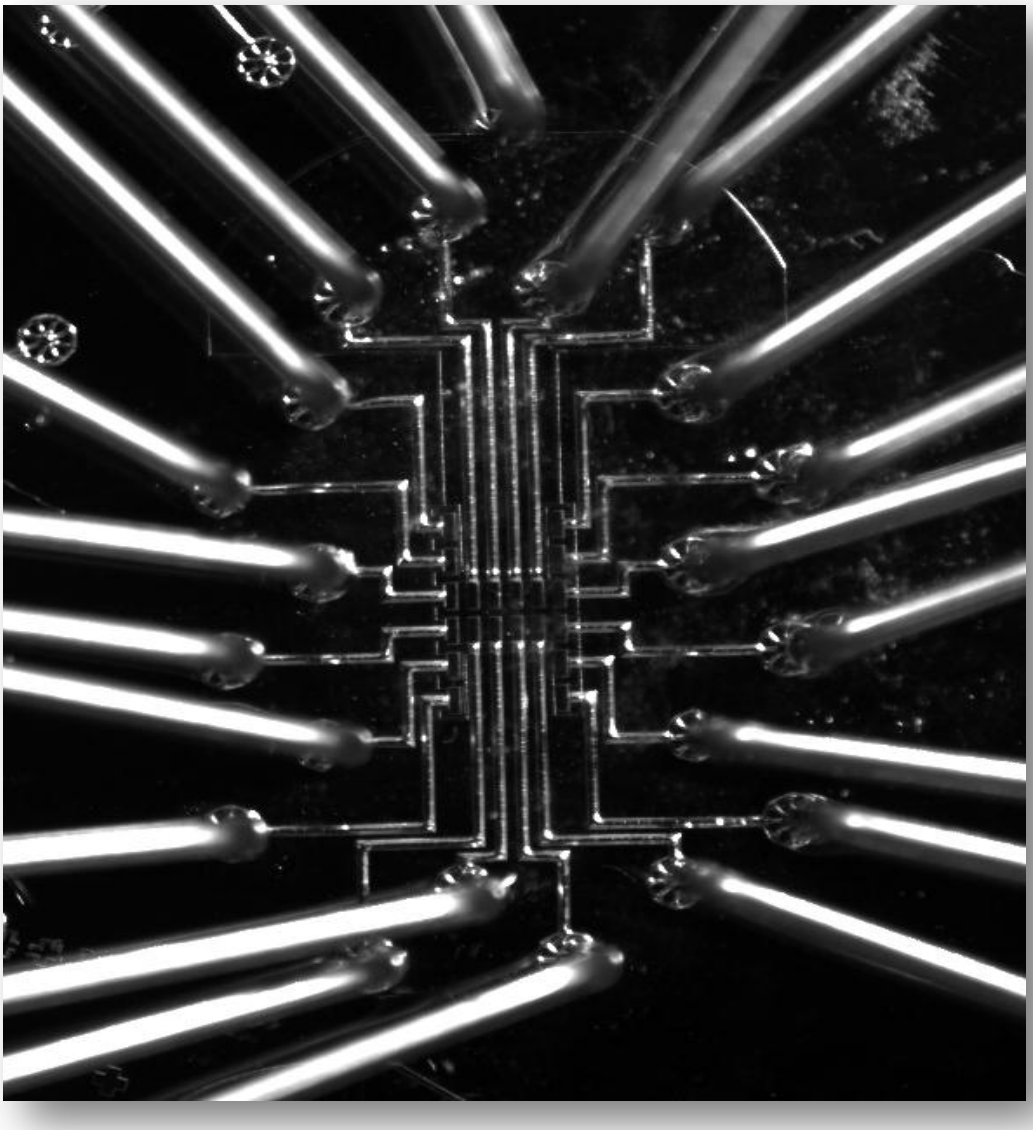

Figure 14: Bright field aerial view of the 20-reactor microfluidic chip. This picture shows how the chip looks like when the reagents are being loaded. The silver objects protruding from each circular aperture are the pins loading the PCR master mix into the reaction vessels through tygon tubing.

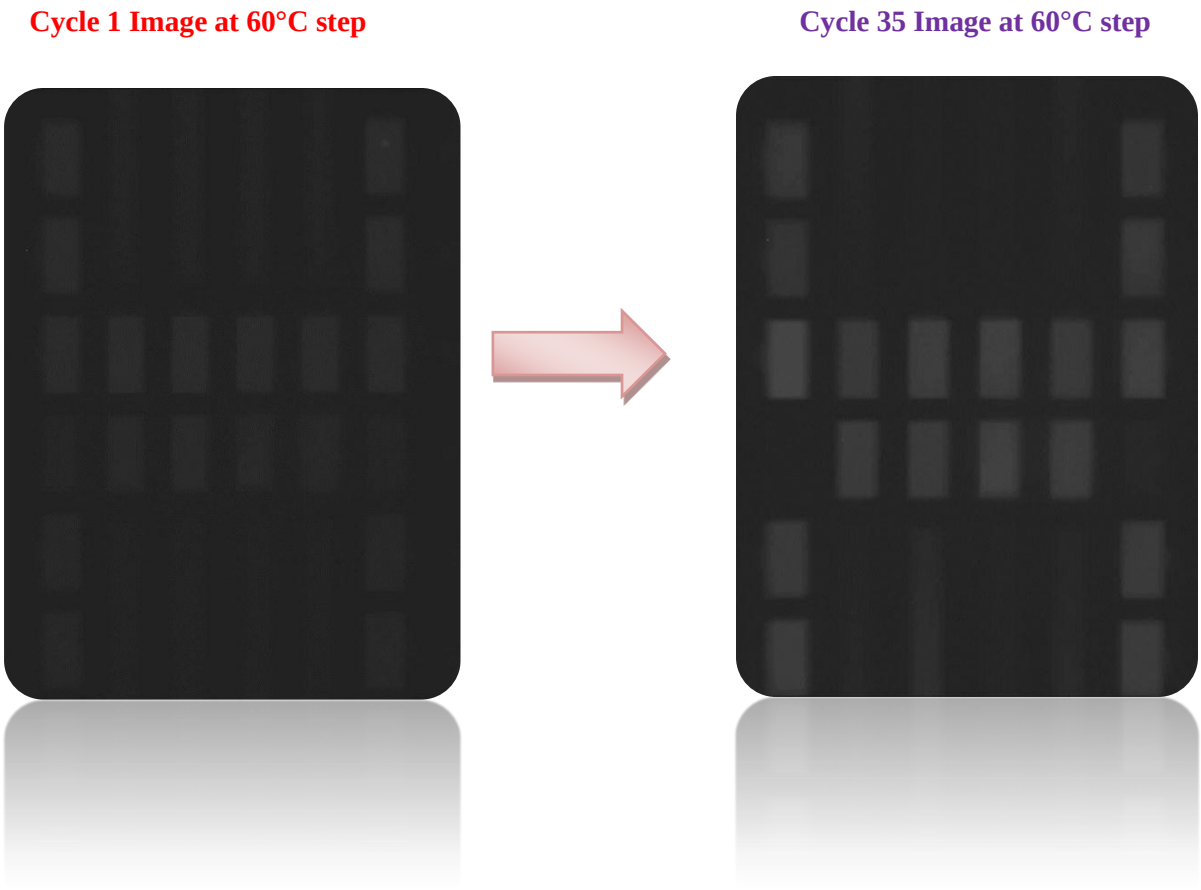

Figure 15: Appearance of the microfluidic chip pre and post amplification using the GFP module on the fluorescent filter wheel. The images above show the change in the fluorescence signal during the amplification of the PCR mix containing *M.tuberculosis* DNA. The images were acquired using a CCD camera controlled by a computer program developed in house i.e. Light Forge system. Light Forge uses a temperature feedback system that captures images when easily programmable temperature and time thresholds are attained. The observed increase in fluorescence from the first to the 35^{th} cycle is a confirmation that amplification was occurring on the chip. It should be noted that two reactors with the non-template control showed no amplification thus remained dark squares, showing that contamination was not an issue in the experiment.

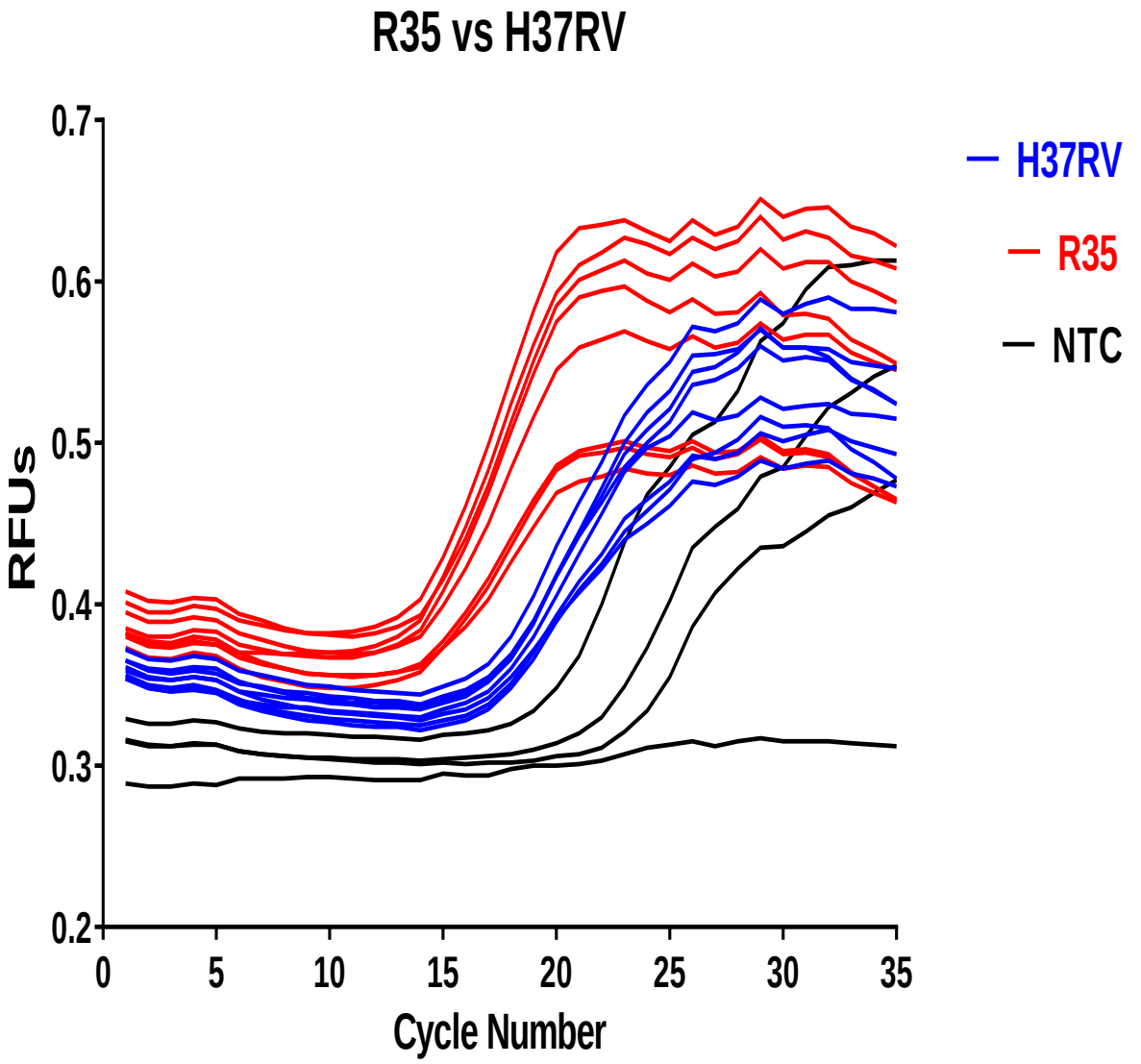

Figure 16 : Amplification profile of R35 and H37Rv *rpoB* amplicons in the Light Forge device. The above graph is showing the progression of the amplification process, both samples reached the exponetial amplification phase before the 20th cycle. Product is detected for the non-template control in later cycles. This suggests the presence of primer dimers, but this can only be concluded from the melt curve data. Thus from this data, it can be concluded that the amplifcation process was efficient in producing the desired amplicons.

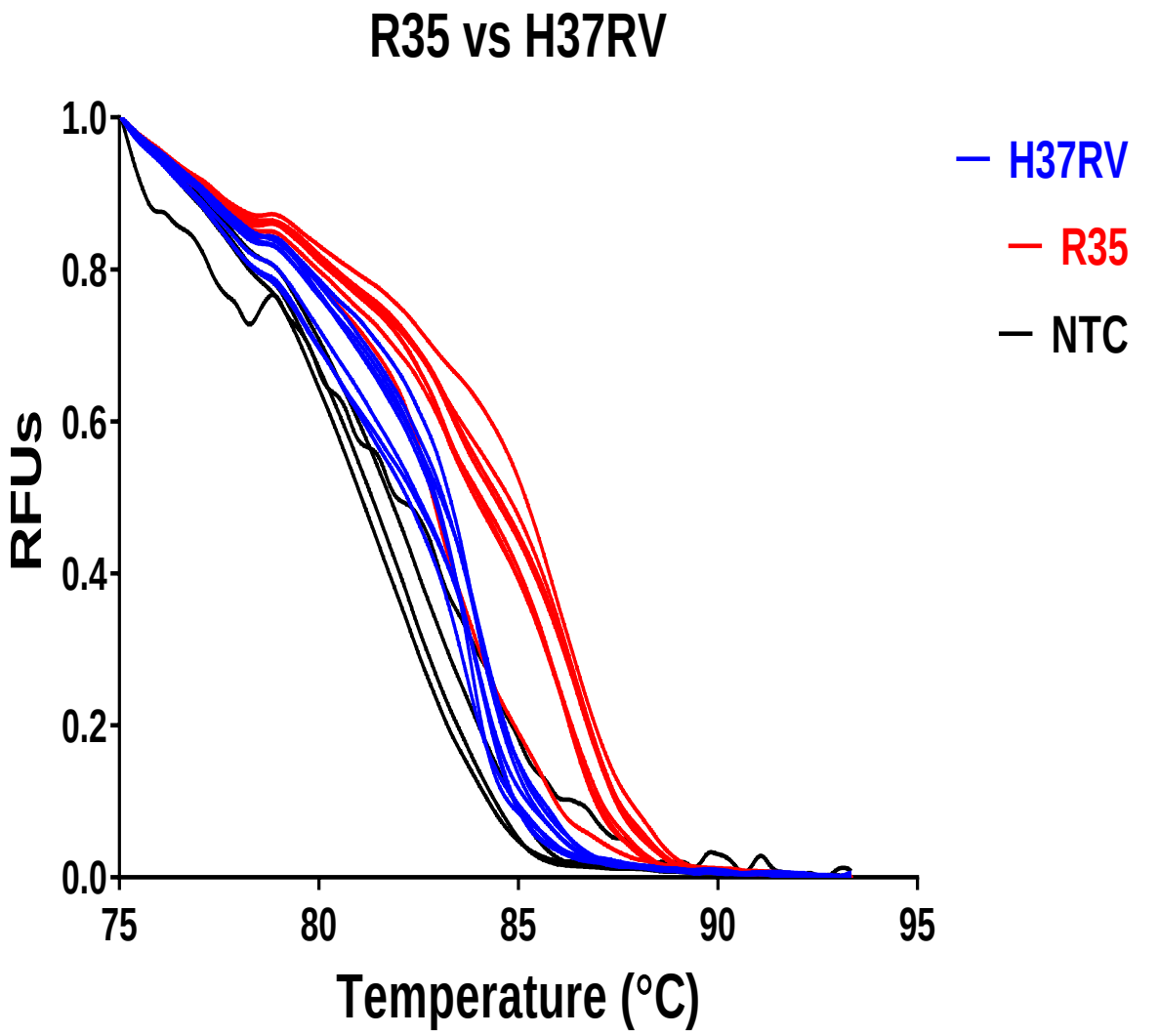

Figure 17: Melt curves comparing R35 and H37Rv amplicons at the rpoB loci. The above graph shows the denaturation profile of the amplicons during the melt curve assay. R35 samples melt at a later temperature in comparison to H37Rv. The non-template control melts at a temperature before both the test amplicons. One of the R35 replicates appears to overlapp with the melt curves of H37Rv. It was concluded that the amplicons from the test strain R35 had a disticnt profile to that of H37Rv.

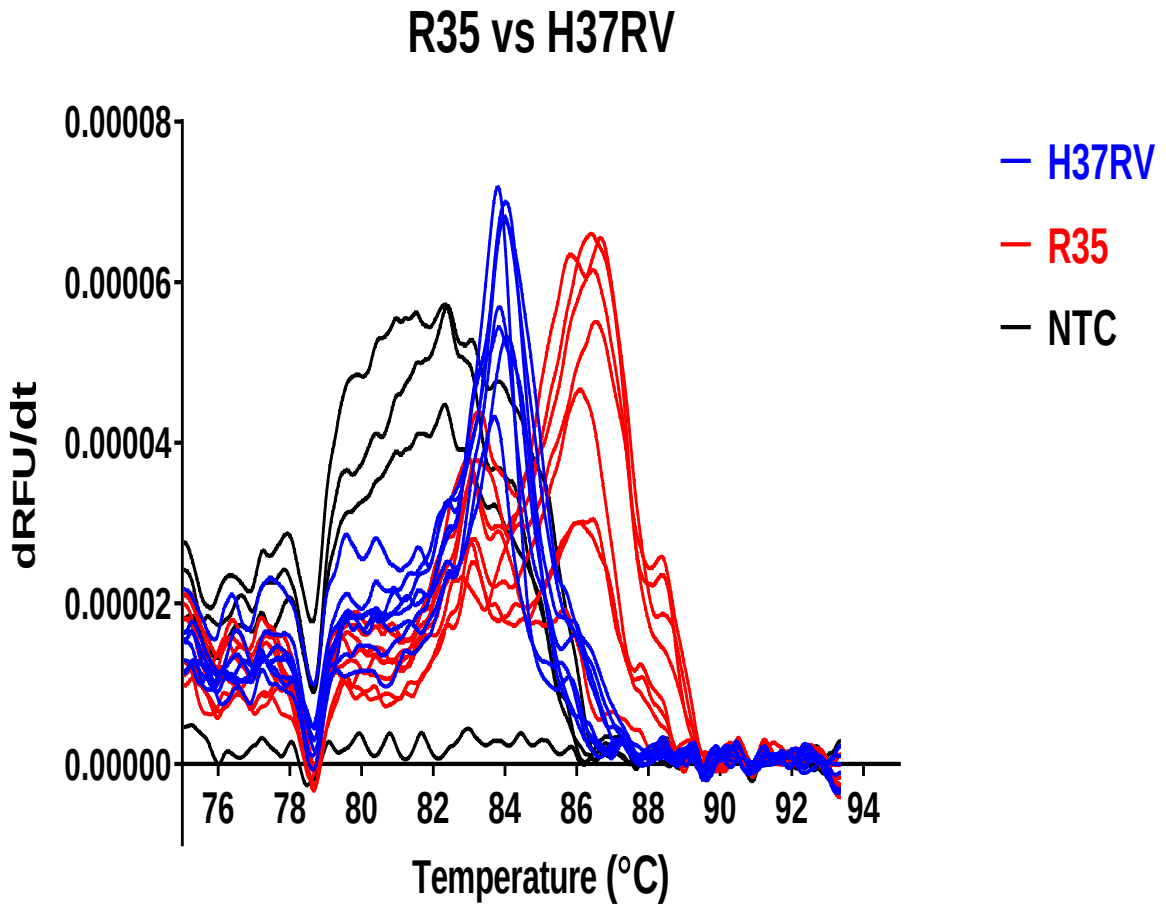

Figure 18: The Derivate plot for R35 and H37Rv rpoB amplicons. H37Rv showed peaks that were lower than the peaks observed for H37Rv. The non-template control showed peaks that located at lower temperatures compared to the target amplicons.

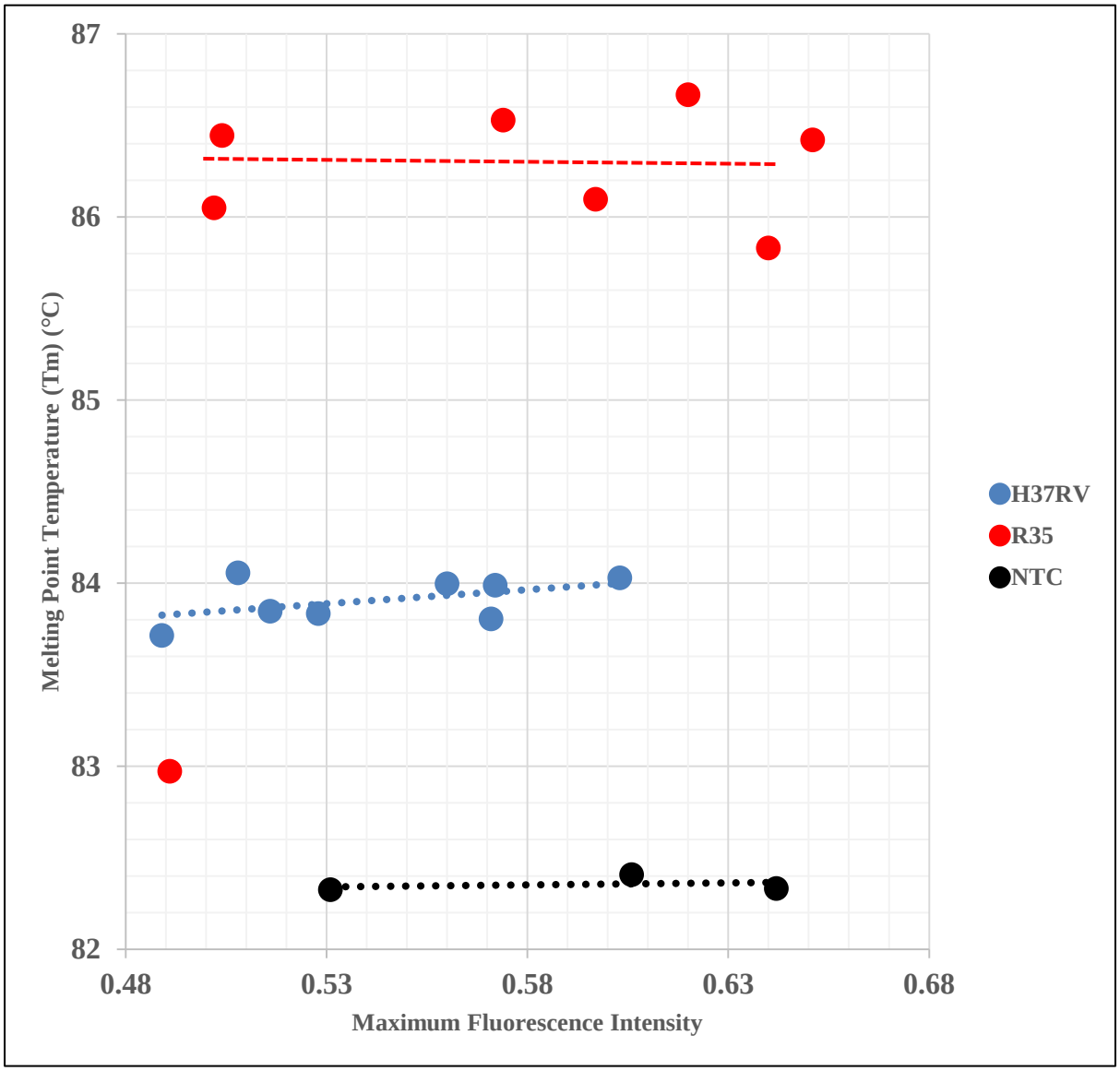

Figure 19: Pictorial representation of the melting point temperatures of H37Rv and R35. The illustration above shows the variation of the melting point temperature of R35 compared with H37Rv. The replicates show that the temperatures were distinct; a 2°C difference compared to the 0.21 observed using the Light Cycler96 system. One outlier was observed in the R35 sample, with a low Tm of 83°C. The non-template showed a melting profile lower than the target amplicon thus the findings are reliable.

Thus in conclusion, Light Forge managed to detect the mutations within the *rpoB* amplicon of R35, increase the temperature difference by 10-fold. This is a marked improvement from the commercial system.

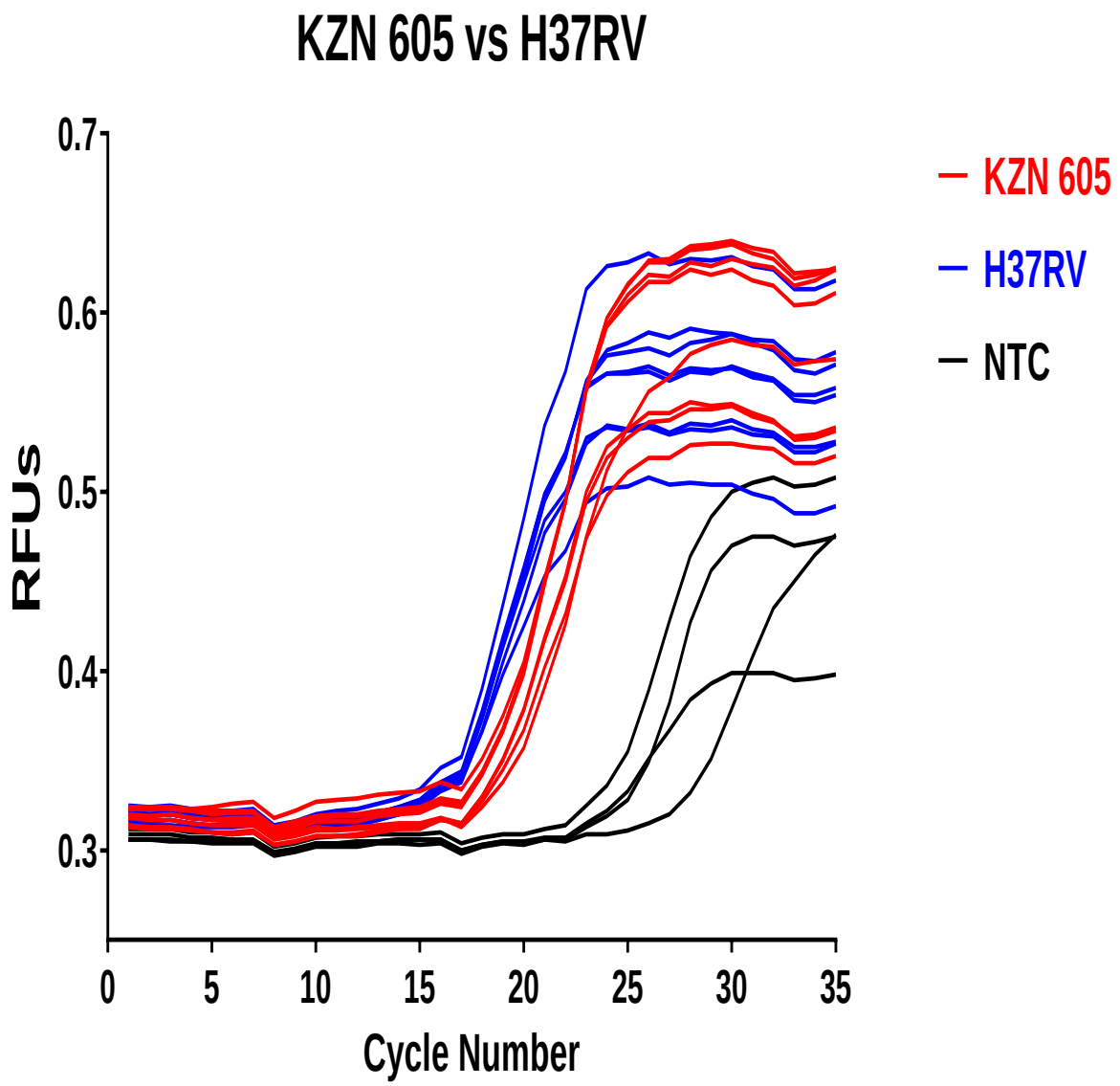

Figure 20: Amplification of the rpoB amplicons from Kzn 605 and H37Rv. Both samples reached the exponential phase before the 20th cycle. The non-template control reactions reached the exponential phase around the 24th cycle. The positive reaction in the either non-template controls suggest that the primer dimers amplified or there was contamination but this is concluded by observation of the subsequent plots.

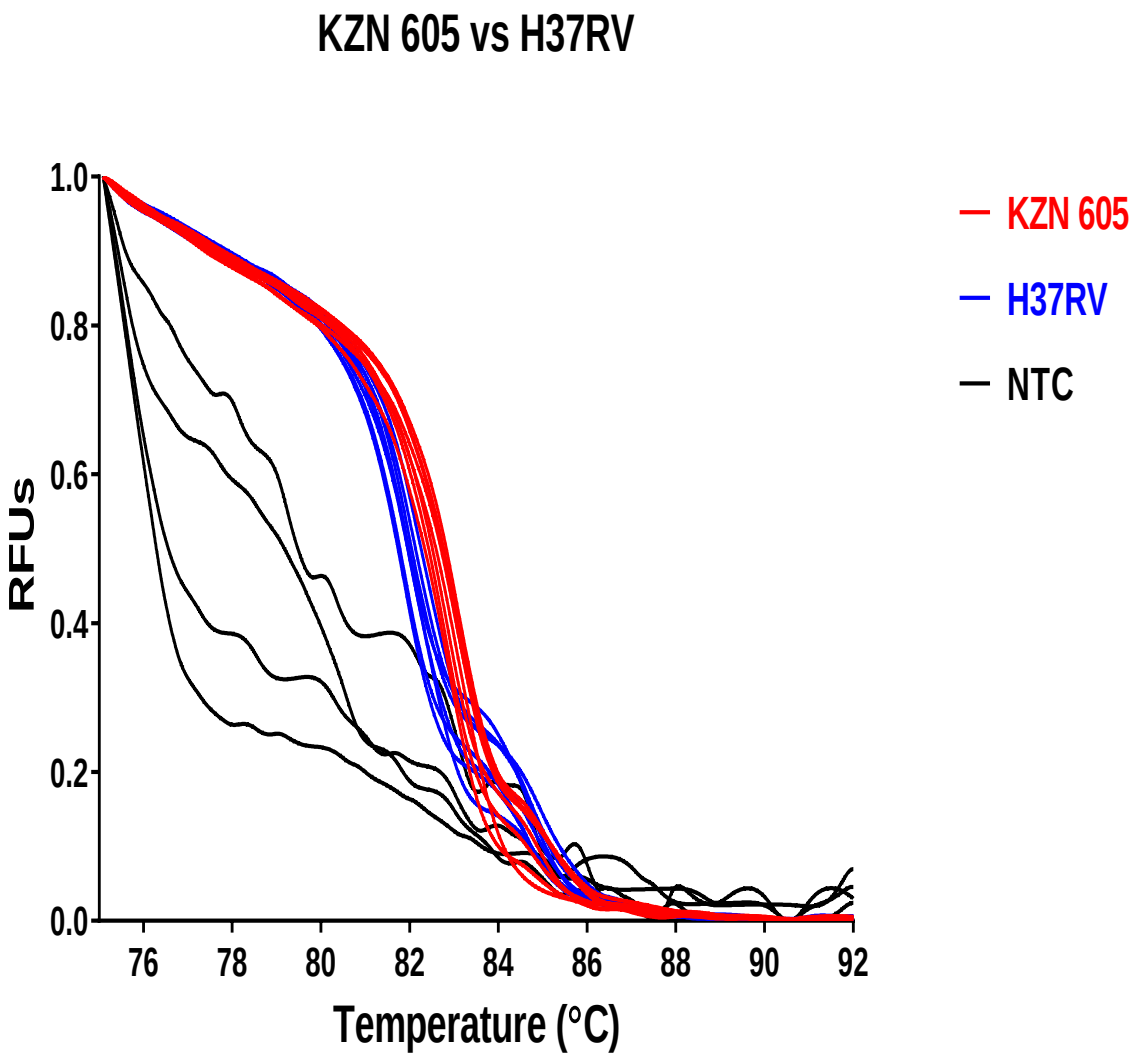

Figure 21: Melt curve profile from the amplification of the *rpoB* amplicons of Kzn 605 and H37Rv. The graph above shows how the amplicons from Kzn 605 and H37Rv denatured during the melting process. Kzn 605 amplicons seem to have a higher melting point temperature in comparison to the H37Rv samples. The graph shows that the non-template control reactions had lower melting point temperatures. Both Kzn 605 and H37Rv showed a biphasic melting curve profile which, in which the product appears to melt in two stages. It can be concluded that H37Rv has as distinct profile compared to Kzn 605.

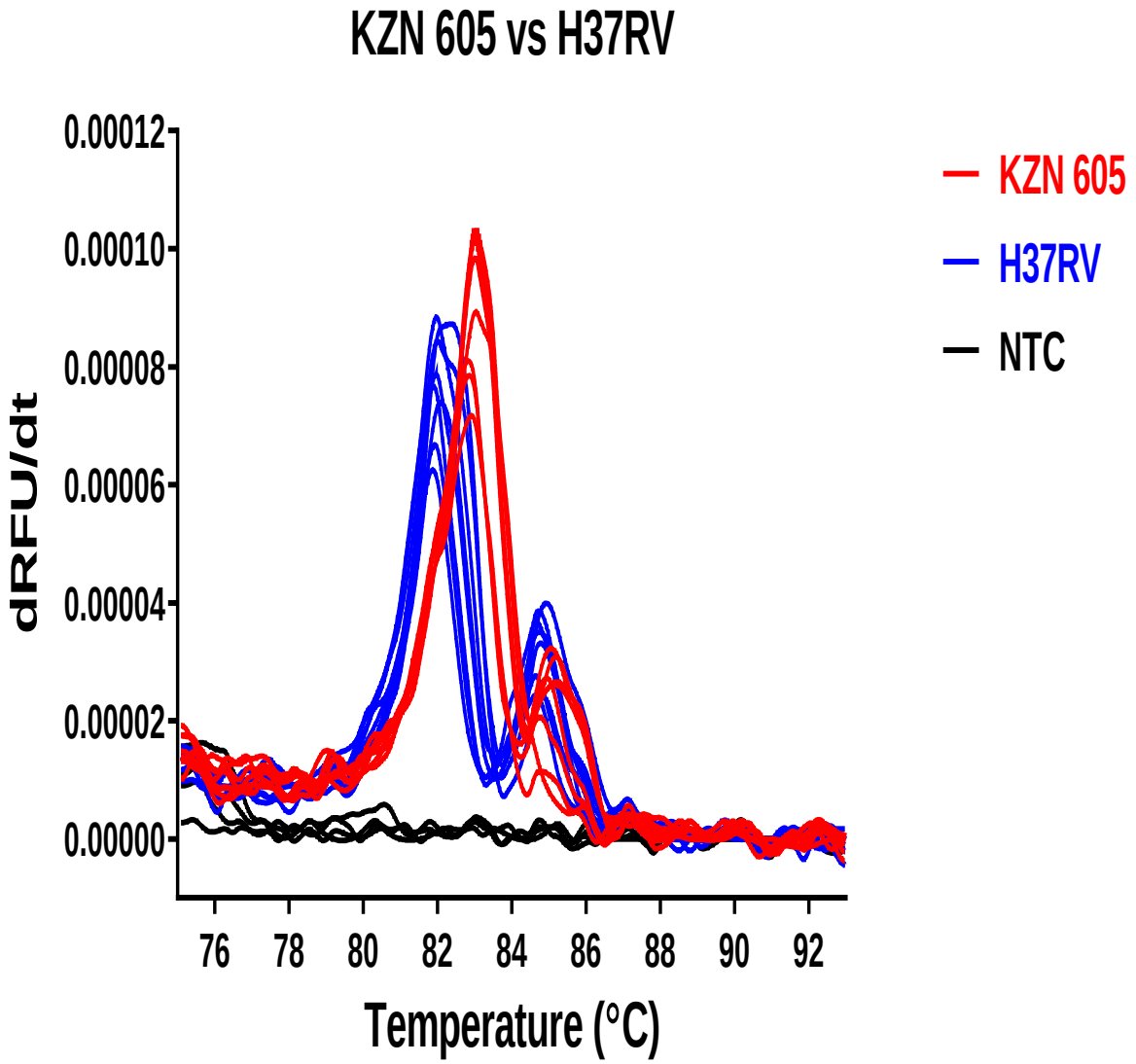

Figure 22: Derivative plot for the H37Rv and Kzn 605 *rpoB* amplicons. The graph above shows the derivative plot from the melt data of H37Rv and Kzn 605. The graph shows two distinct peaks for the replicates of sample, There is no peak in the non-template control with the region were the target amplicon. Thus it can be concluded that the reaction was successful in differentiating the amplicons. Both samples showed a minor peak after the more abundant peak, perhaps due to a glitch in the measurement of the signal.

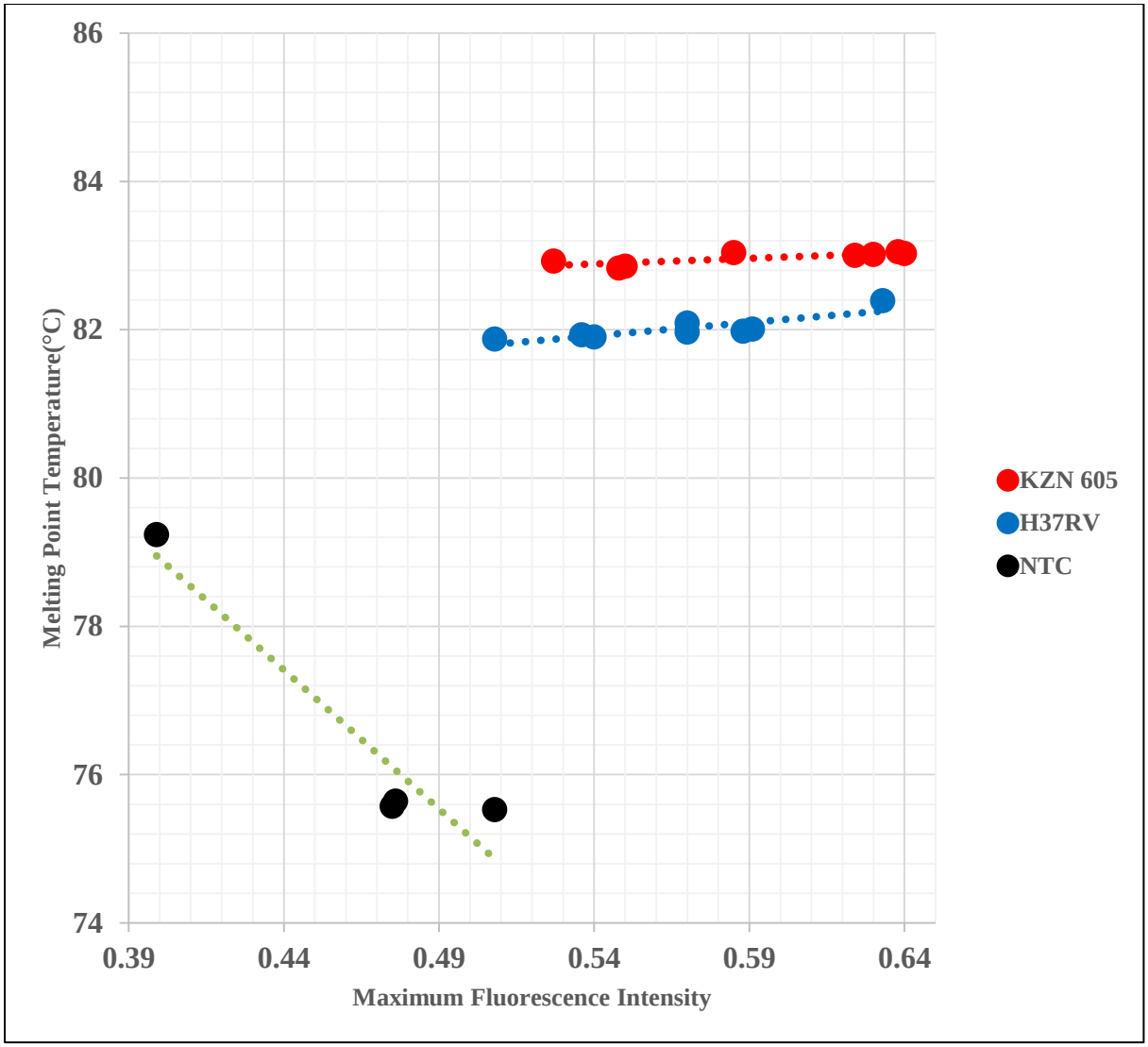

Figure 23: Visual variation of the melting point temperature of H37Rv vs Kzn 605 at the *rpoB* amplicon. The figure above shows the differences in the melting point temperature between H37Rv and Kzn 605. There is a clear and well defined difference between the general melting point temperatures of these two strains of about 1°C. This about a 1.5 fold increase from the 0.62°C observed on the Light Cycler96. However, this difference was lower than expected considering that Kzn 605 showed a higher temperature difference than that of R35 on the Light Ccyler96 system. The lower Tm values from the non-template controls affirm that the reaction was not affected by contamination, as the positive non-template reaction was due to primer dimers.

In summary, it can be concluded that the Light Forge system can detect mutations linked to drug resistance with Kzn 605, increasing the temperature difference by 1.5 fold.

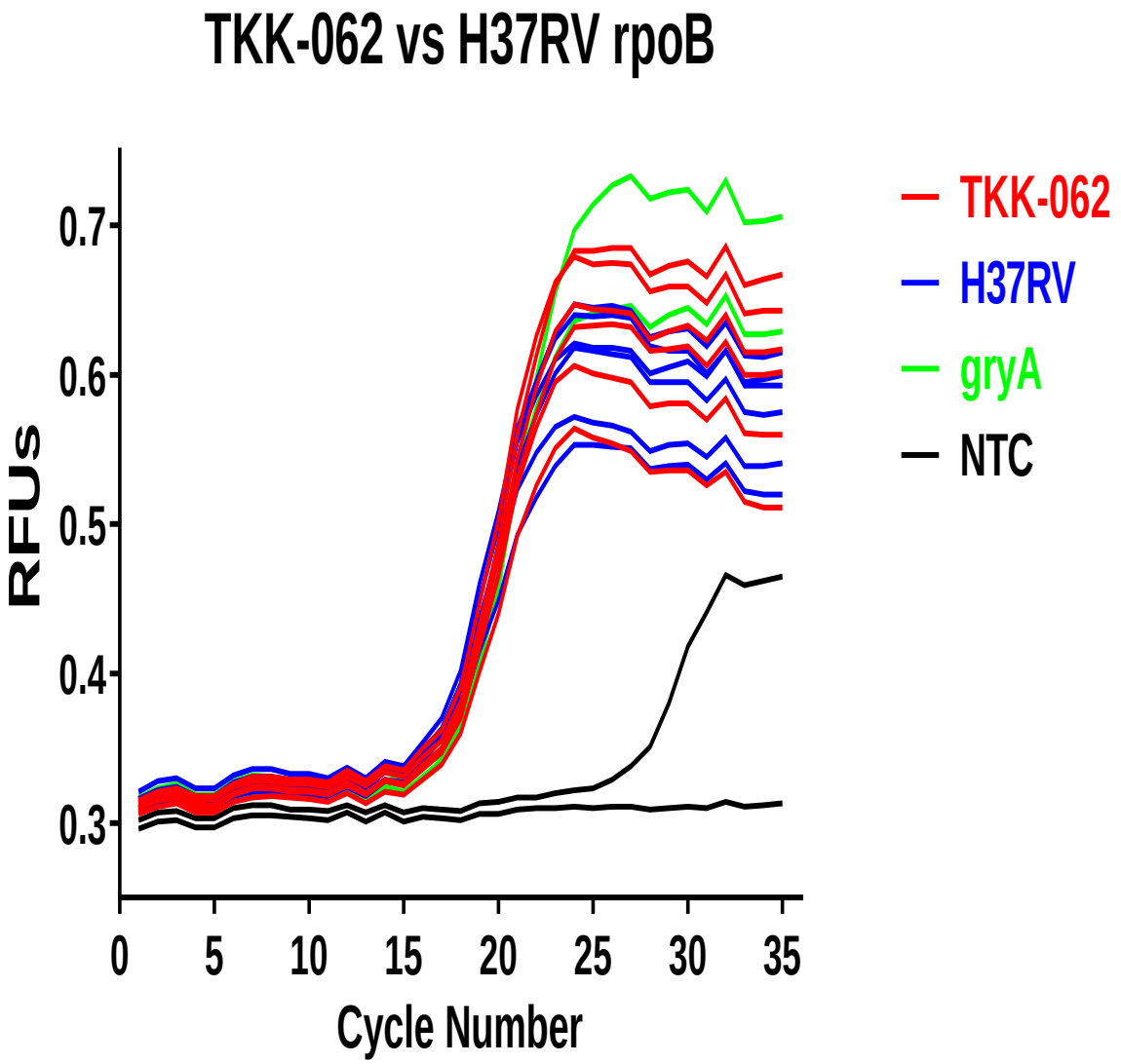

Figure 24: Amplification profile of H37Rv and Tkk-062 samples at the rpoB loci. The above graph shows the amplification profile of Tkk-062 and H37Rv. The graph shows that both H37Rv and Tkk-062 reached the exponential phase around the 17th cycle. One of the non-template control replicates reached the exponential phase around the 27th cycle. A positive control of *gyrA* amplified from H37Rv was used as a positive control. Thus, it was concluded that the amplification process occurred efficiently. The positive reaction in the non-template control can be due to contamination or the presence of primer dimers, but the subsequent plots will assert this.

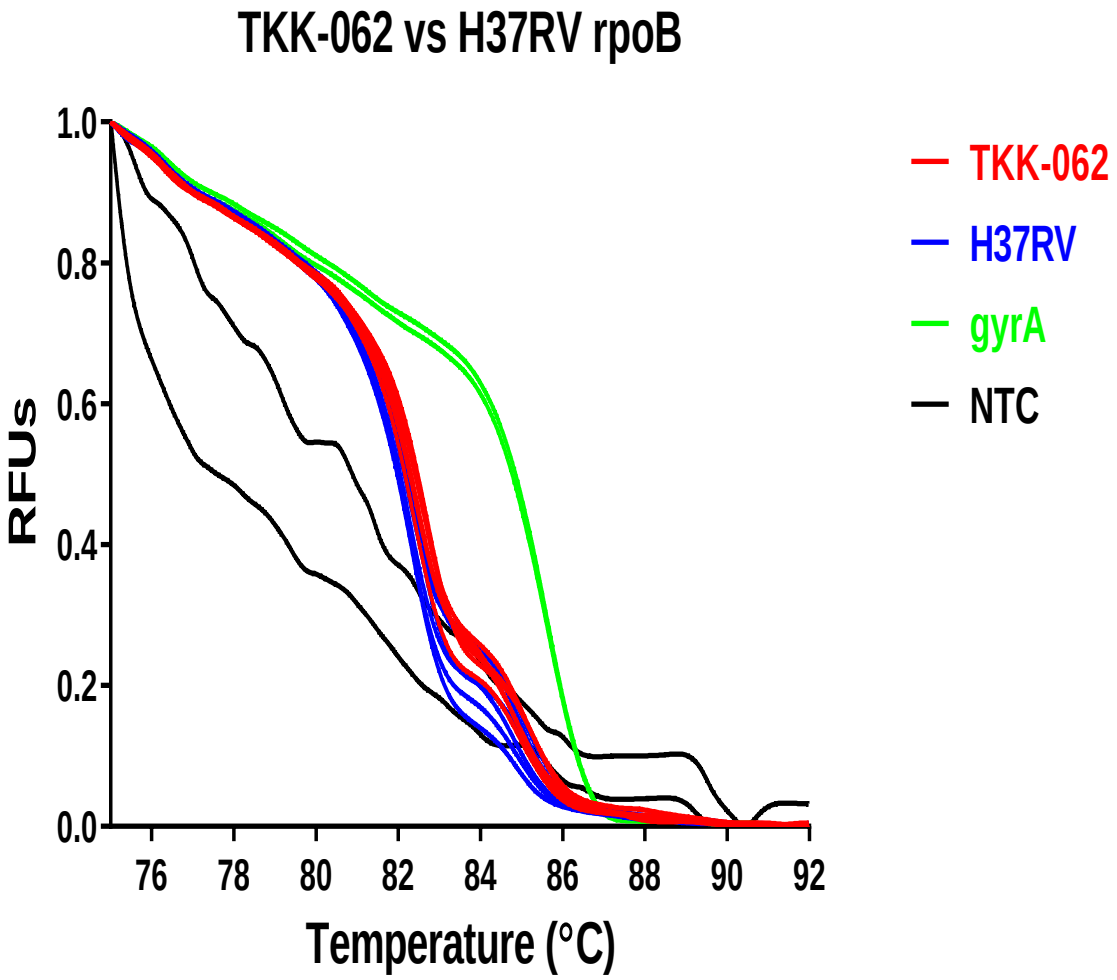

Figure 25: Melt curve of Tkk-062 and H37Rv at the *rpoB* region. The above figure shows the differences in melting profile of the standard strain vs the test Tkk-062. The amplicons showed melt curves that were almost identical with minor deviations. The Tkk-062 shows a profile that is skewed to the right of H37Rv because of the mutations. Both samples showed a curious The *gyrA* amplicons showed melting point temperatures much higher than *rpoB*. From this profile, it is difficult to ascertain with high confidence if the amplicons are distinct because of the overlap. In such cases, subsequent plots are useful to further probe the differences.

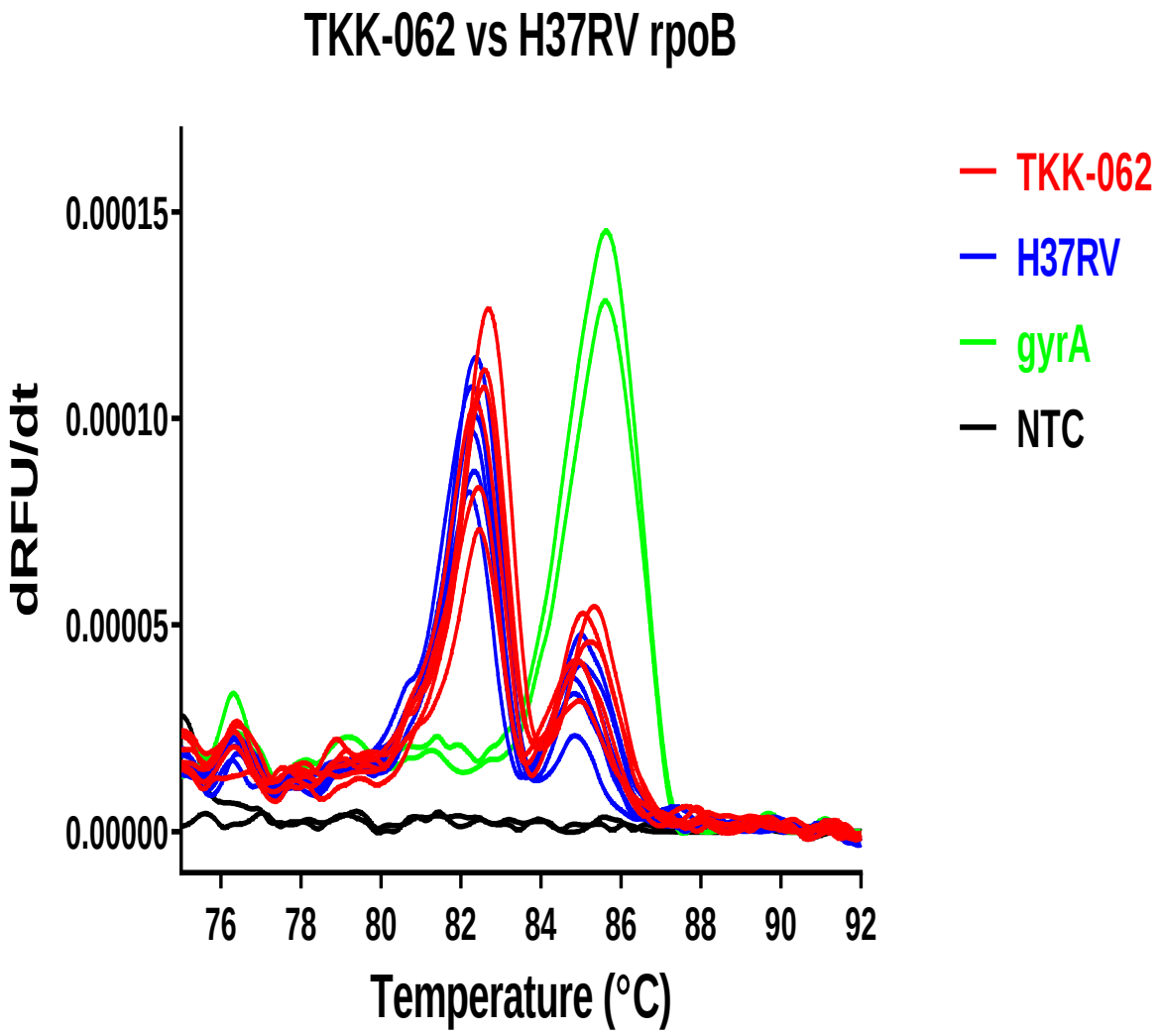

Figure 26: Derivative plot showing the melting point peaks of H37Rv and Tkk-062. The derivative plots show the location of the melt derivative curve peaks for the different samples. H37Rv and Tkk-062 show slightly different locations of the melt peaks around the 82°C. There is a hint of deviation between the samples but it is not easily discernible. The *gyrA* amplicon shows melt peaks located at a higher temperature around 86°C. The non-template control shows that the positive reaction was because of primer dimers. Thus, it is concluded that the derivative peaks managed to detect the slight variation in the melting point temperature albeit with a lower confidence.

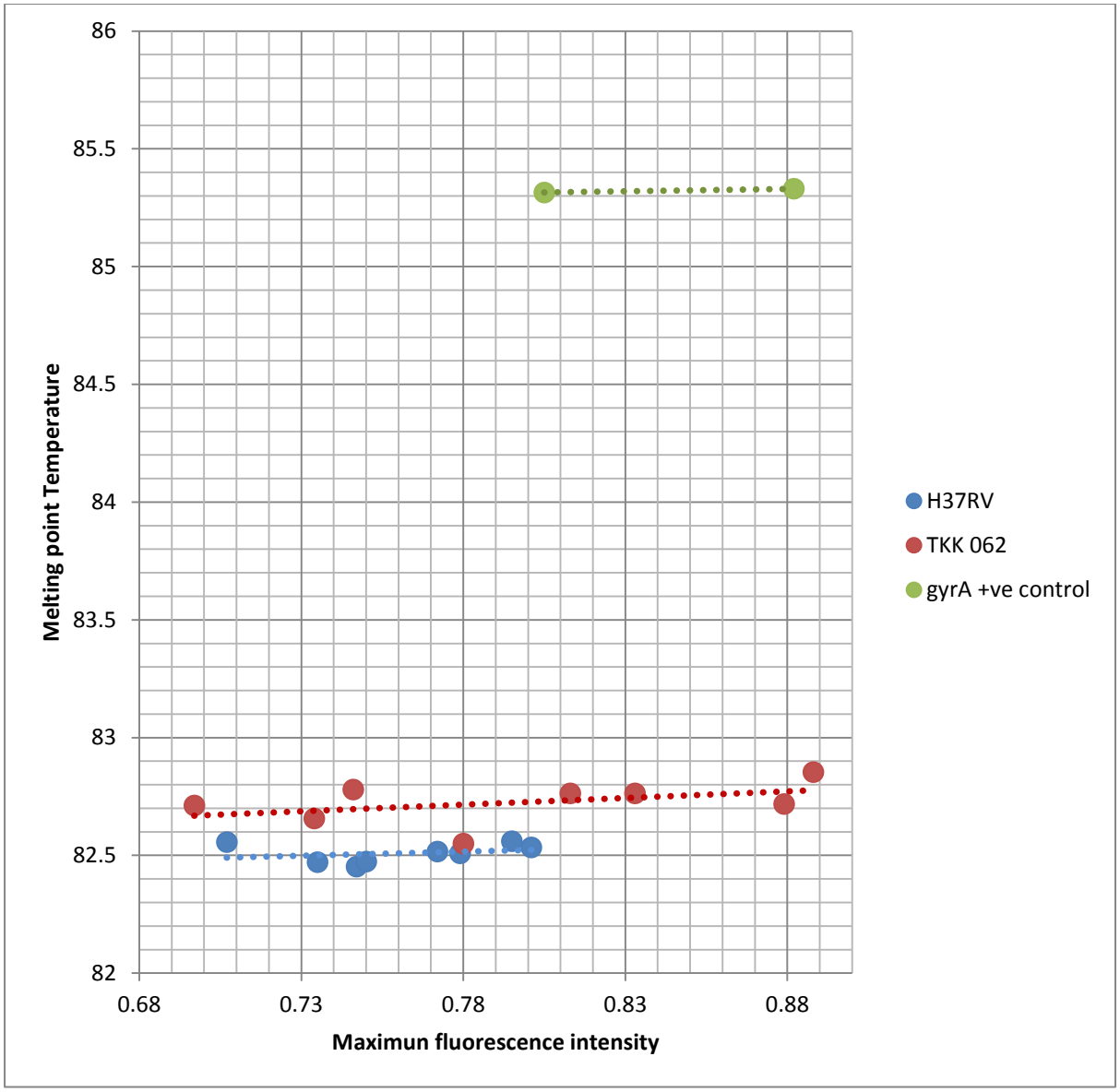

Figure 27: Melting point temperature of H37Rv vs Tkk-062 at the rpoB loci. The figure shows a small difference between the melting point temperature of H37rv and that of Tkk062. The difference in the Tm values of H37Rv and Tkk-062 of approximately 0.1°C (10-fold increase) compared to 0.01°C on the Light Cycler96. The *gyrA* positive control showed a very high Tm value of 85.2°C as opposed to 91.3°C observed on the Light Cycler96. The non-template controls show an expected lower melting point temperature, thus the positive reaction in the non-template controls was a result of the primer dimers**.**

In summary, the Light Forge assay could detect the mutation linked to drug resistance. It should be noted that this finding is a low confidence positive result due to diminished temperature difference.

Thus, Light Forge detected three out three mutations at the *rpoB* loci with **100% sensitivity**.

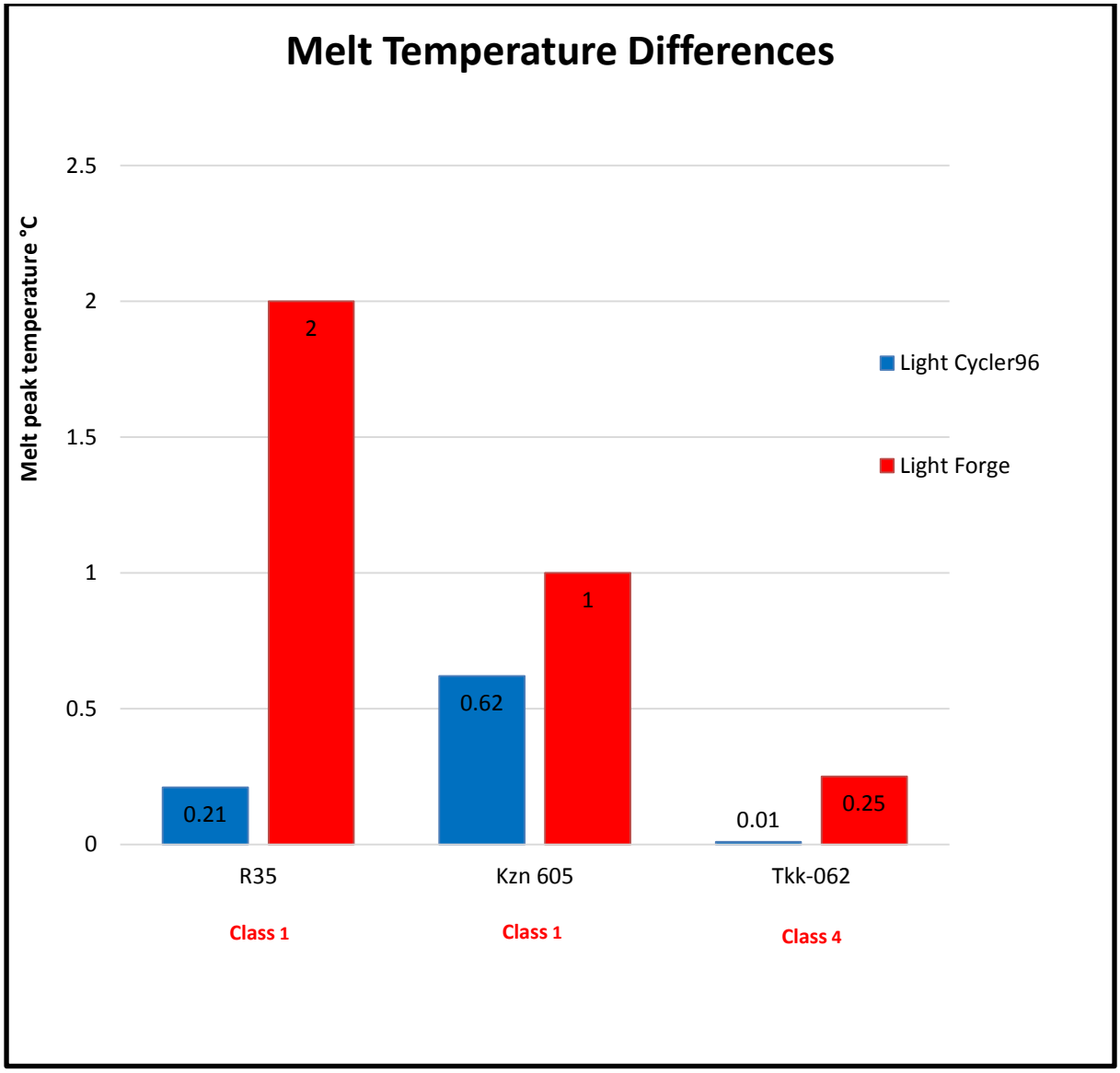

Figure 28: Pictorial summary of derivative peak temperatures as detected by the Light Cycler96 and the Light Forge system. The above graph shows the differences in the average melting point differences observed for the rpoB amplicons of H37Rv and the selected strains. In all iterations, the Light Forge device amplified the size of the deviation detected by the Light Cycler96. Consistently large deviations greater than 0.5°C were observed with the microfluidic system when used to detect class 1 mutation in R35 and Kzn 605. Light Forge also outperformed the Light Cycler96 when used to detect the class 4 mutation present in Tkk-062. In summary, the Light Forge amplified the sensitivy of the rifampin assay .

CHAPTER 4: DISCUSSION

Resistance to rifampin has been largely attributed to mutation of bases in the *rpoB* 81bp region, from codons 507 to 533 [53]. This region accounts for 95% of the incidence of rifampin resistance[264]. The remaining 5% is attributed to mutations outside this region such as V176F or Rv2629 gene [269]. Resistance to isoniazid, is determined by multiple genes such as *katG*, *mab-inhA* promoter region, *kasA*, *oxyR* and *aphC*, mainly as compensatory mechanisms by which the *M.tuberculosis* averts drug pressure [53]. The *katG* gene is thought to account for 50 to 70% of isoniazid resistance isolates, whilst *mab-inhA* is responsible for 15 to 20% of the resistance isolates[53]. Combining these two in a diagnostic assay increases the chances of detecting strains of *M.tuberculosis* with resistance to the drug. Quinolone resistance is due to mutations in the *gyrA* gene, which has been reported to be the cause of this phenotype in 42 to 85% of the cases [270,271].

In this study, six out of the seven (86% sensitivity) strains with the *rpoB* mutations were detected using the Light Cycler96 system, producing four distinct profiles during the rifampin resistance assay. The only exception was Tkk062, which registered as a susceptible strain. This was caused by the presence of a class 4 mutation (A to T) at codon 526, which involves switching of the nucleotides from one strand to another, thereby causing a diminished thermal aberration [270]. Literature suggests that the most frequently observed mutations in the *rpoB* region are located on codon 531, which was not the case for this panel of test strains[272].

For isoniazid resistance, the two genes with the most understood influence, *katG* and *mab-inhA* were separately analysed. As shown by the difference plot in Figure 7, HRMA managed to detect one out of a possible six (17% sensitivity) mutations in the *katG* region. However, a rather interesting profile was observed in figure 6, where R35 and Tkk043, which contain the same mutation at codon 315 (as shown in table 8), appear to have an identical temperature profile. However, this deviation is undetectable in the difference plot. It is difficult to assign resistance based on temperature variation, especially since the Light Cycler96 technical specification document states that the melting temperature can vary with ±0.4°C. All the other strains with the exception of R271, showed a similar melting point temperature as they all harboured the guanine to cytosine mutation which is associated with a low temperature change of less than 0.4°C [270]. Tkk039 displayed a curiously lower melting point temperature in spite of harbouring the same S315T mutation as Kzn 605, Tkk050 and Tkk039. For the *mab-inhA* promoter region, Light Cycler96 detected none of the three mutants, inexplicably detecting R35 as mutant, even though it has no mutation in this region. Careful analysis of the actual melting point temperatures show a more expected profile in figure 9, with the mutants clearly deviating from the reference strain. The apparent deviation between the difference plot and the melting point temperature plot suggests that more optimisation is required to establish which is more superior, as the results for both these genes were rather confounding. Consistent with these findings, a study by Yadav *et al* reported that two strains which were shown to be isoniazid susceptible via both

culture methods and sequencing, produced variant HRMA profiles[120]. These deviations could have been because of instrument, reagent or even PCR variations. In light of these drawbacks, these two genes were not used on the microfluidic platform.

For ofloxacin resistance, the *gyrA* gene was used and managed to detect the only strain with the resistance-linked mutations, which was the Kzn 605. The rest of the test strains had the S95T mutation, a rather unfortunate finding, as this is a non-synonymous mutation. This means that the particular mutation has no bearing on the drug resistance profile of the *M.tuberculosis*. It is commonly detected in *M.tuberculosis* strains of the beijing genotype [271]. This can be addressed by using H37Ra as the standard strain, as it contains this mutation or developing primer sets that circumvent the 95 codon [167]. Kzn 605 showed a very distinct profile in the difference plot as shown in figure 13, which corresponded moderately well with the melting point graph shown in figure 12. As observed during the isoniazid resistance assay, R35 behaved unexpectedly as it gave a distinct profile in the difference profile but a typical orientation in the melting point temperature plot. Again, the disparities observed when probing mutations with the commercial system for this gene meant that the strains could not be studied using the microfluidic system. It is interesting to note that R35 amplified late for the *katG*, *mab-inhA* and *gyrA* reactions as shown by figure 5, figure 8 and figure 11 respectively. This suggests that the R35 might have contained a constituent that somehow delayed the amplification process. This is feasible considering that the sample originates from a complex multi-step DNA extraction protocol with several salts and solvents that can affect the activity of the polymerase.

Based on the results from the conventional HRMA Light Cycler96 system, further testing of the test strains was done for the *rpoB* gene on the Light Forge device. R35 was clearly distinguished from H37Rv as shown in figure 17-19. An impressive observation was that the melting point temperature difference between the strains was approximately 2°C, a 10-fold increase in comparison with the Light Cycler96 system as shown by the average melting point temperatures in table 4. A similar distinction was observed when Kzn 605 was compared to the H37Rv, in which the melting point temperature difference was 1°C as opposed to the 0.62°C as observed in the conventional system. However, this was unexpected, as Kzn 605 had a larger melting point deviation on the commercial system than R35. This can be explained by the mechanical variation often observed during HRMA as a result of suspected non-uniformity in the heating and optical system [273]. Tkk-062 yielded a very small thermal deviation of approximately 0.1°C when compared to H37Rv as shown in figure 18, again a tenfold increase from the largely insignificant 0.01°C observed on the commercial system. Examination of figure 22 and 26 shows a minor peak in the derivative plots after the pronounced peaks, an occurrence not observed in the commercial system. Green suggested that appearance of double peaks is a result of either amplification of short length chimeric products or background nucleic acids depending on the sample source[113]. These claims were discounted as the non-specific products melt before the pronounced peak and the DNA originated from pure cultures of the strains as

opposed to mammalian samples where this occurrence is frequent. A more plausible explanation is that the various electronic components used during data acquisition might be subject to random deviations because of fluxes leading to an artificial peak. Considering the fact that Wi-Fi signals are abundant in the laboratory, a manner to shield the system from this interference should be considered in a bid to improve the measurement.

These findings suggest that the microfluidic system, when properly optimized could yield better analytical performance of the HRMA that can ultimately lead to adoption of this protocol in the clinical setting. A study by Phowlat *et al* reported the use of TaqMan array card which can perform the same HRMA on 10 genes linked with *M.tuberculosis* resistance [163]. The study used HRMA in combination with mutation specific hydrolysis probes, using the former to detect unknown mutations on a platform that performed 48 separate reactions, with a volume of 1µl, for eight separate samples. Such a device is brilliant in principle but further designing is required for this system to be adaptable to the emerging market where this innovation is needful when the cost of the probes, machinery and maintenance services are considered, creating a void systems such as the Light Forge can fill.

In spite of the potential that such approaches possess in terms of *M.tuberculosis* diagnosis, HRMA needs to address the several drawbacks. The saturating dyes used to detect the PCR product are not specific to any sequence thus sometimes atypical PCR products are detected [169]. HRMA is dependent on a high quality and quantity input DNA sample, which is not guaranteed when working with clinical samples such as sputum. Such a challenge can be avoided by adding a sputum processing module on a microfluidic chip that can extract DNA [274], which would help in the capture and detection of wild strains of tuberculosis. Alternatively, the cheap methods currently used to decontaminate sputum samples can be used in conjuction with PCR additives that enhance amplification such α-casein or BSA, increasing sensitivity of the assay [275]. Nagai et al showed in a study that wild strains are detectable with very high accuracy with HRMA using strains from Mie-Chuo Medical centre, confirming results with culture and sanger sequencing[162].

HRMA is also prone to the detection of false positives [276] i.e. silent mutations which are not actually linked with drug resistance, suggesting that more research is required to fully comprehend the mechanisms that lead to drug tolerance. As a consequence, molecular assays still require phenotypic testing before a high confidence resistance profile can be confirmed [277]. Since molecular assays target nucleic acids, there is a high chance of them detecting DNA from dead *M.tuberculosis* cells which would be culture negative as reported in the study by Rachow and *et al* with the Gene Xpert system [274]. Unfortunately, patients are subsequently receiving treatment they do not require.

Conclusion

Light Forge demonstrated its ability to detect mutations that are linked to rifampin resistance in the test *M.tuberculosis* strains. This ability can be translated to an affordable, quick and easily accessible assay that can be used in resource poor communities, as the platform is cost conscious as reflective in the use of saturating dyes and miniaturization. With reported increases in the cases of drug resistance [277], there is a need for efforts to be rapidly channelled towards providing patients, within the emerging markets, a diagnostic solution with the potential to positively shift the Tuberculosis pandemic.

Recommendations

The first recommendation would be to include other genes that are associated with drug resistance such as *gyrA,gyrB katG,mab-inhA, embB, pncA*, rrs etc in a bid to understand the profile of the *M.tuberculosis* pathogen. This can be an extension of the concept of personalized medicine, in which the treatment plan is fully instructed by the patient specific profile [278]. This can lead to more powerful, precise and predictable health management systems at a very personal level. Such an approach would also require patient genetic and environmental backgrounds to be considered as these also play a key role in how patients respond to any given treatment[279]. This would require an increase in the number of reactors to accommodate the other targets and re-optimisation but it is quite easily achievable as all the expertise required are available in house. An increase in the number of test strains is needful, especially increasing the number of strains lacking the mutation to have a much more reliable specificity estimate. Following from the reviewed articles summarised in table 2, a minimum number of 50 samples in the assay can easily achieve the desired specificity.

The second recommendation would be to design a microfluidic device that can probe the various mechanisms of heteroresistance in *M.tuberculosis* [280]. This is when a host is simultaneously infected with drug resistant and drug susceptible strains of *M.tuberculosis* [281]. It is suggested that this is a preliminary phase to full resistance but is often missed due to detection limits of the current methods. This is shown by the fact that a mutant strain of *M.tuberculosis* can only be detected if it is above 65% of the population of microorganisms when, for example, using the Gene Xpert device [282]. A microfluidic device with an increased number of partitions which can capture, amplify and detect sequence variants would be an indispensable tool for understanding the significance of this occurrence. Phowlat and *et al* have already carried out preliminary work by performing digital PCR on artificial mixtures of DNA from various strains of *M.tuberculosis* with very encouraging success [86].

References

1. Weis, S.E., *et al.* The effect of directly observed therapy on the rates of drug resistance and relapse in tuberculosis. *New England journal of medicine* **330**, 1179-1184 (1994).
2. Organization, W.H. The global plan to stop TB 2011-2015: transforming the fight towards elimination of tuberculosis. (2010).
3. Antony, S.J., Harrell, V., Christie, J.D., Adams, H.G. & Rumley, R.L. Clinical differences between pulmonary and extrapulmonary tuberculosis: a 5-year retrospective study. *Journal of the National Medical Association* **87**, 187 (1995).
4. Sheet, L.T.I.F. Latent Tuberculosis Infection.
5. Centre for disease control and prevention. (2013).Tuberculosis. (2013).
6. Abayomi, A. & Cowan, M.N. The HIV/AIDS epidemic in South Africa: Convergence with tuberculosis, socioecological vulnerability, and climate change patterns. *SAMJ: South African Medical Journal* **104**, 583-584 (2014).
7. Jamison, D.T. *Disease and mortality in sub-Saharan Africa*, (World Bank Publications, 2006).
8. Das, R., *et al.* Macrophage migration inhibitory factor (MIF) is a critical mediator of the innate immune response to Mycobacterium tuberculosis. *Proceedings of the National Academy of Sciences* **110**, E2997-E3006 (2013).
9. Naresh, R. & Tripathi, A. Modelling and analysis of HIV-TB co-infection in a variable size population. *Mathematical Modelling and Analysis* **10**, 275-286 (2005).
10. Pawlowski, A., Jansson, M., Skold, M., Rottenberg, M.E. & Kallenius, G. Tuberculosis and HIV co-infection. *PLoS Pathog* **8**, e1002464 (2012).
11. Bank, T.W. Incidence of Tuberculosis cases per 100000 people. Vol. 2015 (2015).
12. Mootoo, A., Stylianou, E., Arias, M.A. & Reljic, R. TNF-α in Tuberculosis: A Cytokine with a Split Personality. *Inflammation & Allergy-Drug Targets (Formerly Current Drug Targets-Inflammation & Allergy)* **8**, 53-62 (2009).
13. Lin, P.L., Plessner, H.L., Voitenok, N.N. & Flynn, J.L. Tumor necrosis factor and tuberculosis. in *Journal of Investigative Dermatology Symposium Proceedings*, Vol. 12 22-25 (Nature Publishing Group, 2007).
14. Patel, N.R., *et al.* HIV impairs TNF-α mediated macrophage apoptotic response to Mycobacterium tuberculosis. *The Journal of Immunology* **179**, 6973-6980 (2007).
15. Fauci, A.S. The human immunodeficiency virus: infectivity and mechanisms of pathogenesis. *Science* **239**, 617-622 (1988).
16. Rosas-Taraco, A.G., Arce-Mendoza, A.Y., Caballero-Olín, G. & Salinas-Carmona, M.C. Mycobacterium tuberculosis upregulates coreceptors CCR5 and CXCR4 while HIV

modulates CD14 favoring concurrent infection. *AIDS Research & Human Retroviruses* **22**, 45-51 (2006).

17. de Noronha, A.L., Bafica, A., Nogueira, L., Barral, A. & Barral-Netto, M. Lung granulomas from Mycobacterium tuberculosis/HIV-1 co-infected patients display decreased in situ TNF production. *Pathology-Research and Practice* **204**, 155-161 (2008).
18. Nakata, K., *et al.* Mycobacterium tuberculosis enhances human immunodeficiency virus-1 replication in the lung. *American journal of respiratory and critical care medicine* **155**, 996-1003 (1997).
19. Kedzierska, K., Crowe, S.M., Turville, S. & Cunningham, A.L. The influence of cytokines, chemokines and their receptors on HIV-1 replication in monocytes and macrophages. *Reviews in medical virology* **13**, 39-56 (2003).
20. Geijtenbeek, T.B., *et al.* DC-SIGN, a dendritic cell–specific HIV-1-binding protein that enhances trans-infection of T cells. *cell* **100**, 587-597 (2000).
21. Jiao, X., *et al.* Dendritic cells are host cells for mycobacteria in vivo that trigger innate and acquired immunity. *The Journal of Immunology* **168**, 1294-1301 (2002).
22. Brindle, R.J., *et al.* Infection and morbidity in patients with tuberculosis in Nairobi, Kenya. *AIDS* **7**, 1469-1474 (1993).
23. Reid, M.J. & Shah, N.S. Approaches to tuberculosis screening and diagnosis in people with HIV in resource-limited settings. *The Lancet infectious diseases* **9**, 173-184 (2009).
24. Getahun, H., Harrington, M., O'Brien, R. & Nunn, P. Diagnosis of smear-negative pulmonary tuberculosis in people with HIV infection or AIDS in resource-constrained settings: informing urgent policy changes. *The Lancet* **369**, 2042-2049 (2007).
25. Mukolo, A., Villegas, R., Aliyu, M. & Wallston, K.A. Predictors of late presentation for HIV diagnosis: a literature review and suggested way forward. *AIDS and Behavior* **17**, 5-30 (2013).
26. Crum, N.F., *et al.* Comparisons of causes of death and mortality rates among HIV-infected persons: analysis of the pre-, early, and late HAART (highly active antiretroviral therapy) eras. *JAIDS Journal of Acquired Immune Deficiency Syndromes* **41**, 194-200 (2006).
27. Badri, M., Wilson, D. & Wood, R. Effect of highly active antiretroviral therapy on incidence of tuberculosis in South Africa: a cohort study. *The Lancet* **359**, 2059-2064 (2002).
28. Leonard, M.K., *et al.* Increased survival of persons with tuberculosis and human immunodeficiency virus infection, 1991–2000. *Clinical infectious diseases* **34**, 1002-1007 (2002).
29. Wood, A.J., Piscitelli, S.C. & Gallicano, K.D. Interactions among drugs for HIV and opportunistic infections. *New England Journal of Medicine* **344**, 984-996 (2001).

30. Lecoeur, H.F., Truffot-Pernot, C. & Grosset, J.H. Experimental short-course preventive therapy of tuberculosis with rifampin and pyrazinamide. *American Journal of Respiratory and Critical Care Medicine* **140**, 1189-1193 (1989).
31. Blumberg, H., *et al.* American Thoracic Society/Centers for Disease Control and Prevention/Infectious Diseases Society of America: treatment of tuberculosis. *American journal of respiratory and critical care medicine* **167**, 603 (2003).
32. Raviglione, M.C., Narain, J.P. & Kochi, A. HIV-associated tuberculosis in developing countries: clinical features, diagnosis, and treatment. *Bulletin of the World Health Organization* **70**, 515 (1992).
33. Sharma, S., Mohan, A. & Kadhiravan, T. HIV-TB co-infection: epidemiology, diagnosis & management. *Indian Journal of Medical Research* **121**, 550-567 (2005).
34. Dean, G.L., *et al.* Treatment of tuberculosis in HIV-infected persons in the era of highly active antiretroviral therapy. *Aids* **16**, 75-83 (2002).
35. Murdoch, D.M., Venter, W.D., Van Rie, A. & Feldman, C. Immune reconstitution inflammatory syndrome (IRIS): review of common infectious manifestations and treatment options. *AIDS research and therapy* **4**, 9 (2007).
36. Abdool Karim, S.S., *et al.* Timing of initiation of antiretroviral drugs during tuberculosis therapy. *New England Journal of Medicine* **362**, 697-706 (2010).
37. Niemi, R. Tuberculosis Treatments Past and Present. Vol. 2015 (Intellectual Ventures Laboratory, 2014).
38. Daniel, T.M. The history of tuberculosis. *Respiratory medicine* **100**, 1862-1870 (2006).
39. Keers, R. Pneumoperitoneum: Its place in treatment. *British Journal of Tuberculosis and Diseases of the Chest* **42**, 58-IN56 (1948).
40. Matson, R.W. Exairesis of the phrenic nerve in the treatment of pulmonary tuberculosis. *Am. Rev. Tuberc.* **22**, 1-34 (1930).
41. Iseman, M.D., Madsen, L., Goble, M. & Pomerantz, M. Surgical intervention in the treatment of pulmonary disease caused by drug-resistant Mycobacterium tuberculosis. *American Journal of Respiratory and Critical Care Medicine* **141**, 623-625 (1990).
42. Lerner, K.L. & Lerne, B.W. World of microbiology and immunology. (2003).
43. Kolyva, A.S. & Karakousis, P.C. *Old and new TB drugs: Mechanisms of action and resistance*, (INTECH Open Access Publisher, 2012).
44. Zumla, A., Nahid, P. & Cole, S.T. Advances in the development of new tuberculosis drugs and treatment regimens. *Nature reviews Drug discovery* **12**, 388-404 (2013).
45. Robitzek, E.H. & Selikoff, I.J. Hydrazine derivatives of isonicotinic acid (rimifon marsilid) in the treatment of active progressive caseous-pneumonic tuberculosis; a preliminary report. *American review of tuberculosis* **65**, 402-428 (1952).

46. Raynaud, C., *et al.* Mechanisms of pyrazinamide resistance in mycobacteria: importance of lack of uptake in addition to lack of pyrazinamidase activity. *Microbiology* **145**, 1359-1367 (1999).
47. Gangadharam, P., Harold, F. & Schaefer, W. Selective inhibition of nucleic acid synthesis in Mycobacterium tuberculosis by isoniazid. *Nature* **198**, 712-714 (1963).
48. Winder, F. & Collins, P. Inhibition by isoniazid of synthesis of mycolic acids in Mycobacterium tuberculosis. *Journal of general microbiology* **63**, 41-48 (1970).
49. Banerjee, A., *et al.* inhA, a gene encoding a target for isoniazid and ethionamide in Mycobacterium tuberculosis. *Science* **263**, 227-230 (1994).
50. Lin, S.-J. & Guarente, L. Nicotinamide adenine dinucleotide, a metabolic regulator of transcription, longevity and disease. *Current opinion in cell biology* **15**, 241-246 (2003).
51. Rozwarski, D.A., Grant, G.A., Barton, D.H., Jacobs, W.R. & Sacchettini, J.C. Modification of the NADH of the isoniazid target (InhA) from Mycobacterium tuberculosis. *Science* **279**, 98-102 (1998).
52. Wade, M. & Zhang, Y. Mechanisms of drug resistance in Mycobacterium tuberculosis. *Frontiers in bioscience: a journal and virtual library* **9**, 975-994 (2004).
53. Ramaswamy, S. & Musser, J.M. Molecular genetic basis of antimicrobial agent resistance inMycobacterium tuberculosis: 1998 update. *Tubercle and Lung disease* **79**, 3-29 (1998).
54. Karakousis, P.C. Mechanisms of action and resistance of antimycobacterial agents. in *Antimicrobial drug resistance* 271-291 (Springer, 2009).
55. Grosset, J., *et al.* Once-weekly rifapentine-containing regimens for treatment of tuberculosis in mice. *American journal of respiratory and critical care medicine* **157**, 1436-1440 (1998).
56. Cynamon, M.H., Klemens, S.P., Chou, T.S., Gimi, R.H. & Welch, J.T. Antimycobacterial activity of a series of pyrazinoic acid esters. *Journal of medicinal chemistry* **35**, 1212-1215 (1992).
57. Heifets, L. & Lindholm-Levy, P. Pyrazinamide sterilizing activity in vitro against semidormant Mycobacterium tuberculosis bacterial populations. *Am Rev Respir Dis* **145**, 1223-1225 (1992).
58. Mitchison, D. Mechanisms of the action of drugs in the short-course chemotherapy. *Bulletin of the International Union against Tuberculosis* **60**, 36 (1985).
59. Zhang, Y., Wade, M.M., Scorpio, A., Zhang, H. & Sun, Z. Mode of action of pyrazinamide: disruption of Mycobacterium tuberculosis membrane transport and energetics by pyrazinoic acid. *Journal of Antimicrobial Chemotherapy* **52**, 790-795 (2003).
60. Keiler, K.C. Biology of trans-translation. *Annu. Rev. Microbiol.* **62**, 133-151 (2008).
61. Juréen, P., Werngren, J., Toro, J.-C. & Hoffner, S. Pyrazinamide resistance and pncA gene mutations in Mycobacterium tuberculosis. *Antimicrobial agents and chemotherapy* **52**, 1852-1854 (2008).

62. Donald, P., Maher, D., Maritz, S. & Qazi, S.A. Ethambutol efficacy and toxicity: literature review and recommendations for daily and intermittent dosage in children. (2006).
63. Mikusová, K., Slayden, R.A., Besra, G.S. & Brennan, P.J. Biogenesis of the mycobacterial cell wall and the site of action of ethambutol. *Antimicrobial agents and chemotherapy* **39**, 2484-2489 (1995).
64. Cheema, S. & Khuller, G. Metabolism of phospholipids in Mycobacterium smegmatis ATCC 607 in the presence of ethambutol. *The Indian journal of medical research* **82**, 207-213 (1985).
65. Da Silva, P.E.A. & Palomino, J.C. Molecular basis and mechanisms of drug resistance in Mycobacterium tuberculosis: classical and new drugs. *Journal of antimicrobial chemotherapy* **66**, 1417-1430 (2011).
66. Bosne-David, S., Barros, V., Verde, S.C., Portugal, C. & David, H.L. Intrinsic resistance of Mycobacterium tuberculosis to clarithromycin is effectively reversed by subinhibitory concentrations of cell wall inhibitors. *Journal of antimicrobial chemotherapy* **46**, 391-395 (2000).
67. Baquero, F. Epigenetics, epistasis and epidemics. *Evolution, Medicine, and Public Health* **2013**, 86-88 (2013).
68. Bierne, H., Hamon, M. & Cossart, P. Epigenetics and bacterial infections. *Cold Spring Harbor perspectives in medicine* **2**, a010272 (2012).
69. Dhar, N. & McKinney, J.D. Mycobacterium tuberculosis persistence mutants identified by screening in isoniazid-treated mice. *Proceedings of the National Academy of Sciences* **107**, 12275-12280 (2010).
70. Gandhi, N.R., *et al.* Multidrug-resistant and extensively drug-resistant tuberculosis: a threat to global control of tuberculosis. *The Lancet* **375**, 1830-1843 (2010).
71. David, H.L. Probability distribution of drug-resistant mutants in unselected populations of Mycobacterium tuberculosis. *Applied microbiology* **20**, 810-814 (1970).
72. Menzies, D., *et al.* Standardized treatment of active tuberculosis in patients with previous treatment and/or with mono-resistance to isoniazid: a systematic review and meta-analysis. *PLoS medicine* **6**, 1057 (2009).
73. Jassal, M. & Bishai, W.R. Extensively drug-resistant tuberculosis. *The Lancet infectious diseases* **9**, 19-30 (2009).
74. Gandhi, N.R., *et al.* Extensively drug-resistant tuberculosis as a cause of death in patients co-infected with tuberculosis and HIV in a rural area of South Africa. *The Lancet* **368**, 1575-1580 (2006).
75. Facts, T. TB Drugs: First line, second line and new TB drugs. Vol. 2015 (2013).

76. Dooley, K.E., *et al.* World Health Organization group 5 drugs for the treatment of drug-resistant tuberculosis: unclear efficacy or untapped potential? *Journal of Infectious Diseases*, jis460 (2012).
77. Kuaban, C., *et al.* High effectiveness of a 12-month regimen for MDR-TB patients in Cameroon. *The International Journal of Tuberculosis and Lung Disease* **19**, 517-524 (2015).
78. Udwadia, Z.F. MDR, XDR, TDR tuberculosis: ominous progression. *Thorax* **67**, 286-288 (2012).
79. Migliori, G., De Iaco, G., Besozzi, G., Centis, R. & Cirillo, D. First tuberculosis cases in Italy resistant to all tested drugs. *Euro surveill* **12**, E070517 (2007).
80. Slomski, A. South Africa warns of emergence of "totally" drug-resistant tuberculosis. *Jama* **309**, 1097-1098 (2013).
81. Hofmann-Thiel, S., *et al.* Mechanisms of heteroresistance to isoniazid and rifampin of Mycobacterium tuberculosis in Tashkent, Uzbekistan. *European Respiratory Journal* **33**, 368-374 (2009).
82. Rinder, H. Hetero-resistance: an under-recognised confounder in diagnosis and therapy? *Journal of Medical Microbiology* **50**, 1018-1020 (2001).
83. Canetti, G., *et al.* Advances in techniques of testing mycobacterial drug sensitivity, and the use of sensitivity tests in tuberculosis control programmes. *Bulletin of the World Health Organization* **41**, 21 (1969).
84. Rinder, H., Mieskes, K. & Löscher, T. Heteroresistance in Mycobacterium tuberculosis. *The International Journal of Tuberculosis and Lung Disease* **5**, 339-345 (2001).
85. Gilliland, G., Perrin, S. & Bunn, H.F. Competitive PCR for quantitation of mRNA. *PCR protocols: A guide to methods and applications*, 60-69 (1990).
86. Pholwat, S., Stroup, S., Foongladda, S. & Houpt, E. Digital PCR to detect and quantify heteroresistance in drug resistant Mycobacterium tuberculosis. *PloS one* **8**, e57238 (2013).
87. Morand, B. & Mühlemann, K. Heteroresistance to penicillin in Streptococcus pneumoniae. *Proceedings of the National Academy of Sciences* **104**, 14098-14103 (2007).
88. Sakoulas, G., Alder, J., Thauvin-Eliopoulos, C., Moellering, R.C. & Eliopoulos, G.M. Induction of daptomycin heterogeneous susceptibility in Staphylococcus aureus by exposure to vancomycin. *Antimicrobial Agents and Chemotherapy* **50**, 1581-1585 (2006).
89. Gler, M.T., *et al.* Delamanid for multidrug-resistant pulmonary tuberculosis. *New England Journal of Medicine* **366**, 2151-2160 (2012).
90. Rodriguez, D. The Importance of Tuberculosis Awareness. Vol. 2015 (ed. Marcellin, L.) (2009).
91. Dorman, S.E. New diagnostic tests for tuberculosis: bench, bedside, and beyond. *Clinical Infectious Diseases* **50**, S173-S177 (2010).

92. Keeler, E., *et al.* Reducing the global burden of tuberculosis: the contribution of improved diagnostics. *Nature* **444**, 49-57 (2006).
93. Zumla, A., George, A., Sharma, V., Herbert, N. & of Ilton, B.M. WHO's 2013 global report on tuberculosis: successes, threats, and opportunities. *The Lancet* **382**, 1765-1767 (2013).
94. Andersen, P., Munk, M., Pollock, J. & Doherty, T. Specific immune-based diagnosis of tuberculosis. *The Lancet* **356**, 1099-1104 (2000).
95. Pai, M., Dheda, K., Cunningham, J., Scano, F. & O'Brien, R. T-cell assays for the diagnosis of latent tuberculosis infection: moving the research agenda forward. *The Lancet infectious diseases* **7**, 428-438 (2007).
96. Falkinham 3rd, J. Epidemiology of infection by nontuberculous mycobacteria. *Clinical microbiology reviews* **9**, 177 (1996).
97. Katoch, V. Newer diagnostic techniques for tuberculosis. *Indian Journal of Medical Research* **120**, 418-428 (2004).
98. Desikan, P. Sputum smear microscopy in tuberculosis: Is it still relevant? *The Indian journal of medical research* **137**, 442 (2013).
99. Hopewell, P.C., Pai, M., Maher, D., Uplekar, M. & Raviglione, M.C. International standards for tuberculosis care. *The Lancet infectious diseases* **6**, 710-725 (2006).
100. Steingart, K.R., *et al.* Sputum processing methods to improve the sensitivity of smear microscopy for tuberculosis: a systematic review. *The Lancet infectious diseases* **6**, 664-674 (2006).
101. Swingler, G., Du Toit, G., Andronikou, S., Van der Merwe, L. & Zar, H. Diagnostic accuracy of chest radiography in detecting mediastinal lymphadenopathy in suspected pulmonary tuberculosis. *Archives of disease in childhood* **90**, 1153-1156 (2005).
102. Van Cleeff, M., Kivihya-Ndugga, L., Meme, H., Odhiambo, J. & Klatser, P. The role and performance of chest X-ray for the diagnosis of tuberculosis: a cost-effectiveness analysis in Nairobi, Kenya. *BMC infectious diseases* **5**, 111 (2005).
103. Kim, S. Drug-susceptibility testing in tuberculosis: methods and reliability of results. *European Respiratory Journal* **25**, 564-569 (2005).
104. Trajstman, A. Diagnostic tests, sensitivity, specificity, efficiency and prevalence. *Australian veterinary journal* **55**, 501-501 (1979).
105. Simel, D.L., Samsa, G.P. & Matchar, D.B. Likelihood ratios with confidence: sample size estimation for diagnostic test studies. *Journal of clinical epidemiology* **44**, 763-770 (1991).
106. Šimundić, A.-M. Measures of diagnostic accuracy: basic definitions. *Med Biol Sci* **22**, 61-65 (2008).
107. Reitsma, J.B., *et al.* Bivariate analysis of sensitivity and specificity produces informative summary measures in diagnostic reviews. *Journal of clinical epidemiology* **58**, 982-990 (2005).

108. Alberg, A.J., Park, J.W., Hager, B.W., Brock, M.V. & Diener-West, M. The use of "overall accuracy" to evaluate the validity of screening or diagnostic tests. *Journal of general internal medicine* **19**, 460-465 (2004).
109. Migliori, G.B., Matteelli, A., Cirillo, D. & Pai, M. Diagnosis of multidrug-resistant tuberculosis and extensively drug-resistant tuberculosis: Current standards and challenges. *The Canadian Journal of Infectious Diseases & Medical Microbiology* **19**, 169 (2008).
110. Venkataraman, P., Herbert, D. & Paramasivan, C. Evaluation of the BACTEC radiometric method in the early diagnosis of tuberculosis. *Indian Journal of Medical Research* **108**, 120-127 (1998).
111. Tortoli, E., *et al.* Use of BACTEC MGIT 960 for recovery of mycobacteria from clinical specimens: multicenter study. *Journal of clinical microbiology* **37**, 3578-3582 (1999).
112. Moore, D.A., *et al.* Microscopic-observation drug-susceptibility assay for the diagnosis of TB. *New England Journal of Medicine* **355**, 1539-1550 (2006).
113. Green, M.R. & Sambrook, J. *Molecular cloning: a laboratory manual*, (Cold Spring Harbor Laboratory Press New York, New York, United States, 2012).
114. Palomino, J. Nonconventional and new methods in the diagnosis of tuberculosis: feasibility and applicability in the field. *European Respiratory Journal* **26**, 339-350 (2005).
115. Abe, C., *et al.* Detection of Mycobacterium tuberculosis in clinical specimens by polymerase chain reaction and Gen-Probe Amplified Mycobacterium Tuberculosis Direct Test. *Journal of clinical microbiology* **31**, 3270-3274 (1993).
116. Dalovisio, J.R., *et al.* Comparison of the amplified Mycobacterium tuberculosis (MTB) direct test, Amplicor MTB PCR, and IS6110-PCR for detection of MTB in respiratory specimens. *Clinical infectious diseases* **23**, 1099-1106 (1996).
117. Pandey, B.D., *et al.* Development of an in-house loop-mediated isothermal amplification (LAMP) assay for detection of Mycobacterium tuberculosis and evaluation in sputum samples of Nepalese patients. *Journal of medical microbiology* **57**, 439-443 (2008).
118. Bi, A., *et al.* A rapid loop-mediated isothermal amplification assay targeting hspX for the detection of Mycobacterium tuberculosis complex. *Japanese journal of infectious diseases* **65**, 247-251 (2012).
119. Boehme, C.C., *et al.* Operational feasibility of using loop-mediated isothermal amplification for diagnosis of pulmonary tuberculosis in microscopy centers of developing countries. *Journal of clinical microbiology* **45**, 1936-1940 (2007).
120. Yadav, R.N., *et al.* Comparative evaluation of GenoType MTBDRplus line probe assay with solid culture method in early diagnosis of multidrug resistant tuberculosis (MDR-TB) at a tertiary care centre in India. *PloS one* **8**, e72036 (2013).
121. Anek-vorapong, R., *et al.* Validation of the GenoType® MTBDRplus assay for detection of MDR-TB in a public health laboratory in Thailand. *BMC infectious diseases* **10**, 123 (2010).

122. Huyen, M.N., *et al.* Validation of the GenoType® MTBDRplus assay for diagnosis of multidrug resistant tuberculosis in South Vietnam. *BMC infectious diseases* **10**, 149 (2010).
123. Ling, D.I., Zwerling, A.A. & Pai, M. Rapid diagnosis of drug-resistant TB using line probe assays: from evidence to policy. (2008).
124. Martin, K.J. & Rygiewicz, P.T. Fungal-specific PCR primers developed for analysis of the ITS region of environmental DNA extracts. *BMC microbiology* **5**, 28 (2005).
125. Hillemann, D., Rüsch-Gerdes, S. & Richter, E. Evaluation of the GenoType MTBDRplus assay for rifampin and isoniazid susceptibility testing of Mycobacterium tuberculosis strains and clinical specimens. *Journal of clinical microbiology* **45**, 2635-2640 (2007).
126. Ulrich, M., *et al.* Evaluation of the Cepheid GeneXpert® system for detecting Bacillus anthracis. *Journal of applied microbiology* **100**, 1011-1016 (2006).
127. Zeka, A.N., Tasbakan, S. & Cavusoglu, C. Evaluation of the GeneXpert MTB/RIF assay for rapid diagnosis of tuberculosis and detection of rifampin resistance in pulmonary and extrapulmonary specimens. *Journal of clinical microbiology* **49**, 4138-4141 (2011).
128. Piatek, A.S., *et al.* Molecular beacon sequence analysis for detecting drug resistance in Mycobacterium tuberculosis. *Nature biotechnology* **16**, 359-363 (1998).
129. Tyagi, S. & Kramer, F.R. Molecular beacons: probes that fluoresce upon hybridization. *Nature biotechnology* **14**, 303-308 (1996).
130. Lawn, S.D. & Nicol, M.P. Xpert® MTB/RIF assay: development, evaluation and implementation of a new rapid molecular diagnostic for tuberculosis and rifampicin resistance. *Future microbiology* **6**, 1067-1082 (2011).
131. Meyer-Rath, G., *et al.* The impact and cost of scaling up GeneXpert MTB/RIF in South Africa. (2012).
132. Walusimbi, S., *et al.* Meta-analysis to compare the accuracy of GeneXpert, MODS and the WHO 2007 algorithm for diagnosis of smear-negative pulmonary tuberculosis. *BMC infectious diseases* **13**, 507 (2013).
133. Nakiyingi, L., Nankabirwa, H. & Lamorde, M. Tuberculosis diagnosis in resource-limited settings: clinical use of GeneXpert in the diagnosis of smear-negative PTB: a case report. *African health sciences* **13**, 522-524 (2013).
134. Rie, A.V., Page-Shipp, L., Scott, L., Sanne, I. & Stevens, W. Xpert® MTB/RIF for point-of-care diagnosis of TB in high-HIV burden, resource-limited countries: hype or hope? (2010).
135. Helb, D., *et al.* Rapid detection of Mycobacterium tuberculosis and rifampin resistance by use of on-demand, near-patient technology. *Journal of clinical microbiology* **48**, 229-237 (2010).
136. Evans, C.A. Genexpert-a game-changer for tuberculosis control? *PLoS medicine* **8**, 882 (2011).

137. Scott, L.E., *et al.* Comparison of Xpert MTB/RIF with other nucleic acid technologies for diagnosing pulmonary tuberculosis in a high HIV prevalence setting: a prospective study. *PLoS medicine* **8**, 976 (2011).
138. Omrani, A.S., *et al.* GeneXpert MTB/RIF Testing in the Management of Patients with Active Tuberculosis; A Real Life Experience from Saudi Arabia. *Infection & chemotherapy* **46**, 30-34 (2014).
139. McNerney, R., *et al.* Field test of a novel detection device for Mycobacterium tuberculosis antigen in cough. *BMC infectious diseases* **10**, 161 (2010).
140. Jassal, M.S., *et al.* 13 [C]-urea breath test as a novel point-of-care biomarker for tuberculosis treatment and diagnosis. *PLoS One* **5**(2010).
141. Hamasur, B., *et al.* Rapid diagnosis of tuberculosis by detection of mycobacterial lipoarabinomannan in urine. *Journal of microbiological methods* **45**, 41-52 (2001).
142. Hunter, S.W., Gaylord, H. & Brennan, P. Structure and antigenicity of the phosphorylated lipopolysaccharide antigens from the leprosy and tubercle bacilli. *Journal of Biological Chemistry* **261**, 12345-12351 (1986).
143. Shah, M., *et al.* Diagnostic accuracy of a urine lipoarabinomannan test for tuberculosis in hospitalized patients in a High HIV prevalence setting. *Journal of acquired immune deficiency syndromes (1999)* **52**, 145 (2009).
144. Lawn, S.D. Point-of-care detection of lipoarabinomannan (LAM) in urine for diagnosis of HIV-associated tuberculosis: a state of the art review. *BMC infectious diseases* **12**, 103 (2012).
145. Drain, P.K., *et al.* Diagnostic accuracy of a point-of-care urine test for tuberculosis screening among newly-diagnosed hiv-infected adults: a prospective, clinic-based study. *BMC infectious diseases* **14**, 110 (2014).
146. Nakamura, R., *et al.* MPB64 mycobacterial antigen: a new skin-test reagent through patch method for rapid diagnosis of active tuberculosis. *The International Journal of Tuberculosis and Lung Disease* **2**, 541-546 (1998).
147. Bekmurzayeva, A., Sypabekova, M. & Kanayeva, D. Tuberculosis diagnosis using immunodominant, secreted antigens of Mycobacterium tuberculosis. *Tuberculosis* **93**, 381-388 (2013).
148. Khan, S., Andries, A., Pherwani, A., Saranchuk, P. & Isaakidis, P. Patch-testing for the management of hypersensitivity reactions to second-line anti-tuberculosis drugs: a case report. *BMC research notes* **7**, 537 (2014).
149. Barman, P. & Gadre, D. A study of phage based diagnostic technique for tuberculosis. *INDIAN JOURNAL OF TUBERCULOSIS* **54**, 36 (2007).

150. Minion, J. & Pai, M. Bacteriophage assays for rifampicin resistance detection in Mycobacterium tuberculosis: updated meta-analysis [Review article]. *The International Journal of Tuberculosis and Lung Disease* **14**, 941-951 (2010).
151. Mi, X., He, F., Xiang, M., Lian, Y. & Yi, S. Novel phage-piezoelectric sensor for rapid drug susceptibility testing of Mycobacterium tuberculosis. *Sensors and Actuators B: Chemical* **193**, 715-722 (2014).
152. Montgomery, J.L., Sanford, L.N. & Wittwer, C.T. High-resolution DNA melting analysis in clinical research and diagnostics. (2010).
153. Bhatt, N. Extensively Drug Resistance Tuberculosis & Molecular Tools. (2014).
154. Wittwer, C.T., Reed, G.H., Gundry, C.N., Vandersteen, J.G. & Pryor, R.J. High-resolution genotyping by amplicon melting analysis using LCGreen. *Clinical chemistry* **49**, 853-860 (2003).
155. Erali, M. & Wittwer, C.T. High resolution melting analysis for gene scanning. *Methods* **50**, 250-261 (2010).
156. Mackay, J.F. & Wittwer, C.T. High-resolution melting analysis. *PCR troubleshooting and optimization: The essential guide*, 201-206 (2011).
157. Mackay, J.F., Wright, C.D. & Bonfiglioli, R.G. A new approach to varietal identification in plants by microsatellite high resolution melting analysis: application to the verification of grapevine and olive cultivars. *Plant Methods* **4**, 8 (2008).
158. Reed, G.H., Kent, J.O. & Wittwer, C.T. High-resolution DNA melting analysis for simple and efficient molecular diagnostics. (2007).
159. Choi, G.E., *et al.* High-resolution melting curve analysis for rapid detection of rifampin and isoniazid resistance in Mycobacterium tuberculosis clinical isolates. *Journal of clinical microbiology* **48**, 3893-3898 (2010).
160. Chen, X., *et al.* Rapid detection of isoniazid, rifampin, and ofloxacin resistance in Mycobacterium tuberculosis clinical isolates using high-resolution melting analysis. *Journal of clinical microbiology* **49**, 3450-3457 (2011).
161. Haeili, M., *et al.* Rapid screening of rpoB and katG mutations in Mycobacterium tuberculosis isolates by high-resolution melting curve analysis. *Indian journal of medical microbiology* **32**, 398 (2014).
162. Nagai, Y., *et al.* High resolution melting curve assay for rapid detection of drug-resistant Mycobacterium tuberculosis. *Journal of Infection and Chemotherapy* **19**, 1116-1125 (2013).
163. Pholwat, S., *et al.* Integrated Microfluidic Card with TaqMan Probes and High-Resolution Melt Analysis To Detect Tuberculosis Drug Resistance Mutations across 10 Genes. *mBio* **6**, e02273-02214 (2015).

164. Pietzka, A.T., *et al.* Rapid identification of multidrug-resistant Mycobacterium tuberculosis isolates by rpoB gene scanning using high-resolution melting curve PCR analysis. *Journal of antimicrobial chemotherapy* **63**, 1121-1127 (2009).
165. Yin, X., *et al.* High-resolution melting curve analysis for rapid detection of rifampin resistance in Mycobacterium tuberculosis: a meta-analysis. *Journal of clinical microbiology* **51**, 3294-3299 (2013).
166. Hoek, K., *et al.* Fluorometric assay for testing rifampin susceptibility of Mycobacterium tuberculosis complex. *Journal of clinical microbiology* **46**, 1369-1373 (2008).
167. Lee, A.S.G. & Ong, D.C.T. Molecular diagnostic methods for the detection of Mycobacterium tuberculosis resistance: the potential of high-resolution melting analysis. (2012).
168. Yadav, R., *et al.* Rapid detection of rifampicin, isoniazid and streptomycin resistance in Mycobacterium tuberculosis clinical isolates by high-resolution melting curve analysis. *Journal of applied microbiology* **113**, 856-862 (2012).
169. Newby, D.T., Hadfield, T. & Roberto, F.F. Real-time PCR detection of Brucella abortus: A comparative study of SYBR green I, 5′-exonuclease, and hybridization probe assays. *Applied and environmental microbiology* **69**, 4753-4759 (2003).
170. Lawn, S.D., *et al.* Advances in tuberculosis diagnostics: the Xpert MTB/RIF assay and future prospects for a point-of-care test. *The Lancet infectious diseases* **13**, 349-361 (2013).
171. Lienhardt, C., *et al.* Global tuberculosis control: lessons learnt and future prospects. *Nature Reviews Microbiology* **10**, 407-416 (2012).
172. Weyer, K., Carai, S. & Nunn, P. Viewpoint TB diagnostics: what does the world really need? *Journal of Infectious Diseases* **204**, S1196-S1202 (2011).
173. El-Ali, J., Sorger, P.K. & Jensen, K.F. Cells on chips. *Nature* **442**, 403-411 (2006).
174. Squires, T.M. & Quake, S.R. Microfluidics: Fluid physics at the nanoliter scale. *Reviews of modern physics* **77**, 977 (2005).
175. Erickson, D. & Li, D. Integrated microfluidic devices. *Analytica Chimica Acta* **507**, 11-26 (2004).
176. Whitesides, G.M. The origins and the future of microfluidics. *Nature* **442**, 368-373 (2006).
177. Armani, M., Chaudhary, S., Probst, R., Walker, S. & Shapiro, B. Control of microfluidic systems: two examples, results, and challenges. *International Journal of Robust and Nonlinear Control* **15**, 785-803 (2005).
178. Zhang, Y. & Ozdemir, P. Microfluidic DNA amplification—a review. *Analytica chimica acta* **638**, 115-125 (2009).
179. Hansen, C.L., Skordalakes, E., Berger, J.M. & Quake, S.R. A robust and scalable microfluidic metering method that allows protein crystal growth by free interface diffusion. *Proceedings of the National Academy of Sciences* **99**, 16531-16536 (2002).

180. Sackmann, E.K., Fulton, A.L. & Beebe, D.J. The present and future role of microfluidics in biomedical research. *Nature* **507**, 181-189 (2014).
181. Bao, N., Zhang, Q., Xu, J.-J. & Chen, H.-Y. Fabrication of poly (dimethylsiloxane) microfluidic system based on masters directly printed with an office laser printer. *Journal of Chromatography A* **1089**, 270-275 (2005).
182. Zhang, C. & Xing, D. Miniaturized PCR chips for nucleic acid amplification and analysis: latest advances and future trends. *Nucleic acids research* **35**, 4223-4237 (2007).
183. Easley, C.J., Karlinsey, J.M. & Landers, J.P. On-chip pressure injection for integration of infrared-mediated DNA amplification with electrophoretic separation. *Lab on a Chip* **6**, 601-610 (2006).
184. Gong, X. & Wen, W. Polydimethylsiloxane-based conducting composites and their applications in microfluidic chip fabrication. *Biomicrofluidics* **3**, 012007 (2009).
185. Regehr, K.J., *et al.* Biological implications of polydimethylsiloxane-based microfluidic cell culture. *Lab on a Chip* **9**, 2132-2139 (2009).
186. Makamba, H., Hsieh, Y.-Y., Sung, W.-C. & Chen, S.-H. Stable permanently hydrophilic protein-resistant thin-film coatings on poly (dimethylsiloxane) substrates by electrostatic self-assembly and chemical cross-linking. *Analytical chemistry* **77**, 3971-3978 (2005).
187. West, J., *et al.* Application of magnetohydrodynamic actuation to continuous flow chemistry. *Lab on a Chip* **2**, 224-230 (2002).
188. Mukhopadhyay, R. When PDMS isn't the best. *Analytical chemistry* **79**, 3248-3253 (2007).
189. Hupert, M.L., *et al.* Polymer-based microfluidic devices for biomedical applications. in *Micromachining and Microfabrication* 52-64 (International Society for Optics and Photonics, 2003).
190. Martynova, L., *et al.* Fabrication of plastic microfluid channels by imprinting methods. *Analytical Chemistry* **69**, 4783-4789 (1997).
191. Easley, C.J., *et al.* A fully integrated microfluidic genetic analysis system with sample-in–answer-out capability. *Proceedings of the National Academy of Sciences* **103**, 19272-19277 (2006).
192. Bu, M., Melvin, T., Ensell, G., Wilkinson, J.S. & Evans, A.G. Design and theoretical evaluation of a novel microfluidic device to be used for PCR. *Journal of Micromechanics and Microengineering* **13**, S125 (2003).
193. Khandurina, J., *et al.* Integrated system for rapid PCR-based DNA analysis in microfluidic devices. *Analytical Chemistry* **72**, 2995-3000 (2000).
194. Erill, I., *et al.* Development of a CMOS-compatible PCR chip: comparison of design and system strategies. *Journal of Micromechanics and Microengineering* **14**, 1558 (2004).

195. Slyadnev, M.N., Tanaka, Y., Tokeshi, M. & Kitamori, T. Photothermal temperature control of a chemical reaction on a microchip using an infrared diode laser. *Analytical chemistry* **73**, 4037-4044 (2001).
196. Focke, M., *et al.* Lab-on-a-Foil: microfluidics on thin and flexible films. *Lab on a Chip* **10**, 1365-1386 (2010).
197. Hoang, V.N., Kaigala, G.V. & Backhouse, C.J. Optimization of Thin Film Heater/Sensor Design for Miniature Devices Using Finite Element Analysis. in *COMSOL Multiphysics User's conference* (2005).
198. Daniel, J.H., *et al.* Silicon microchambers for DNA amplification. *Sensors and Actuators A: Physical* **71**, 81-88 (1998).
199. Daniel, J., *et al.* Silicon microchambers for DNA amplification. *Sensors and Actuators A: Physical* **71**, 81-88 (1998).
200. Miralles, V., Huerre, A., Malloggi, F. & Jullien, M.-C. A review of heating and temperature control in microfluidic systems: techniques and applications. *Diagnostics* **3**, 33-67 (2013).
201. Zhang, C., Xu, J., Ma, W. & Zheng, W. PCR microfluidic devices for DNA amplification. *Biotechnology advances* **24**, 243-284 (2006).
202. Wittwer, C., Fillmore, G.C. & Hillyard, D. Automated polymerase chain reaction in capillary tubes with hot air. *Nucleic acids research* **17**, 4353-4357 (1989).
203. Wu, J., Kodzius, R., Cao, W. & Wen, W. Extraction, amplification and detection of DNA in microfluidic chip-based assays. *Microchimica Acta* **181**, 1611-1631 (2014).
204. Giordano, B.C., Copeland, E.R. & Landers, J.P. Towards dynamic coating of glass microchip chambers for amplifying DNA via the polymerase chain reaction. *Electrophoresis* **22**, 334-340 (2001).
205. Pak, N., Saunders, D.C., Phaneuf, C.R. & Forest, C.R. Plug-and-play, infrared, laser-mediated PCR in a microfluidic chip. *Biomedical microdevices* **14**, 427-433 (2012).
206. Pal, D. & Venkataraman, V. A portable battery-operated chip thermocycler based on induction heating. *Sensors and Actuators A: Physical* **102**, 151-156 (2002).
207. Lee, T.M., Hsing, I.-M., Lao, A.I. & Carles, M.C. A miniaturized DNA amplifier: its application in traditional Chinese medicine. *Analytical chemistry* **72**, 4242-4247 (2000).
208. Quake, S. A nanoliter rotary device for polymerase chain reaction. *Electrophoresis* **23**, 1531-1536 (2002).
209. Basson, M. & Pottebaum, T.S. Measuring the temperature of fluid in a micro-channel using thermochromic liquid crystals. *Experiments in fluids* **53**, 803-814 (2012).
210. Mark, D., Haeberle, S., Roth, G., von Stetten, F. & Zengerle, R. Microfluidic lab-on-a-chip platforms: requirements, characteristics and applications. *Chemical Society Reviews* **39**, 1153-1182 (2010).

211. Posthuma-Trumpie, G.A., Korf, J. & van Amerongen, A. Lateral flow (immuno) assay: its strengths, weaknesses, opportunities and threats. A literature survey. *Analytical and bioanalytical chemistry* **393**, 569-582 (2009).
212. Hicks, J. & Iosefsohn, M. Reliability of home pregnancy-test kits in the hands of laypersons. *The New England journal of medicine* **320**, 320-321 (1989).
213. Pollack, M.G., Fair, R.B. & Shenderov, A.D. Electrowetting-based actuation of liquid droplets for microfluidic applications. *Applied Physics Letters* **77**, 1725-1726 (2000).
214. Kamholz, A.E. & Yager, P. Theoretical analysis of molecular diffusion in pressure-driven laminar flow in microfluidic channels. *Biophysical journal* **80**, 155-160 (2001).
215. Spielman, L. & Goren, S.L. Improving resolution in Coulter counting by hydrodynamic focusing. *Journal of Colloid and Interface Science* **26**, 175-182 (1968).
216. Alizadeh, A., De Castro, C.N. & Wakeham, W. The theory of the Taylor dispersion technique for liquid diffusivity measurements. *International Journal of thermophysics* **1**, 243-284 (1980).
217. Holtze, C., *et al.* Biocompatible surfactants for water-in-fluorocarbon emulsions. *Lab on a Chip* **8**, 1632-1639 (2008).
218. Glass, N.R., Shilton, R.J., Chan, P.P., Friend, J.R. & Yeo, L.Y. Miniaturized Lab-on-a-Disc (miniLOAD). *small* **8**, 1881-1888 (2012).
219. Sasaki, N., Kitamori, T. & Kim, H.-B. AC electroosmotic micromixer for chemical processing in a microchannel. *Lab on a Chip* **6**, 550-554 (2006).
220. Kumar, A. & Whitesides, G.M. Features of gold having micrometer to centimeter dimensions can be formed through a combination of stamping with an elastomeric stamp and an alkanethiol ‘‘ink’’followed by chemical etching. *Applied Physics Letters* **63**, 2002-2004 (1993).
221. Rogers, J.A. & Nuzzo, R.G. Recent progress in soft lithography. *Materials today* **8**, 50-56 (2005).
222. Unger, M.A., Chou, H.-P., Thorsen, T., Scherer, A. & Quake, S.R. Monolithic microfabricated valves and pumps by multilayer soft lithography. *Science* **288**, 113-116 (2000).
223. Anderson, M.J., Hansen, C.L. & Quake, S.R. Phase knowledge enables rational screens for protein crystallization. *Proceedings of the National Academy of Sciences* **103**, 16746-16751 (2006).
224. Hong, J.W., Studer, V., Hang, G., Anderson, W.F. & Quake, S.R. A nanoliter-scale nucleic acid processor with parallel architecture. *Nature biotechnology* **22**, 435-439 (2004).
225. Kartalov, E.P., *et al.* High-throughput multi-antigen microfluidic fluorescence immunoassays. *BioTechniques* **40**, 85 (2006).

226. Thorsen, T., Maerkl, S.J. & Quake, S.R. Microfluidic large-scale integration. *Science* **298**, 580-584 (2002).
227. Gu, W., Zhu, X., Futai, N., Cho, B.S. & Takayama, S. Computerized microfluidic cell culture using elastomeric channels and Braille displays. *Proceedings of the National Academy of Sciences of the United States of America* **101**, 15861-15866 (2004).
228. Manz, A., Graber, N. & Widmer, H.á. Miniaturized total chemical analysis systems: a novel concept for chemical sensing. *Sensors and actuators B: Chemical* **1**, 244-248 (1990).
229. Pires, N.M.M., Dong, T., Hanke, U. & Hoivik, N. Recent developments in optical detection technologies in lab-on-a-chip devices for biosensing applications. *Sensors* **14**, 15458-15479 (2014).
230. Lee, T.M.-H., Carles, M.C. & Hsing, I.-M. Microfabricated PCR-electrochemical device for simultaneous DNA amplification and detection. *Lab on a Chip* **3**, 100-105 (2003).
231. van den Hurk, R. & Evoy, S. Deflection cantilever detection of interferon gamma. *Sensors and Actuators B: Chemical* **176**, 960-965 (2013).
232. Sharma, H., Lakshmanan, R.S., Johnson, B.N. & Mutharasan, R. Piezoelectric cantilever sensors with asymmetric anchor exhibit picogram sensitivity in liquids. *Sensors and Actuators B: Chemical* **153**, 64-70 (2011).
233. Genet, C. & Ebbesen, T. Light in tiny holes. *Nature* **445**, 39-46 (2007).
234. Kuswandi, B., Huskens, J. & Verboom, W. Optical sensing systems for microfluidic devices: a review. *Analytica chimica acta* **601**, 141-155 (2007).
235. Du, W.B., Fang, Q., He, Q.H. & Fang, Z.L. High-throughput nanoliter sample introduction microfluidic chip-based flow injection analysis system with gravity-driven flows. *Analytical Chemistry* **77**, 1330-1337 (2005).
236. Watson, G., Slocombe, R., Robinson, N. & Sleight, S. Definition of chemiluminescence and superoxide production responses of bovine neutrophils to selected soluble and particulate stimulants, and comparisons with the responses to Pasteurella haemolytica. *American journal of veterinary research* **56**, 1045-1054 (1995).
237. Amatatongchai, M., Hofmann, O., Nacapricha, D. & Chailapakul, O. A microfluidic system for evaluation of antioxidant capacity based on a peroxyoxalate chemiluminescence assay. *Analytical and bioanalytical chemistry* **387**, 277-285 (2007).
238. Hofmann, O., *et al.* Monolithically integrated dye-doped PDMS long-pass filters for disposable on-chip fluorescence detection. *Lab on a Chip* **6**, 981-987 (2006).
239. Delaney, J.L., Hogan, C.F., Tian, J. & Shen, W. Electrogenerated chemiluminescence detection in paper-based microfluidic sensors. *Analytical chemistry* **83**, 1300-1306 (2011).
240. Valeur, B. & Berberan-Santos, M.N. *Molecular fluorescence: principles and applications*, (John Wiley & Sons, 2012).

241. Auroux, P.-A., Iossifidis, D., Reyes, D.R. & Manz, A. Micro total analysis systems. 2. Analytical standard operations and applications. *Analytical chemistry* **74**, 2637-2652 (2002).
242. Gao, J., Yin, X.-F. & Fang, Z.-L. Integration of single cell injection, cell lysis, separation and detection of intracellular constituents on a microfluidic chip. *Lab on a Chip* **4**, 47-52 (2004).
243. Karlinsey, J.M. & Landers, J.P. Multicolor fluorescence detection on an electrophoretic microdevice using an acoustooptic tunable filter. *Analytical chemistry* **78**, 5590-5596 (2006).
244. Miyaki, K., *et al.* Fabrication of an integrated PDMS microchip incorporating an LED-induced fluorescence device. *Analytical and bioanalytical chemistry* **382**, 810-816 (2005).
245. Belgrader, P., *et al.* A reusable flow-through polymerase chain reaction instrument for the continuous monitoring of infectious biological agents. *Analytical chemistry* **75**, 3446-3450 (2003).
246. Mao, X. & Huang, T.J. Microfluidic diagnostics for the developing world. *Lab on a Chip* **12**, 1412-1416 (2012).
247. Wang, S., Inci, F., De Libero, G., Singhal, A. & Demirci, U. Point-of-care assays for tuberculosis: role of nanotechnology/microfluidics. *Biotechnology advances* **31**, 438-449 (2013).
248. Ke, C., Berney, H., Mathewson, A. & Sheehan, M. Rapid amplification for the detection of Mycobacterium tuberculosis using a non-contact heating method in a silicon microreactor based thermal cycler. *Sensors and Actuators B: Chemical* **102**, 308-314 (2004).
249. Rosenfeld, L., Cheng, Y., Rao, J. & Tang, S.K.Y. Rapid detection of tuberculosis using droplet-based microfluidics. Vol. 8976 897611-897611-897618 (2014).
250. Xie, H., *et al.* Rapid point-of-care detection of the tuberculosis pathogen using a BlaC-specific fluorogenic probe. *Nature chemistry* **4**, 802-809 (2012).
251. Tsai, T.-T., Shen, S.-W., Cheng, C.-M. & Chen, C.-F. Paper-based tuberculosis diagnostic devices with colorimetric gold nanoparticles. *Science and Technology of Advanced Materials* **14**, 044404 (2013).
252. Veigas, B., *et al.* Au-nanoprobes for detection of SNPs associated with antibiotic resistance in Mycobacterium tuberculosis. *Nanotechnology* **21**, 415101 (2010).
253. Chun, A.L. Nanoparticles offer hope for TB detection. *Nature nanotechnology* **4**, 698 (2009).
254. Merritt, A.J., Keehner, T., O'Reilly, L.C., McInnes, R.L. & Inglis, T.J. MANTRA, a rapid genotyping method for Mycobacterium tuberculosis by multiplex PCR and microfluidic labchip. *Journal of Clinical Microbiology* (2010).
255. Żaczek, A., Brzostek, A., Wojtasik, A., Dziadek, J. & Sajduda, A. Genotyping of Clinical Mycobacterium tuberculosis Isolates Based on IS6110 and MIRU-VNTR Polymorphisms. *BioMed research international* **2013**(2013).
256. Koul, A., *et al.* Delayed bactericidal response of Mycobacterium tuberculosis to bedaquiline involves remodelling of bacterial metabolism. *Nature communications* **5**(2014).

257. Peter, J., *et al.* Urine for the diagnosis of tuberculosis: current approaches, clinical applicability, and new developments. *Current opinion in pulmonary medicine* **16**, 262-270 (2010).
258. Ahlburg, D.A. & Initiative, S.T. The economic impacts of tuberculosis. (2000).
259. McNerney, R., Cunningham, J., Hepple, P. & Zumla, A. New tuberculosis diagnostics and rollout. *International Journal of Infectious Diseases* **32**, 81-86 (2015).
260. Padmapriyadarsini, C., Narendran, G. & Swaminathan, S. Diagnosis & treatment of tuberculosis in HIV co-infected patients. *The Indian journal of medical research* **134**, 850 (2011).
261. Raviglione, M., *et al.* Scaling up interventions to achieve global tuberculosis control: progress and new developments. *The Lancet* **379**, 1902-1913 (2012).
262. Velayati, A.A., *et al.* Emergence of new forms of totally drug-resistant tuberculosis bacilli: super extensively drug-resistant tuberculosis or totally drug-resistant strains in Iran. *Chest Journal* **136**, 420-425 (2009).
263. Pang, Y., Liu, G., Wang, Y., Zheng, S. & Zhao, Y.-l. Combining COLD-PCR and high-resolution melt analysis for rapid detection of low-level, rifampin-resistant mutations in Mycobacterium tuberculosis. *Journal of microbiological methods* **93**, 32-36 (2013).
264. Telenti, A., Imboden, P., Marchesi, F., Schmidheini, T. & Bodmer, T. Direct, automated detection of rifampin-resistant Mycobacterium tuberculosis by polymerase chain reaction and single-strand conformation polymorphism analysis. *Antimicrobial agents and chemotherapy* **37**, 2054-2058 (1993).
265. Higuchi, R., Fockler, C., Dollinger, G. & Watson, R. Kinetic PCR analysis: real-time monitoring of DNA amplification reactions. *Biotechnology* **11**, 1026-1030 (1993).
266. Pfaffl, M.W. A new mathematical model for relative quantification in real-time RT–PCR. *Nucleic acids research* **29**, e45-e45 (2001).
267. Palais, R. & Wittwer, C.T. Mathematical algorithms for high-resolution DNA melting analysis. *Methods in enzymology* **454**, 323-343 (2009).
268. Altman, D.G. & Bland, J.M. Statistics notes: detecting skewness from summary information. *Bmj* **313**, 1200 (1996).
269. Wang, Q., *et al.* A newly identified 191A/C mutation in the Rv2629 gene that was significantly associated with rifampin resistance in Mycobacterium tuberculosis. *Journal of proteome research* **6**, 4564-4571 (2007).
270. Ginsburg, A.S., Grosset, J.H. & Bishai, W.R. Fluoroquinolones, tuberculosis, and resistance. *The Lancet infectious diseases* **3**, 432-442 (2003).
271. Zhou, J., *et al.* Selection of antibiotic-resistant bacterial mutants: allelic diversity among fluoroquinolone-resistant mutations. *Journal of infectious Diseases* **182**, 517-525 (2000).

272. Chaves, F., *et al.* rpoB mutations as an epidemiologic marker in rifampin-resistant Mycobacterium tuberculosis. *The International Journal of Tuberculosis and Lung Disease* **4**, 765-770 (2000).
273. Herrmann, M.G., Durtschi, J.D., Wittwer, C.T. & Voelkerding, K.V. Expanded instrument comparison of amplicon DNA melting analysis for mutation scanning and genotyping. *Clinical chemistry* **53**, 1544-1548 (2007).
274. Rachow, A., *et al.* Rapid and accurate detection of Mycobacterium tuberculosis in sputum samples by Cepheid Xpert MTB/RIF assay–a clinical validation study. *PloS one* **6**, e20458 (2011).
275. Suffys, P., *et al.* Inhibition of the polymerase chain reaction by sputum samples from tuberculosis patients after processing using a silica-guanidiniumthiocyanate DNA isolation procedure. *Memórias do Instituto Oswaldo Cruz* **96**, 1137-1139 (2001).
276. Sreevatsan, S., *et al.* Restricted structural gene polymorphism in the Mycobacterium tuberculosis complex indicates evolutionarily recent global dissemination. *Proceedings of the National Academy of Sciences of the United States of America* **94**, 9869-9874 (1997).
277. Glaziou, P., Falzon, D., Floyd, K. & Raviglione, M. Global epidemiology of tuberculosis. *Semin Respir Crit Care Med* **34**, 3-16 (2013).
278. Hamburg, M.A. & Collins, F.S. The path to personalized medicine. *New England Journal of Medicine* **363**, 301-304 (2010).
279. Schork, N.J. Personalized medicine: Time for one-person trials. *Nature* **520**, 609-611 (2015).
280. Zhang, X., *et al.* Co-occurrence of amikacin-resistant and-susceptible Mycobacterium tuberculosis isolates in clinical samples from Beijing, China. *Journal of Antimicrobial Chemotherapy* **68**, 1537-1542 (2013).
281. Kumar, P., *et al.* High degree of multi-drug resistance and hetero-resistance in pulmonary TB patients from Punjab state of India. *Tuberculosis* **94**, 73-80 (2014).
282. Blakemore, R., *et al.* Evaluation of the analytical performance of the Xpert MTB/RIF assay. *Journal of clinical microbiology* **48**, 2495-2501 (2010).

Appendix

Isolates	Mutations detected by Sanger sequencing				HRMA result (LightCycler®96)				HRMA result (Light Forge)	Mutation Class				Phenotype		
	rpoB	*mab-inhA*	*katG*	*gyrA*	*rpoB*	*mab-inhA*	*katG*	*gyrA*	*rpoB*	*rpoB*	*mab-inhA*	*katG*	*gyrA*	RIF	INH	OFLX
R35	CTG→CCG (L533P)	ND	AGC→AAC (S315N)	AGC→ACC (S95T)	V	V	V	V	V	1	-	1	3	R	R	S
Kzn 605	GAC →GGC (D516G) CTG→CCG (L533P)	T→A (-8)	AGC→ACC (S315T)	AGC→ACC (S95T) GCG→GTG (A90V)	V	WT	WT	V	V	1	4	3	1&3	R	R	R
R271	TCG→TTG (S531L)	ND	ND	AGC→ACC (S95T)	V	WT	WT	WT	NT	1	-	-	3	R	R	S
Tkk-050	CAC →TAC (H526Y)	C→T (-15)	AGC→ACC (S315T)	AGC→ACC (S95T)	V	WT	WT	WT	NT	1	1	3	3	R	R	S
Tkk-062	GAC→GTC (D516V)	G →T (-17)	AGC→ACC (S315T)	AGC→ACC (S95T)	WT	WT	WT	WT	V	4	2	3	3	R	R	S
Tkk-043	TCG→TTG (S531L)	ND	AGC→AAC (S315N)	AGC→ACC (S95T)	V	WT	WT	WT	NT	1	-	1	3	R	R	S
Tkk-039	CAC →TAC (H526Y)	ND	AGC→ACC (S315T)	AGC→ACC (S95T)	V	WT	WT	WT	NT	1	-	3	3	R	R	S

Table 8: Mutations detected in the seven test strains of Tuberculosis (Mtb) compared with the HRMA profiles from the Roche commercial system, Light Forge and the Phenotypic

V-variant, WT-wild type/ none variant, ND- none detected, NT- not tested, R-resistant, S-susceptible

The graph shows a comparative summary of the drug susceptibility testing using the Light Cycler96, Light Forge, Sanger sequencing and phenotypic methods. In spite of some cases of discordance, a high degree of agreement across the tests is observed.

Isolate	Initial Sample Concentration (ng μl^{-1})	Initial $A_{260}/_{280}$	DNA (ng) content per reaction	Volume of sample added	Volume of TE Buffer added (µl)-	Final Concentration of mixture (ng μl^{-1})	Final A_{260}/A_{280}	Volume added to PCR master mix (µl)
H37Rv	114	1.91	200	1.75	98.25	0.8	1.98	5
R35	30.6	1.88	200	6.5	93.5	1.9	1.44	5
Kzn 605	34.5	1.93	200	5.8	94.2	1.1	1.74	5
R271	29.6	1.92	200	6.8	93.2	0.9	1.53	5
Tkk-050	16.4	1.91	200	12.2	87.8	1.5	1.59	5
Tkk-062	33.2	1.89	200	6.02	94	0.8	1.52	5
Tkk-043	97.6	1.95	200	2.05	97.95	0.7	1.34	5
Tkk-039	33.8	1.93	200	5.92	94.08	1.1	1.29	5

Table 9: Quantity and purity of M.tuberculosis DNA samples. The A_{260}/A_{280} for pure DNA preparations is around 1.8.

The table above shows the quantity and purity of the DNA samples used in the assay. The initial extracts were measured for the total DNA and purity using the A260/A280 number. All samples were then adjusted to contain 200ng per reaction by diluting with TE Buffer according to sample specific instructions in the table. This meant that the same volume and quantity of DNA is added per reaction to remove variability that these two factors might possibly introduce. Thus for all the genes studied by all the molecular DST methods used these adjusted DNA samples for unifor